## Novel approaches for biocatalytic oxyfunctionalization reactions

# Novel approaches for biocatalytic oxyfunctionalization reactions

#### Proefschrift

ter verkrijging van de graad van doctor aan de Technische Universiteit Delft, op gezag van de Rector Magnificus prof. ir. K.C.A.M. Luyben, voorzitter van het College voor Promoties, in het openbaar te verdedigen op vrijdag 20 juni 2014 om 12:30 uur

door

#### Ekaterina CHURAKOVA

Master of Science in Chemistry, Novosibirsk State University, Russia geboren te Igra, Udmurt Republic, Russia

Dit proefschrift is goedgekeurd door de promotor:

Prof. Dr. I.W.C.E. Arends

Copromotor Dr. F. Hollmann

#### Samenstelling promotiecommissie:

Rector Magnificus voorzitter

Prof. Dr. I.W.C.E. Arends

Technische Universiteit Delft, promotor

Dr. F. Hollmann

Technische Universiteit Delft, supervisor

Prof. Dr. R. Wever University of Amsterdam

Prof. Dr. V.B. Urlacher Heinrich-Heine-Universität Düsseldorf

Prof. Dr. S. de Vries Technische Universiteit Delft

Dr. Ir. M.C.R. Franssen Wageningen University

Prof. Dr. R.H. Kaul Lund University

Prof. Dr. U. Hanefeld Technische Universiteit Delft, reservelid

The research reported in this thesis was supported by the Marie Curie Initial Training Network BIOTRAINS, financed by the European Union through the 7th Framework People Programme (grant agreement number 238531).

ISBN: 978-94-6203-607-9

## Table of contents

Preface	1
Chapter 1. Introduction	4
Biocatalysis as a valuable tool for oxyfunctionalization	
Chapter 2	33
Increasing the productivity of peroxidase - catalyzed oxyfunctionalization – a case study on the potential of two liquid phase systems	
Chapter 3	51
Specific photobiocatalytic oxyfunctionalization reactions	
Chapter 4	71
A novel approach to utilize cytochrome P450 peroxygenases	
Chapter 5	87
Artificial metalloenzymes for in situ regeneration of the reduced nicotinamide cofactor	
Chapter 6	107
Hydrophobic formic acid esters for cofactor regeneration in aqueous/organic two-liquid phase systems	
Chapter 7	120
Conclusions and outlook	
Summary	127
Samenvatting	129
Acknowledgements	131
List of publications	134

### Preface

Modern everyday life inherently involves an enormous variety of goods produced by the chemical industry. Fossil fuels represent not only the energy source, but also the raw material for a vast amount of organic chemicals. Nowadays, over 95% of organic chemicals are derived from petroleum and natural gas <sup>[1]</sup>. Hydrocarbons (alkanes, alkenes and (alkyl)aromatics) are the main building blocks on which most of the organic chemical industry is based. Selective oxidations of hydrocarbons are widely used for oil processing towards oxygenated derivatives - alcohols, aldehydes, ketones, epoxides and carboxylic acids, which are the starting materials in the manufacturing of plastics, resins, fibers, lubricants, detergents, agrochemicals, cosmetics, health care products, pharmaceuticals, etc. <sup>[1-2]</sup>

Modern oxidation methods require the use of selective catalysts and environmentally friendly oxidants. Therefore, traditional stoichiometric use of hazardous oxidants such as chromium reagents, permanganate, manganese dioxide, periodate, chlorine is being replaced by catalytic processes using oxygen or hydrogen peroxide as oxidants (which produce water as byproduct) <sup>[3]</sup>. For example, catalytic oxidation of ethylene is an important process for the production of ethylene oxide – a starting material for manufacturing of ethylene glycol (1,2-diol) produced annually on a multimillion tons scale as polyester monomers and antifreeze agents <sup>[2]</sup>. Gas - phase partial aerobic oxidation of ethylene using silver supported catalyst replaced the traditional chlorohydrin method: hypochlorination of ethylene followed by dehydrochlorination using Ca(OH)<sub>2</sub>, which generates considerable amount of calcium chloride as byproduct <sup>[2]</sup>. Other relevant examples of gas phase oxidations include oxidation of butane to maleic anhydride (involving vanadyl pyrophosphate catalyst  $(VO)_2P_2O_7$ ) <sup>[4]</sup> and *o*-xylene to phthalic anhydride (over  $V_2O_5$  catalyst) <sup>[2]</sup>.

The liquid phase catalytic oxidation, which is generally referred to as autooxidation, is extensively practiced world - wide. These processes occur with the use of oxygen or (alkyl)peroxides, in the presence or absence of a metal catalyst, and involve the formation of free radicals as intermediates <sup>[3]</sup>. Propylene oxide, benzoic acid, terephthalic acid and phenol are produced by liquid phase catalytic oxidations of propylene and alkylbenzenes <sup>[2]</sup>. These reactions require harsh conditions and the efficiency of the process is not always high due to competing radical pathways.

Generally, partial oxidation of hydrocarbons, especially alkanes, via C-H activation towards alcohols and carbonyl compounds remains challenging due to higher reactivity of the products than starting material. One exceptional example is the gas phase oxidation of butane to maleic anhydride (stable product), which proceeds with a maximum 50-60% selectivity at a butane conversion of 10-15% <sup>[2]</sup>. Partial oxidation is more challenging, when the substrate lacks reactive C-H bonds and the products

are unstable. For example, liquid phase oxidation of cyclohexane to cyclohexanol/cyclohexanone (KA oil) is an important industrial process for the production of adipic acid used on million tones scale for the manufacture of nylon-6,6 <sup>[2]</sup>. However, due to a complicated radical mechanism, the bio-product formation is excessive and the overall conversion is retained at 4% in order to keep KA oil selectivity at 75-80% <sup>[2]</sup>.

In conclusion, modern catalytic oxidation of hydrocarbons remain inefficient and energy demanding process ( $120 - 450^{\circ}$  C). Additionally, despite of the progress of catalytic oxidations using  $O_2$  or  $H_2O_2$  in bulk industry, selective oxidation with  $O_2/H_2O_2$  of fine chemicals remains a difficult transformation due to the multifunctional nature of the molecules of interest. Therefore, the fine chemical industry still suffers from significant waste formation due to the stoichiometric use of inorganic oxidants  $^{[3, 5]}$ . Moreover, a large variety of desirable oxyfunctionalized molecules are rather obtained in multistep synthesis, e.g. via halogenation followed by dehydrohalogenation, or reduction of the molecules with higher oxidation state, thus obviating more challenging catalytic oxidation  $^{[1, 3]}$ . An example of the latter is asymmetric hydrogenation of prochiral ketones towards chiral alcohols using e.g. transition metal catalysts  $^{[5]}$ .

Nowadays, increasing demands of energy and ecology concerns require more sustainable chemical processes. Hence, the search for efficient and environmentally benign catalytic systems for the selective oxyfunctionalizations of hydrocarbons to valuable oxygenated compounds is an ongoing challenge in research <sup>[6-10]</sup>. Although tremendous results have been achieved in homogeneous and heterogeneous catalysis for selective oxyfunctionalizations, various enzyme-mediated transformations come into sight, which become attractive for industrial use <sup>[3, 6-10]</sup>. Throughout this thesis various examples in the area of selective enzymatic oxyfunctionalization will be shown, demonstrating the great potential of biocatalysis for synthetic organic chemistry.

#### References

- [1] H. A. Wittcoff, B. G. Reuben, J. S. Plotkin, Industrial organic chemicals, 2nd ed., *John Wiley & Sons, Inc.*, **2004**
- [2] K. Weissermel, H.-J. Arpe, Industrial Organic Chemistry, 4th ed., *Wiley-VCH Verlag GmbH & Co. KGaA*, **2003**
- [3] R. Sheldon, I. W. C. E. Arends, U. Hanefeld, Green Chemistry and Catalysis, *Wiley-VCH Verlag GmbH & Co. KGaA*, **2007**
- [4] N. Ballarini, F. Cavani, C. Cortelli, S. Ligi, F. Pierelli, F. Trifirò, C. Fumagalli, G. Mazzoni, T. Monti, VPO catalyst for n-butane oxidation to maleic anhydride: A goal achieved, or a still open challenge?, *Top Catal*, **2006**, *38*, 147-156.
- [5] M. Breuer, K. Ditrich, T. Habicher, B. Hauer, M. Keßeler, R. Stürmer, T. Zelinski, Industrial Methods for the Production of Optically Active Intermediates, *Angew. Chem. Int. Ed.*, **2004**, *43*, 788-824.

- [6] E. Roduner, W. Kaim, B. Sarkar, V. B. Urlacher, J. Pleiss, R. Glaser, W. D. Einicke, G. A. Sprenger, U. Beifuss, E. Klemm, C. Liebner, H. Hieronymus, S. F. Hsu, B. Plietker, S. Laschat, Selective Catalytic Oxidation of C-H Bonds with Molecular Oxygen, *ChemCatChem*, **2013**, *5*, 82-112.
- [7] M. Bordeaux, A. Galarneau, J. Drone, Catalytic, Mild, and Selective Oxyfunctionalization of Linear Alkanes: Current Challenges, *Angew. Chem. Int. Ed.*, **2012**, *51*, 10712-10723.
- [8] F. Hollmann, I. Arends, K. Buehler, A. Schallmey, B. Buhler, Enzyme-mediated oxidations for the chemist, *Green Chem.*, **2011**, *13*, 226-265.
- [9] J. C. Lewis, P. S. Coelho, F. H. Arnold, Enzymatic functionalization of carbon-hydrogen bonds, *Chem. Soc. Rev.*, **2011**, *40*, 2003-2021.
- [10] D. Monti, G. Ottolina, G. Carrea, S. Riva, Redox Reactions Catalyzed by Isolated Enzymes, *Chem. Rev.*, **2011**, *111*, 4111-4140.

### Chapter 1. Introduction

## Biocatalysis as a valuable tool for oxyfunctionalization

### Chapter 1. Introduction

#### Biocatalysis as a valuable tool for oxyfunctionalization

#### 1. The challenge of C-H oxyfunctionalization

The controlled partial oxidation of hydrocarbons is the key reaction for the conversion of oil and gas feedstock to industrial organic chemicals <sup>[1]</sup>. One of the hurdles towards oxidation of hydrocarbons is the inertness of C-H bonds, especially in saturated hydrocarbons, where the bond energy amounts to  $400 \text{ kJ mol}^{-1}$  [2]. Moreover, the formed product needs to be stabilized as it is often more reactive than the starting material <sup>[3]</sup>. Thus, the formed alcohols can be further oxidized to e.g. the aldehyde, acid and even  $CO_2^{[4]}$ .

The use of molecular oxygen as the primary oxidant is desirable from economic and environmental points of view. However, the ground state of the dioxygen contains two unpaired electrons (triplet  ${}^3O_2$ ), and therefore is spin forbidden to react with spin-paired singlet C-H bonds  ${}^{[4-5]}$ . Hence, catalysts are needed to activate molecular oxygen and to direct the selectivity of the reaction. Transition metals containing unpaired electrons are able to react directly with the triplet state of oxygen, forming dioxygen adducts, which can incorporate an oxygen into the C-H bond or oxidize an organic substrate  ${}^{[5]}$ .

Despite the progress in transition—metal and organocatalysis, the selective catalytic oxidation of C-H bonds using molecular oxygen is accompanied by many problems, e.g. the oxidative destruction of organic ligands and competition with free radical oxidation pathways <sup>[1-2, 4]</sup>. In addition, chemical catalysts suffer from low selectivity when it comes to converting C-H bonds in functionalized molecules. In this respect, enzymes have a key advantage because of their possibility to stir chemo-, regio- and stereoselectivity even in multifunctional molecules. Furthermore, biocatalytic reactions operate under mild reaction conditions, which is essential from an environmental point of view <sup>[6-9]</sup>. Thus, there is a vast area of oxidation reactions to be disclosed using enzymes as catalysts.

#### 2. Enzymatic oxyfunctionalizations

Several enzymatic systems have emerged in nature that are able to incorporate oxygen into non-activated C - H bonds using  $O_2$  or  $H_2O_2$  as an oxidant  $^{[2, 8-9]}$ . Nowadays, mainly 5 classes of redox enzymes are probed for oxyfunctionalization of non - activated C - H bonds (Table 1). The active site commonly contains either a heme - iron, non - heme di - iron, copper or flavin as a cofactor, which is involved in an oxygen activation  $^{[2]}$ . Essentially all these cofactors are placed in the enzyme scaffold in a manner that controls a substrate scope and a selectivity of the reaction.

Table 1. Enzymes involved in oxyfunctionalization of non - activated C-H bonds

Enzyme class	Prosthetic group	Substrate range
Methane monooxygenase: sMMO	Non - heme di – iron	C <sub>1</sub> - C <sub>8</sub> alkanes, alkenes, cycloalkenes
рММО	Copper	C <sub>1</sub> - C <sub>5</sub> alkanes, alkenes
Alkane 1-monooxygenase (AlkB)	Non – heme di – iron	$C_5$ - $C_{16}$ alkanes, fatty acids, alkylbenzenes, cycloalkanes, etc.
Cytochrome P450 monooxygenase (CYP)	Heme - iron	$C_5$ - $C_{16}$ alkanes, cycloalkanes, alkenes, fatty acids, alkylbenzenes, etc.
Heme – thiolate peroxidases	Heme - iron	$C_3$ - $C_{16}$ alkanes, cycloalkanes alkenes, alkylbenzenes, aromatics, heterocyclic compounds, sulfides
Flavin monooxygenase	Flavins	C <sub>15</sub> - C <sub>36</sub> alkanes, aromatics, alkylbenzenes

The cytochromes P450 monooxygenases (CYPs) are perhaps one of the most versatile enzymes in nature. P450s are heme-iron containing enzymes that catalyze the monooxygenation of various non-activated hydrocarbons using oxygen with high regio-, stereo- and enantioselectivity. Many P450s microbial biotransformations have already been industrialized mainly for steroid and terpenoid hydroxylations  $^{[8, 10]}$ . One example is the enantio- and regioselective  $11\beta$ -hydroxylation of a steroid 17,21-dihydroxypregn-4-ene-3,20-dione (commercialized as Reichstein S) catalyzed by microorganism *Curvularia* sp. for the production of hydrocortisone at a scale of ~100 tons per year by Bayer  $^{[10-11]}$ . Other relevant examples include the conversion of progesterone to cortisone with *Rhizopus* sp. established by Pfizer  $^{[12]}$ , and the production of cholesterol lowering drug pravastatin with *Streptomyces* sp. by Daiichi - Sankyo  $^{[13]}$  and Bristol - Myers Squibb Company  $^{[10, 14]}$ . Lately, promising results have been achieved for the P450 catalyzed oxyfunctionalization of short chain and cyclic alkanes  $^{[2, 4, 15-17]}$ .

The methane monooxygenases (MMOs) have been found in methanotrophic bacteria. The active site of sMMO (soluble MMO) contains two irons, which are connected through two carboxylate-bridges. The pMMOs (particulate MMOs), expressed under copper saturated conditions, have a dicopperbased active site  $^{[1-2]}$ . sMMOs have a broad substrate scope, catalyzing not only methane hydroxylation, but also oxygen insertion into a wide range of  $C_1$ -  $C_8$  alkanes, alkenes, cycloalkanes, ethers and aromatic compounds  $^{[18-19]}$ . Substrate scope of pMMO is limited to alkanes and alkenes with a length up to  $C_5$   $^{[20]}$ . One issue with MMOs is their difficult production due to multicomponent structure (and membrane bound nature in case of pMMO). Although methane oxidation to methanol catalyzed by sMMO proceeds with a relatively high turnover frequency (TF) of 220 min<sup>-1</sup>, in general MMOs suffer from product inhibition and are quite unstable, thus leading to poor productivity  $^{[2]}$ .

Alkane 1- monooxygenases (AlkB) are non – heme di – iron monooxygenases, which have been found within several *n*-alkane degrading bacteria such as *Pseudomonas putida*, *Alcanivorax*, etc. They catalyze terminal hydroxylation of the substrates, generally ranging from pentane to dodecane, and terminal epoxidation of alkenes <sup>[8, 21-22]</sup>. Although reactions are performed with relatively high TF (e.g. 200 min<sup>-1</sup> for octane hydroxylation), AlkBs are not well suited for in vitro applications due to their membrane – bound and multicomponent nature <sup>[2]</sup>.

Within the group of non-heme iron oxygenases, it is also worth mentioning enzymes bearing the 2-His-1-carboxylate facial triad <sup>[23-24]</sup>. These enzymes feature two histidines and one carboxylate ligand, which flank one side of the iron in triangle and play the important role in oxygen activation. The notable examples of these enzymes are mononuclear dioxygenases and aromatic amino acid hydroxylases (AAAHs). AAAHs catalyze the hydroxylation of aromatic rings of amino acids <sup>[23]</sup>. Mononuclear dioxygenases can perform dihydroxylation of aromatics, the cleavage of catechol and hydroperoxidation of lipids <sup>[8, 24]</sup>.

Another important class of oxygenases are the flavin monooxygenases, which are capable of efficient epoxidation, phenol hydroxylation, benzylic hydroxylation and Baeyer–Villiger oxidation <sup>[8]</sup>. Notably, one representative – a long chain alkane monooxygenase, LadA (isolated from thermofilic bacterium *G. thermodenitrificans* NG80-2) enables the selective but slow terminal oxidation of  $C_{15}$  –  $C_{36}$  alkanes <sup>[25]</sup>.

All the above examples are dependent on the nicotinamide cofactors NADH (nicotinamide adenine dinucleotide) or NADPH (nicotinamide adenine dinucleotide phosphate), which play the role of sacrificial reductant for oxygen activation. Moreover, the enzymes usually require electron transfer partners, which are needed to provide reducing equivalents to an enzyme active site. For these reasons, application of isolated enzymes is not straightforward and aforementioned biotransformations are usually performed using whole cells as catalysts. However microbial transformations are not always optimal due to (i) further metabolic degradation of products, (ii) toxicity of (co)-substrates/(co)-products for the cell, (iii) complicated recovery of the product, and (iv) presence of competing enzymatic system, which may impair the purity of the product [8, 26-27]. Therefore, use of isolated enzymes is desirable. In this respect, promising results in the area of aliphatic oxidation have been obtained with natural or man-made self-sufficient P450 monooxygenases, independent of redox partners (vide infra). However, these enzymes remain nicotinamide cofactor dependent and require appropriate cofactor regeneration system for economic reasons (vide infra) [Chapter 5].

The need for а cofactor is circumvented in the case of heme - dependent peroxidases/peroxygenases. The main catalytic property of these enzymes is oxygen transfer from H<sub>2</sub>O<sub>2</sub> or organic peroxides ROOH to a substrate, which is referred to as peroxygenase activity. These enzymes need neither NAD(P)H cofactor nor specific electron transfer partners for function. The most prominent examples, which possess respective activity, are heme-thiolate peroxidases, comprising the Caldariomyces fumago chloroperoxidase (EC 1.11.1.10) and unspecific Arocybe aegerita peroxygenase (EC 1.11.2.1), and atypical P450 fatty acid peroxygenases (EC 1.11.2.4).

#### 2.1. Cytochrome P450 monooxygenases – recent developments

Cytochrome P450 enzymes (CYPs) are heme - containing monooxygenases that are found in all life kingdoms: archaea, bacteria, fungi, plants, and animals <sup>[29]</sup>. They catalyze a broad range of regio-, stereo- and enantioselective reactions as oxidation of non-activated C-H bonds, aromatic hydroxylation, epoxidation of C=C double bonds, N-oxidation, sulfoxidation, deamination, dehalogenation, N-, O- and S – dealkylation <sup>[30]</sup>. These transformations appear in the biosynthesis of fatty acids, steroids, antibiotics; detoxification and clearance of xenobiotics; utilization of primary nutrients <sup>[31]</sup>.

The active site of P450s contains a heme prosthetic group that consists of an iron coordinated by four nitrogen atoms of porphyrin (Figure 1) <sup>[31]</sup>. The heme group is linked to the protein by a cysteine amino acid residue that is covalently ligated to the iron. Most of the P450s use molecular oxygen as an oxidant introducing one oxygen atom into the substrate. In order to promote the reaction P450s require redox equivalents that come from the nicotinamide cofactors NADH or NADPH. The overall reaction catalyzed by P450s is shown in Equation 1, where RH represents the substrate and ROH the resulting monooxygenated product:

P450 monooxygenase
$$RH + O_2 + NAD(P)H + H^+$$

$$ROH + H_2O + NAD(P)^+ (1)$$

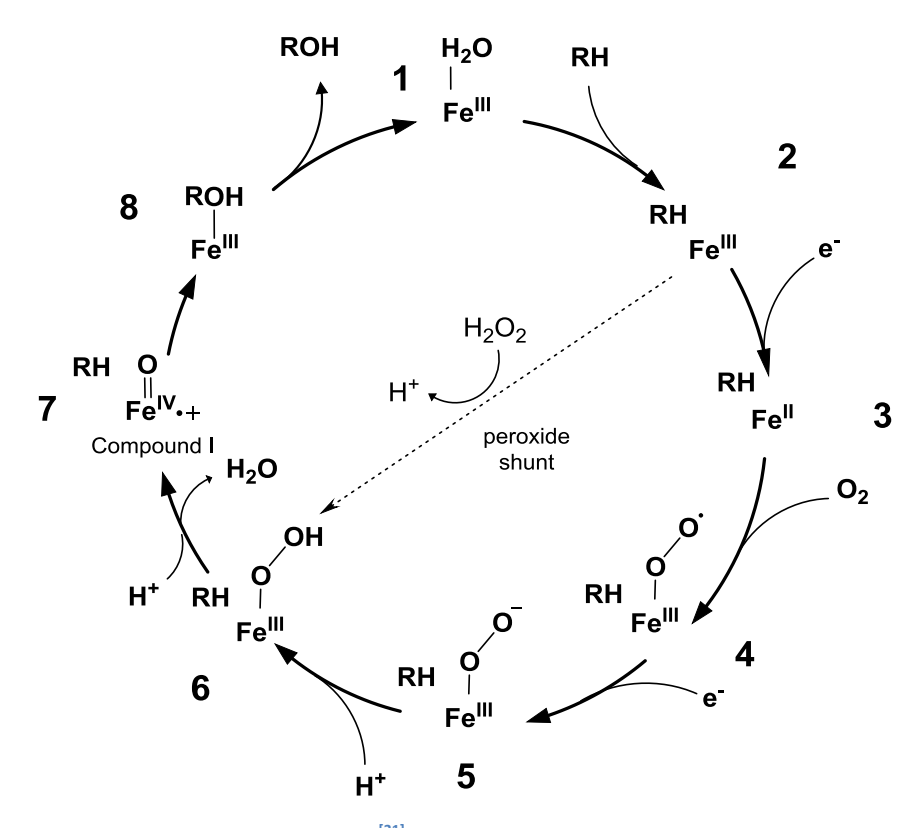
$$OH$$

$$OH$$

$$OH$$

Figure 1. Heme prosthetic group.

The P450 reaction cycle starts by substrate binding and displacement of the distal water ligand from the heme – thiolated group (2) (Scheme 1) [31-32]. Then redox partners supply single electrons to reduce the heme - iron to the ferrous state (3). Next, oxygen binding takes place (4) followed by the reduction to the ferric peroxo state (5). This intermediate is protonated to form ferric hydroperoxo compound (6), which transforms after the second protonation and scission of bound oxygen to the oxo-ferryl state [Fe(IV)=O]<sup>+-</sup> known as a Compound I. Compound I predominantly is present as an iron(IV)oxo porphyrin radical cation with an electron delocalized in the porphyrin ring and on the oxygen [33]. Compound I is the key oxidant that promotes the oxyfunctionalization of the substrate and returns the heme to its ferric state (Scheme 1).

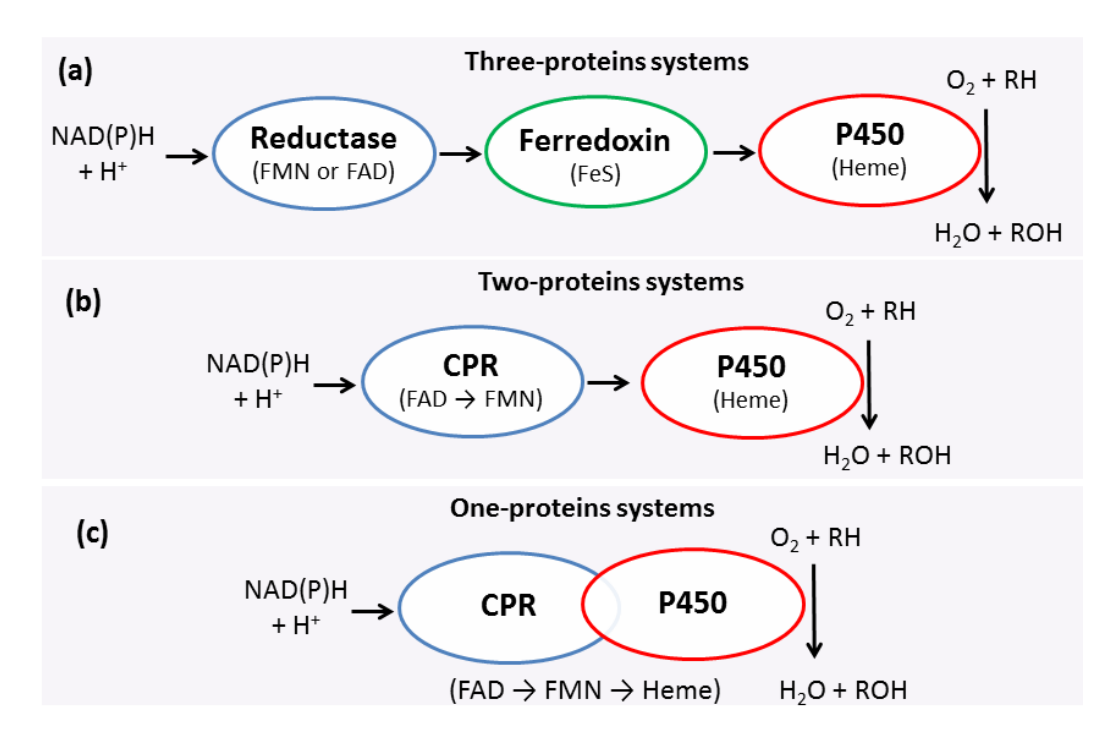


Scheme 1. Catalytic cycle of P450 monooxygenases [31].

P450 catalytic cycle commonly encounters the three major abortive reactions: (i) release of superoxide anion returning enzyme to resting state; (ii) dissociation of coordinated peroxide or hydroperoxide anion yielding  $H_2O_2$ ; and (iii) oxidation of oxo-ferryl species to water instead of oxygenation of the substrate <sup>[31]</sup>. These side reactions are determined as uncoupling. Uncoupling leads to the loss of the reducing equivalents, i.e. the unproductive NAD(P)H oxidation, and the formation of strong oxidative species toxic to a cell/enzyme. Uncoupling is commonly observed in the absence of a substrate or if a substrate does not fit well to active site <sup>[26]</sup>.

As already mentioned, the full reaction mechanism necessitates redox partners to transfer electrons from NAD(P)H to the P450 heme - center. P450 can be classified depending on the type of the redox

partners involved in the catalytic cycle. In class I the redox partners are two distinct proteins: a flavin adenine dinucleotide (FAD) containing protein (reductase) and 2Fe - 2S iron - sulfur protein (ferredoxin) (Scheme 2a) [30]. In class II electrons are transferred via FAD- and FMN- (flavin adenine mononucleotide) containing cytochrome P450 reductase (CPR) (Scheme 2b). Besides, so called self sufficient P450s have been identified, which do not belong neither to Class I or Class II. For example, a naturally fused systems of diflavin reductase (FAD and FMN) and heme via aminoacid linker, which afford efficient internal electron transfer and - high activity (Scheme 2c) [30, 34]. Besides, peculiar P450nor, produced by fungus *Fusarium oxysporum*, proceeds via the direct electron transfer from NADH to the heme group without redox partners [35-36].



Scheme 2. General steps in typical P450 catalyzed reactions. (a) Three-protein systems: P450 and reductase can either be soluble or membrane-bound. (b) Two-protein systems: CPR and P450 are membrane-bound. (c) One-protein systems: soluble or membrane-bound systems formed by fusions of a CPR-like reductase and P450 [30]

Involvement of the redox proteins is one the main limitations for the in vitro use of multicomponent P450s. Therefore, self-sufficient single component enzymes are desirable. One of the best characterized bacterial P450 monooxygenase is CYP102A1 from *Bacillus megaterium* (P450 BM3). P450 BM3 is a natural fusion protein between a monooxygenase and diflavin domain (Scheme 2c), and is easy to handle. Wild type P450 BM3 is a  $C_{12}$ -  $C_{20}$  fatty acid hydroxylase (at  $\omega$ -1 to  $\omega$ -3), which possesses the highest avtivity measured for P450s: hydroxylation of arachidonic acid proceeds with a  $k_{cat}$  value of 17 000 min<sup>-1</sup> [37]. Moreover, the coupling efficiency – electron transfer from NADPH oxidation to the product formation reaches 88-98 % [38].

Many efforts have been undertaken to exploit P450 BM3 activity for alkane oxyfunctionalizations. Thus, the substrate spectrum of P450 BM3 has been evolved from fatty acids to short chain alkanes by protein engineering tools: the large, long, and hydrophobic funnel was shrinked for better interaction with small molecules <sup>[2]</sup>. For example, P450 BM3 variant 139-3 (11 amino acids changes in heme domain) exhibited a higher activity than the WT towards a variety of fatty acid and alkane substrates, including  $C_3$ -  $C_8$  alkanes <sup>[16]</sup>. Remarkably, a TF of 3840 min<sup>-1</sup> was reported for subterminal hexane hydroxylation yielding 3-hexanole as a main product, whereas overoxidation rate did not exceed 5% (Table 2, entry 1) <sup>[16]</sup>. P450 BM3 mutant 139-3 is also capable of benzene, styrene, cyclohexene, hexene and propylene oxidation surpassing the activity of the wild type (between 17-and >100-fold for NADPH oxidation)(Table 2, entries 2 - 3) <sup>[39]</sup>. However, NADPH consumption was only partally coupled towards product formation (14 - 79%).

Table 2. Oxyfunctionalizations catalyzed by self - sufficient P450 monooxygenases.

Entry	Substrate	Catalyst	TTN <sup>a</sup> / TF, min <sup>-1</sup>	Selectivity, %	Ref.
1	n-hexane	P450 BM3 mutant 139-3	n.a. <sup>b</sup> / 3840 <sup>c</sup>	2-hexanole (19 %) 3-hexanole (81 %)	[16]
2	propylene	P450 BM3 mutant 139-3	n.a. / 700 <sup>d</sup>	Propylene oxide (100 %)	[39]
3	cyclohexene	P450 BM3 mutant 139-3	n.a. / 948 <sup>c</sup>	Cyclohexene oxide (85 %) 2-cyclohexene-1-ol (15 %)	[39]
4	propane	P450 BM3 mutant P450 <sub>PMO</sub> R2	45800 /370 <sup>d</sup>	2-propanol (90 %) 1-propanol (10 %)	[40]
5	n-octane	CYP153A	55 / n.a.	1-octanol (91 %)	[2]
6	n-octane	CYP153A13 – red	3000 <sup>f</sup> / n.a.	1-octanol (99 %)	[2]
7	propane	P450 BM3 WT treated by CF <sub>3</sub> (CF <sub>2</sub> ) <sub>9</sub> CO <sub>2</sub> H	1021 / n.a.	2-propanol (>99 %)	[17]
8	methane	P450 BM3 WT treated by CF <sub>3</sub> (CF <sub>2</sub> ) <sub>8</sub> CO <sub>2</sub> H	2500 / n.a.	Methanol (>99 %)	[17]
9	ethylbenzene	P450bsβ in the presence of heptanoic acid	n.a. / 28	(R)-1-phenylethanol ee 68 %	[41]
10	styrene	P450bsβ in the presence of heptanoic acid	n.a. / 290	(S) – styrene oxide (91 %) ee 83 %	[41]

<sup>&</sup>lt;sup>a</sup> Total turnover number calculated as a ratio of mole product produced to mole of enzyme used; <sup>b</sup> n.a. – not available; <sup>c</sup> turnover frequency (mol substrate/min/mol P450); <sup>d</sup> turnover frequency (nmoles NADPH consumed/min/nmoles P450); <sup>e</sup> overoxidation towards cyclohexanone is not reported; <sup>f</sup> By using a NADPH recycling system and in the presence of bovine catalase

In order to improve the coupling effciency, Fasan et al. applied directed evolution on both the heme and reductase domains of P450 BM3 mutant (35 E11 variant), which was previously engineered for ethane and propane hydroxylation. These mutations resulted in an engineered P450<sub>PMO</sub> R2 (propane monooxygenase) variant that is efficient for propane oxidation: the turnover frequency (TF) could be increased from 200 to 370 min<sup>-1</sup>, the total turnover number from 5650 to 45800, and the coupling efficiency from 17 to 98.2% in comparison to the 35 E11 variant (Table 2, entry 4) [40]. This result underlines the importance of high coupling efficiency for the productive P450 catalysis.

The self-sufficient architecture of P450 BM3 inspired researchers to design an artificial single component P450 for regioselective alkane hydroxylation. Natural  $C_5$ - $C_9$  alkane hydroxylases of the CYP153 family (soluble but multicomponent proteins) are at the center of several studies that aim to enhance their efficiency for in vitro applications (Table 2, entry 5) <sup>[2]</sup>. Thus Drone and co-workers created a fusion protein between the hydroxylating domain of alkane hydroxylase CYP153A13a and FMN/Fe<sub>2</sub>S<sub>2</sub> reductase (from self-sufficient P450RhF of *Rhodococcus* sp) <sup>[15]</sup>. The CYP153A13-red monooxygenase showed the highest reported activity for  $\omega$ -hydroxylation of alkanes reaching TN of 3000 in octane oxidation to 1-octanole (Table 2, entry 6) <sup>[2]</sup>.

Alternatively to time and labour demanding protein engeneering, "the substrate misrecognitions approach" was developed in order to achieve the P450 activity on non - natural substrates. In this strategy, the enzyme is treated by different activator molecules initiating the P450 catalytic cycle for further oxidation of a desirable substrate. For example, high activity towards short chain alkanes  $(C_1 - C_8)$  was obtained for the wild-type P450 BM3 using inert perfluorocarboxylic acid to fill the long substrate binding channel but leaving sufficient space for docking of alkane (Table 2, entry 7) [17, 42]. This is the first example of selective methane oxidation towards methanol, catalyzed by P450 enzyme (Table 2, entry 8) [17].

In contrast to most P450s, some atypical P450 peroxygenases (the CYP152 family) originally employ hydrogen peroxide instead of oxygen for oxidation reactions [Chapter 4]. These enzymes act in the so-called hydrogen peroxide shunt pathway utilizing  $H_2O_2$  to generate the Compound I as an active species (Scheme 1) [43]. Therefore, NAD(P)H cofactor and redox partners are not needed in the catalytic cycle, which makes these enzymes attractive for the practical biocatalysis.

P450 peroxygenases include P450s isolated from anaerobic microorganisms *Bacillus subtilis* (P450Bsβ), *Sphingomonas pausimobilis* (P450Sp $\alpha$ ), *Clostridium acetobutylicum* (P450Cl $\alpha$ ). Results of protein sequence and spectral analysis revealed that these enzymes belong to P450s family and they have been given systematic designations CYP152B1 (P450Sp $\alpha$ ), CYP152A1 (P450Bs $\beta$ ) and CYP152A2 (P450Cl $\alpha$ ) [44-46]. As the peroxide shunt is the main catalytic pathway of the CYP152 family, they have

been assigned as P450 peroxygenases rather than monooxygenases (EC 1.11.2.4) . They catalyze hydroxylation of fatty acids and corresponding methylesters at  $\alpha$  - or  $\beta$  - positions with high catalytic turnovers: P450Cl $\alpha$  reaches 200 min<sup>-1</sup> [<sup>44]</sup>, P450Bs $\beta$  - 1000 min<sup>-1</sup> [<sup>47]</sup>, and P450Sp $\alpha$  - 800 min<sup>-1</sup> (measured for myristic acid) [<sup>45]</sup>. The carboxyl group of a fatty acid is located in the proximal position to the heme, thus directing the selectivity to  $\alpha$ - and  $\beta$ - products [<sup>46]</sup>. P450Sp $\alpha$  is 100%  $\alpha$  - selective, whereas P450Cl $\alpha$  and P450Bs $\beta$  produce both  $\alpha$  - and  $\beta$  - hydroxylated fatty acid at the ratios 24:1 and 1:2 ( $\alpha$ :  $\beta$ ) respectively [<sup>44,48]</sup>.

The "substrate misrecognition approach" also has been successfully applied to P450 peroxygenase catalysis. Addition of decoy molecules (bearing carboxylic group) allowed the generation of active species and, therefore, oxidation of non-natural substrates such as guaiacol, styrene, ethylbenzene [41, 49] (Table 2). Furthermore, high enantioselectivity was observed for styrene and ethylbenzene oxidations, suggesting that combination of the decoy molecule and the protein environment may alter the stereoselectivity of the reaction [41, 49].

#### 2.2. Heme – iron thiolate peroxygenases

Heme - iron dependent peroxidases structurally resemble P450s and have the ferriprotoporphyrin IX prosthetic group in common (Figure 1)  $^{[33]}$ . Unlike P450s, peroxidases do not rely on NAD(P)H as cofactor and simply utilize hydrogen peroxide ( $H_2O_2$ ) or organic hydroperoxides (R-OOH) as an oxidant  $^{[33]}$ . The fifth (proximal) ligand of most of the peroxidases is histidine, except for heme-thiolate fungal peroxidases - chloroperoxidase from the ascomycetous fungus *Caldariomyces fumago* (CPO) and aromatic peroxygenase from the basidiomycetous fungus *Agrocybe Aegerita* (*Aae*APO), where the iron is ligated to a cysteine, as in P450s  $^{[50]}$ .

The formation of catalytic active species (Compound I) of peroxidases follows the peroxide shunt pathway (Scheme 1). In the first step the  $H_2O_2$  replaces the water ligand of the ferric protoporphyrin in the active site resulting in a Fe(III) hydroperoxide intermediate. Next, heterolytic cleavage of  $H_2O_2$  occurs, which requires a two-electron transfer from the heme and leads to the formation of iron(IV)oxo porphyrin radical cation (Compound I) and a molecule of water [33, 51].

Reactions catalyzed by peroxidases can be summarized in four classes (Table 3). In the absence of an organic substrate or halide, the catalase reaction is observed: hydrogen peroxide disproportionation to water and oxygen [52-53]. Hydrogen peroxide dismutation usually occurs as a side reaction, whereas other reactions represent synthetic value.

A classical peroxidase reaction (oxidative dehydrogenation, or peroxidative activity) proceeds as one electron transfer oxidation with radical intermediates, particularly of phenolic derivatives or anilines [9, 54-55]. Here, Compound I extracts one electron from the substrate to form a protonated

iron(IV)oxo intermediate called Compound II (Scheme 3). A second electron transfer returns enzyme to the resting state [33]. The resulting radicals (e.g. phenoxy radicals) then can initiate a non enzymatic polymerization.

Table 3. Reactions catalyzed by peroxidases

Reaction type	Example	Ref
1. Oxidative dehydrogenation $2RH + H_2O_2 \rightarrow 2R\cdot + 2H_2O \rightarrow R-R$	2 OH 2H <sub>2</sub> O <sub>2</sub> 4H <sub>2</sub> O O OO	[9, 56]
2. Oxidative halogenation $RH + H_2O_2 + Hal^{-} + H^{+} \rightarrow RHal + 2H_2O$	$H^{+} + CI^{-} + H_{2}O_{2}$ $2H_{2}O$ OH	[57]
3. Oxygen transfer $RH + H_2O_2 \rightarrow ROH + H_2O$	H <sub>2</sub> O <sub>2</sub> H <sub>2</sub> O OH	[58-59]
4. Hydrogen peroxide dismutation $2H_2O_2 \rightarrow O_2 + 2H_2O$		[52-53]

In oxidative halogenation reactions Compound I reacts with halide yielding resting enzyme and hypohalous acid, which acts as a halogenating agent <sup>[51]</sup>. Halogenation occurs with unbound substrate outside of enzyme active site and lacks selectivity, although some vanadium - containing peroxidases are able to catalyze selective halogenation <sup>[60]</sup>.

The oxygen transfer from  $H_2O_2$  or R-OOH to the substrate is the most intriguing property of heme - thiolate peroxidases, which is referred to as peroxygenase activity <sup>[51]</sup>. In an oxygen transfer reaction, the Compound I is reduced to native state via two - electron transfer directly reacting with a substrate (Scheme 1). Heme - thiolate peroxidases showed dramatic differences to all peroxidases with respect to amino - acid sequence, structure (cysteine as 5<sup>th</sup> axial heme ligand) and reactions catalyzed. Due to their unique structure they combine the features of both – P450s (oxygen transfer) and peroxidases (e.g. phenol and halide oxidation) <sup>[50-51]</sup>.

CPO was discovered as a first halogenating enzyme involved in the synthesis of the chlorine containing antibiotic caldariomycin. CPO owes its name thanks to its main catalytic activity - the oxidation of chloride into hypochlorous acid, which further chlorinates organic molecules. Besides, CPO can oxidize bromide, iodide, but not fluoride. In the absence of halides, CPO oxidizes anilines and phenols through peroxidative mechanism (one electron oxidation). Besides, CPO can oxidize primary alcohols to aldehydes [52, 61-62].

CPO was the first discovered heme - thiolate peroxidase, which is able to catalyze oxygen transfer reactions (two electron oxidations), resembling catalytic activity of P450s. Despite similarities in

catalytic properties, the CPO doesn't share any sequence homology with P450s, although molecular architecture - arrangement of  $\alpha$ -helices in tertiary structure shows some similarities <sup>[63]</sup>. Sulfoxidation and indole oxidation are the most efficient oxygen transfer reactions catalyzed by CPO (Table 4, entries 1 - 2), although it is able to promote epoxidation of alkenes as well as benzylic and propargyllic hydroxylations (Table 4, entries 3 - 5) <sup>[33, 50]</sup>. However, oxygen transfer to less activated molecules as alkanes or aromatic rings cannot be catalyzed by CPO <sup>[50]</sup>.

CPO has been an only one heme - thiolate peroxidase characterized for more than 50 years until Hofrichter and co-workers discovered more similar enzymes of this class in the basidiomycetous fungus *Agrocybe Aegerita* (*Aae*APO) <sup>[64]</sup>. Later homologous proteins have been also detected in *Coprinellus radians, Coprinopsis verticillata*, and *Agrocybe alnetorum*, etc. <sup>[51]</sup>. Moreover, several hundred homologous sequences have been identified in genoms of over 20 basidiomycota and over 30 ascomycota encoding putative heme - thiolate peroxidase/peroxygenase <sup>[51]</sup>. Due to the ability to hydroxylate and epoxidize aromatic substrates, these enzymes have been assigned as aromatic peroxygenases (APO), which set them apart from CPO. APOs revealed no homology to classic heme - peroxidases and P450 monooxygenases, and only little homology with CPO (35% similarity in N - terminal moiety; C - terminal part is completely different) <sup>[51]</sup>.

AaeAPO, similarly to CPO, performs one – electron abstractions, brominations (but no chlorinations), and the most interesting – various peroxygenations. In addition to strong hydroxylating activity towards aromatic compounds, AaeAPO possess strong activity for epoxidation and benzylic hydroxylation (Table 4, entries 6 - 9) [Chapter 3], [50-51]. Moreover, it is able to catalyze hydroxylation of fatty acids and alkanes from propane to hexadecane (Table 4, entries 10 - 14). Thus, AaeAPO possess strong activity for the broad range of synthetically valuable oxyfunctionalization reactions with remarkably high specificity.

Preliminary studies show some similarities in structure and several sequence motives of *Aae*APO and CPO enzymes around the active site (heme-thiolate region), but also considerable differences in the heme channel and amino acids in the heme channel <sup>[65]</sup>. The much stronger hydrolylating/oxygenating activity of *Aae*APO than CPO might be due to different positioning of the substrate near the ferryl oxygen of heme or the differences in redox potential of proteins. However the answer is still pending.

Table 4. Oxygen transfer reactions catalyzed by heme – thiolate peroxygenases.

	Substrate	Catalyst	TTN/ TF, min <sup>-1</sup>	Product (Yield, %)	Ref.
1	thioanisole	CPO <sup>a</sup>	250*10 <sup>3</sup> /500	(R) –methyl phenyl sulfoxide (100) ee 99 %	[66]
2	indole	СРО	860*10 <sup>3</sup> / 2000 <sup>b</sup>	Oxindole (100)	[67]
3	cis-2-heptene	СРО	1700 <sup>b</sup> / n.a.	(2 <i>R</i> ,3 <i>S</i> )- epoxide (78) ee 96 %	[68]
4	ethylbenzene	СРО	700/ n.a.	(R)-1-phenylethanol (20) ee 97 %	[58]
5	cis-β-methylstyrene	СРО	1500 <sup>b</sup> / n.a.	(1S,2R)-cis-β-methylstyrene epoxide (67) ee 96 %	[68]
6	ethylbenzene	AaeAPO	43000/ n.a.	1-( <i>R</i> )-phenylethanol ee 99.5 %	[59]
7	toluene	AaeAPO	58570/ 5860 <sup>b</sup>	Benzyl alcohol (37); Benzaldehyde (12); Benzoic acid (4); p-cresol (2); o-cresol (4); Methyl-p-benzoquinone (23)	[69]
8	cis-β-methylstyrene	<i>Aae</i> APO	110 000/ n.a.	(1 <i>R</i> ,2 <i>S</i> )-cis-β-methylstyrene oxide ee 99%	[59]
9	naphthalene	AaeAPO	4760/950 <sup>b</sup>	1-naphthol (64) 2-naphthol (1.9) 1,4-naphthoquinone (1.3)	[69]
10	cyclohexane	AaeAPO	4500/ 75 <sup>b</sup>	cyclohexanol (99) cyclohexanone (1)	[70]
11	propane	AaeAPO	959/ n.a.	2-propanol (100)	[70]
12	n-butane	AaeAPO	1200/ n.a.	2-butanol (100); ee 31% (S)	[70]
13	Heptane	AaeAPO	1434/ n.a.	2-heptanol (60.5; ee 62.2 <i>R</i> ) 3-heptanol (39.5; ee 99.9 <i>R</i> ) ketones (3%)	[70]
14	myristic acid (C <sub>14</sub> )	AaeAPO	6700/ 56 <sup>b</sup>	$(\omega$ -1)-hydroxymyristic acid (34) $(\omega$ -2)- hydroxymyristic acid (30) $(\omega$ -1)-ketomyristic acid (21) <sup>c</sup>	[71]

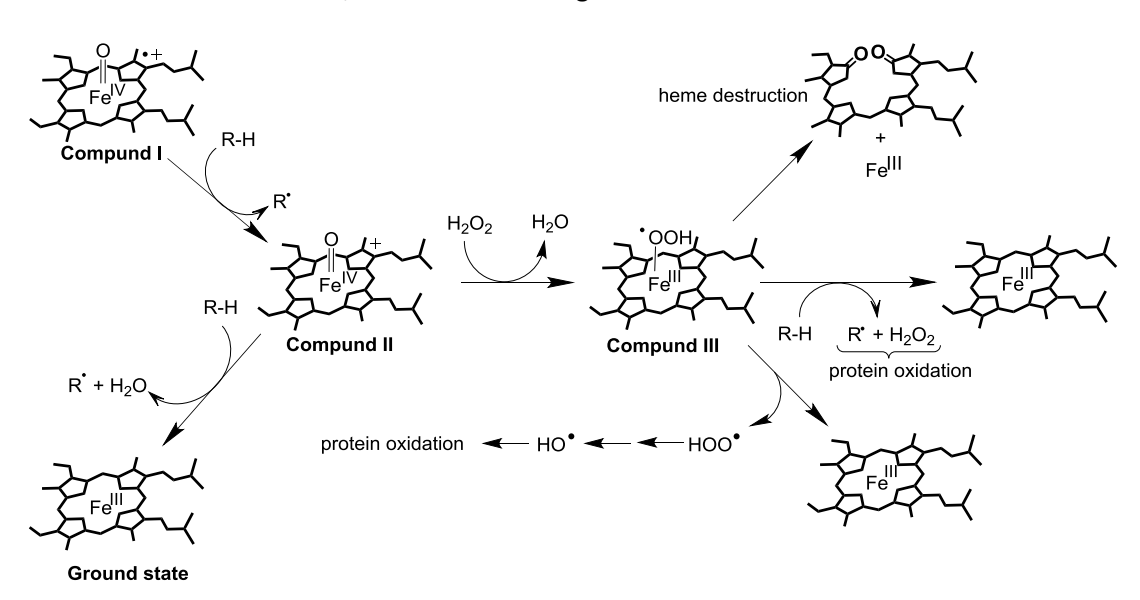
 $<sup>^{</sup>a}$  CPO coimmobilized with glucose oxidase into polyurethane foams;  $^{b}$  Calculated from available data;  $^{c}$  traces of ( $\omega$ -2)-ketomyristic acid, dihydroxylated compounds and several combinations of keto- and hydroxyl- derivatives also have been identified

#### 3. The challenges of the enzymatic oxyfunctionalizations

#### 3.1. Inactivation by $H_2O_2$

Despite of the great potential of the heme-dependent peroxygenases, their present practical application is limited by the low stability even in the presence of catalytic amount of  $H_2O_2$ . The mechanism of inactivation is still under debate. Particularly, in the absence of reducing substrates (RH) or when exposed to high concentration of  $H_2O_2$ , Compound I can react with  $H_2O_2$  in a catalase-like two-electron reduction yielding molecular oxygen (Table 3), or in a two single electron transfers generating so-called Compound II. During two single electron reductions of Compound I, various activated oxygen species can be formed, e.g. superoxide anion or hydroxyl radicals. Heme enzymes are susceptible to oxidative destruction of the porphyrin ring by the activated oxygen species (Scheme 3) [72-75]. Vanadium peroxidases, which have a vanadate as prosthetic group, are more stable towards oxidative destruction as they do not contain a porphyrin ring [76]. These vanadium peroxidases are mainly isolated from marine environment, e.g. bromoperoxidase from seaweed *Ascophyllum nodosum* [76-77].

Another inactivation pathway of heme - peroxidases is the formation of Compound III. Compound III can be formed by adding an excess of  $H_2O_2$  to either Compound II or native enzyme (Scheme 3) <sup>[73]</sup>. Once formed Compound III can follow three degradation pathways: (i) the bound peroxyl radical of Compound III can oxidize porphyrin moiety leading to formation of an open-chain tetra-pyrrole structure and the release of heme iron; (ii) it can oxidize surrounding protein residue or react with a substrate molecule returning enzyme to the ground state; (iii) it can decay liberating reactive oxygen species, e.g. peroxyl or hydroxyl radicals. These radicals may lead to radical chain reaction forming amino acid - based free radicals, which can further generate intermolecular crosslinks <sup>[73]</sup>.



Scheme 3. Alternative inactivation pathways from Compound III intermediate [73].

Different ways to circumvent oxidative inactivation have been proposed. (1) The stability of enzymes can be improved by using less reactive organic peroxides, such as cumene - and tert - butyl hydroperoxide instead of  $H_2O_2$  [33, 78]. (2) Addition of free - radical scavengers, such as tert - butyl alcohol, vitamin C, A and E, mannitol, have been also widely applied [43, 79-80]. (3) Protein engineering in most cases have been applied to alter the catalytic activity of the enzymes rather than stability [73, 79, 81-82]. However, in some cases the stability towards  $H_2O_2$  also could be improved by targeting the amino acids susceptible to oxidation by  $H_2O_2$  [73].

- (4) Various enzyme immobilization techniques showed significant improvement in enzymes stability towards  $H_2O_2$  [66, 83-85]. For example, stability of CPO towards an oxidant could be enhanced by CPO immobilization on silica gel: immobilized CPO retained >20% of its activity in the presence of 10 mM tert-butyl hydroperoxide after 4 hours, while the soluble CPO was completely inactive after 2 hours [86].
- (5) Alternative approaches comprise different methods for regulation of hydrogen peroxide concentration. Thus, the stability of CPO has been significantly improved by stepwise or sensor-controlled addition of hydrogen peroxide [67, 74]. Furthermore, positive results have been obtained by using in situ production of hydrogen peroxide by various methods (Table 5) [Chapter 2,3].

Table 5. CPO - catalyzed sulfoxidation of thioanisole using different H<sub>2</sub>O<sub>2</sub> generation/ -dosage methods.

H <sub>2</sub> O <sub>2</sub> generation method	TTN (CPO)	ee, %	Ref.
Stoichiometric H <sub>2</sub> O <sub>2</sub>	4 900	99	[87]
Sensor – controlled	148 000	n.d.	[33]
Glucose oxidase/glucose/O <sub>2</sub>	250 000	99	[66]
Cathode/ O <sub>2</sub>	58 900	93	[88]
Flavin/ EDTA/ hv/ O <sub>2</sub>	22 400	99	[87]

#### 3.2. Cofactor dependency

Oxidations can be performed by isolated enzymes or whole cells. However, the application of isolated oxygenases for the large - scale synthesis has been hindered by many obstacles including multicomponent architecture of the enzymes and their dependency on the reduced nicotinamide cofactors NAD(P)H providing the reducing equivalents needed for the catalysis [8, 30, 89-90],[Chapter 5,6].

Considering the disadvantages of whole cells catalysis (vide supra), significant efforts have been devoted to establish the processes using isolated P450 enzymes in combination with NAD(P)H supply. However, stoichiometric use of NAD(P)H is not feasible due to its high cost [Chapter 5]. Therefore, for preparative applications NAD(P)H cofactors are usually supplied in the catalytic

amount and continuously regenerated in the reaction media. Up - to - date cofactor regeneration is widely achieved by addition of a second enzyme and a co-substrate (enzyme - coupled reaction system) <sup>[9, 91]</sup>. For example, formate dehydrogenase or glucose dehydrogenase have been extensively applied using formate and glucose as co-substrates respectively <sup>[91-92]</sup>. In addition, the chemical and electrochemical NAD(P)H recycling systems have been investigated intensively <sup>[93-95]</sup>. These regeneration techniques will be discussed in detail in Chapters 5 and 6.

In addition, alternative to NAD(P)H electron sources have been evaluated, such as ascorbic acid, sodium dithionite, and electrochemical means <sup>[96-99]</sup>. However, conversions and initial rates of such systems are much lower than with natural NAD(P)H cofactors. NAD(P)H cofactors can also be substituted by their biomimetic analogs bearing nicotinamide ring required as the redox active site. The development of NAD(P)H - mimics for oxidoreductases catalysis is gaining more attention due to their economic benefits, easy synthesis and high stability <sup>[100-102]</sup>. For example, biomimetic NAD(P)H analogs N-Benzyl-1,4-dihydronicotinamide could substitute the natural NADH for catalysis of P450cam <sup>[103]</sup>.

The great potential of P450s could be also realized via a peroxide shunt pathway completely circumventing the involvement of NAD(P)H (Scheme 1). Generally, under anaerobic conditions ancient prokaryotic P450s may have functioned as peroxidases/peroxygenases [43]. Thus, several reactions have been performed using alkyl peroxides, peracids, sodium chlorite, sodium periodate, and iodosylbenzene as oxidants [104]. For example, the thermofilic archaeal CYP119 from *Sulfolobus acidocaldarius* catalyzes the hydroxylation of laurate, and epoxidation of cis - stilbene and styrene in the presence of  $H_2O_2$ , *tert*-butyl hydroperoxide or *m*-chloroperoxybenzoic acid [43].

Although the shunt pathway was mostly applied for mechanistic studies, some progress using  $H_2O_2$  has been achieved in combination with protein engineering [105-106]. For example, wild-type P450BM3 performed only few turnovers prior to inactivation using  $H_2O_2$  for hydroxylation of fatty acids, whereas the fifth generation mutant 21B3 accepted  $H_2O_2$  and catalyzed hydroxylation without the use of NADPH [106]. The turnover rates and final productivities are generally much lower when using  $H_2O_2$  as oxidant [82]. E.g. the mutant 21B3 achieved a TOF of 50 min<sup>-1</sup> for lauric acid hydroxylation and final turnovers 280, whereas typically P450 BM3 catalyzes the fatty acid hydroxylation with turnover frequencies up to few thousands per minute [37]. Nonetheless, the peroxide shunt pathway represents an important step towards synthetic potential of P450s enzymes in vitro.

#### 3.3. Substrate supply and product removal

One of the major limitations of the enzymatic oxyfunctionalizations is the low solubility of organic substrates in the aqueous media, which leads to high reaction volumes and complicated product

purification. Moreover, (co)-substrates / (co)-products often inhibit enzymes <sup>[Chapter 6]</sup> or cell growth in case of whole cells catalysis <sup>[89, 107]</sup>. Organic co-solvents or ionic liquids are widely used to increase the solubility of hydrophobic substrates <sup>[108-112]</sup>. They can be applied as (a) co-solvents with water; (b) as a second organic phase in water-organic biphasic system; (c) alone as non-aqueous solvents.

Although water-miscible co-solvents are widely applied, high solvent concentrations (that are necessary to achieve high substrate concentrations) often lead to enzyme inactivation and denaturation [113-114]. Moreover, the use of co-solvents does not solve the problem of enzyme inhibition by high concentrations of (co)-substrate or (by)-product.

The situation is different, when water immiscible or poorly miscible organic solvents (or ionic liquids) are used. In this case, the system consists of two phases – aqueous and organic, assuring that the concentration of the solvent in the aqueous phase remains low. Therefore inactivating and denaturing effects are much lower than those induced by hydrophilic co - solvents. The aqueous phase contains enzymes or cell and cofactors, whereas organic solvent contains the hydrophobic organic substrates <sup>[9, 115], [Chapters 2-3, 5-6].</sup> On shaking or gentle stirring, the substrate partitions between the organic and aqueous phase, where biotransformation occurs, and product partitions back to organic phase. This simple method simultaneously solves problems of substrate supply and enzyme inhibition/inactivation by (co)substrate/(by)product, as their concentration remains very low in aqueous phase. Biphasic systems require smaller reaction volumes and facilitate product recovery. If needed, the cofactor regeneration system can be also applied under these conditions <sup>[Chapters 5, 6]</sup>. For example, cyclohexane hydroxylation was established in a biphasic system (cyclohexane/buffer) using the mutant of P450 BM3 coupled with FDH catalyzed NAD(P)H regeneration system. Promising results were obtained revealing 12850 of TTN for double mutant R47L/Y51F and 330 for NADPH <sup>[116]</sup>.

Non - aqueous or low water-content systems are not so common for oxyfunctionalizations and only few examples have been reported <sup>[117-119]</sup>. For example, thioanisole oxidation catalyzed by horseradish peroxidase was 10 to 100 folds faster in isopropyl alcohol or methanol than in aqueous solution <sup>[117]</sup>. Selective oxidation of indole and thioanisole could be catalyzed by immobilized CPO in a range of organic solvents using *tert*-butyl hydroperoxide as an oxidant <sup>[120]</sup>. Indole oxidation catalyzed by CPO immobilized in polyurethane foam proceeded with TF of approx. 260 min<sup>-1</sup> in isooctane or n-hexane and resulted TTN up to 20000 <sup>[120]</sup>. However, the enzyme activity and overall productivity of these reactions are lower than in aqueous solutions.

#### 4. Potential applications

The number of commercial biocatalytic C-H oxyfunctionalizations is slowly growing, especially for the syntheses that are inaccessible by chemical methods <sup>[2, 4, 30]</sup>. E.g., many microbial biotransformations

are already established in pharmaceutical industry, where chemo-, regio- and stereoselectivity are of great importance <sup>[8, 27, 121]</sup>. However, general exploitation of the isolated enzymes is hampered by their multicomponent structure, NAD(P)H cofactor dependency and poor stability. For these reasons, industrial P450 - based oxyfunctionalizations are based on whole cell catalysis, which is not always optimal due to reagent toxicity, low NAD(P)H regeneration rates, and high oxygen consumption by endogenous cell respiration <sup>[8, 27]</sup>.

Protein engineering has played a major role towards adapting and modulating the reactivity of P450s for non-natural substrates as well as creating self-sufficient P450s systems. Other strategies, such as the use of activator molecules to alter P450s selectivity, provide an alternative or synergetic tool for synthetic applications. Recent results showed the great potential of P450s catalysis not only towards selective oxyfunctionalizations of the complex biomolecules, but also for short chain and cyclic alkanes/ alkenes (Table 2). However, these transformations have to become more efficient in terms of productivity in order to lead to an industrial process.

The recently discovered *Aae*APO peroxygenase, represents a promising complimentary tool to P450s for specific C-H oxyfunctionalizations. *Aae*APO is a naturally occurring single component protein, independent of NAD(P)H cofactor and quite stable in broad range of solvents <sup>[70]</sup>. Moreover, *Aae*APO possesses a remarkable activity towards oxyfunctionalizations of activated and non - activated C-H bonds and can be directly applied without demanding techniques of protein engineering (Table 4). To date, *Aae*APO is closest to be the ideal selective biocatalyst for hydroxylation and epoxidation reactions, although its production has not been commercialized yet <sup>[Chapter 3]</sup>.

Biocatalytic oxyfunctionalizations are also attractive from an environmental point of view. In general, biocatalytic processes are considered ecologically advantageous over catalytic processes due to the use of lower temperatures and pressures combined with higher selectivity of the process. Furthermore, biocatalytic oxyfunctionalizations utilize "green" oxidants such as  $H_2O_2$  or oxygen that lead to formation of water as by-product. In comparison, asymmetric catalytic oxidations that are widely applied in industry, usually rely on stoichiometric oxidants such as hypochlorite (Jacobsen's asymmetric epoxidation with (salen)manganese(III) as catalyst) and organic peroxides (Sharpless asymmetric epoxidation with titanium tartrate complex as catalyst) [122].

However, every new bioprocess cannot be taken as more sustainable than existing processes a priori and has to be proven in each individual case. To compare alternative chemical processes Sheldon introduced the concept of E - factor (kg by-products/ kg product) and environmental quotient (EQ), which is obtained by multiplying the E - factor by the arbitrarily chosen unfriendliness quotient Q [123-125]. For example, innocuous salts such as NaCl can be assigned as a Q value of 1, whereas heavy

metal salts, e.g. chromium, can be given a value of 100 or 1000, depending on toxicity. Hence, alternative processes can be compared not solely on the amount of wastes generated, but also on the nature of the wastes.

For example, Friedrich et al performed the ecological assessment for production of (R)-1-phenylethanol using AaeAPO in comparison to: (1) a modern chemical process producing racemic 1-phenylethanol from acetophenone using a titanium catalyst [126] with subsequent enzymatic dynamic kinetic resolution with lipase [127]; and (2) whole-cell procedure using genetically modified E.coli cells and acetophenone as a substrate [128].

This ecological evaluation, expressed as a potential environmental impact (PEI) for production of 1 kg of the product, has been performed using the software *Sabento*. PEI takes into account both the amount of substances used in the synthesis and the nature of the substances. Thus, each substance used in the synthesis assigned in the *Sabento* by corresponding environmental factor (EF), estimated by 14 different impact categories (IC), such as raw material availability, toxicity, global warming potential, acidification potential etc. Each IC has corresponding weighting coefficient, e.g. global warming potential assigned as 100, wherein acidification potential — as 66. Furthermore, for each individual substance mass index (MI) is determined that indicates how much substance (kg) is used per kg of product. Thereafter, PEI can be obtained by multiplying MI (mass index) of each substance by an environmental factor (EF) of a substance (PEI = MI\*EF) [128-129].

During process development the AaeAPO – catalyzed process has been systematically improved with respect to ecological performance (Table 6, entries 1-2):

(1) The content of acetonitrile used as co-solvent was reduced from 25 % to 3 % (v/v) as this compound was shown to possess the most adverse effect in the assessment, expressed as the highest PEI. (2) By the continuous extraction of the products the amount of solvent could be reduced to 50% compared to single product extraction. (3) Initially the by-product acetophenone was removed by derivatization, and the product was separated from the reactant by distillation. In the final procedure the energy consuming distillation was replaced by column chromatography.

Although the product recovery of the revised process was slightly decreased due to the shortening of the reaction time, but simultaneously, the amount of the undesired by-product acetophenone was reduced to less than one-third. Analysis of the wastes revealed that acetonitrile has the highest effect on PEI, despite of drastically reduced amounts and being recycled. All other substances used in the process contribute only marginally to PEI of the revised peroxygenase process. Nevertheless, optimized *Aae*APO-catalyzed process reached the best environmental impact number in comparison

with modern chemical and biotechnological processes (Table 6). Thus, biocatalytic *Aae*APO-catalyzed C-H oxyfunctionalizations are attractive from a synthetic and environmental point of view.

Table 6. Comparison of different procedures for the preparation of (R)-1-phenylethanol with regard to recovery rate (in relation to reactant) and ecological performance, expressed as potential environmental impact (PEI) value determined with Sabento [128].

Entry	Procedure	Recovery rate, %	PEI
1	Primary AaeAPO process	63	14431
2	Revised AaeAPO process	48	832
3	Chemical process with subsequent lipase-catalyzed dynamic kinetic resolution	64	7260
4	Microbial process using <i>E.coli</i> strain BL21(DE)/AW-9	56	1489

In conclusion, it can be stated that the potential of biocatalytic oxyfucntionalizations is immense. The potential of biocatalytic oxyfunctionalizations is definitely recognized by industry, as evidenced by an increasing amount of industrial - academic projects such as Peroxicat <sup>[130]</sup>, INDOX <sup>[131]</sup>. P450s catalyzed systems already have proven their value in the pharmaceutical industry <sup>[27, 132]</sup>. Further studies on *Aae*APO catalyzed processes may lead towards commercial applications in the pharmaceutical and the fine chemical industry. Furthermore, the optimization of P450/*Aae*APO activity towards short chain and cyclic alkane/ alkenes might be of great importance for the petrochemical industry. In this respect, future research needs to focus on further improvement of the reactions productivities through combined enzyme, cell, reaction, and process engineering.

#### Research aim

Aim of this thesis is to setup robust and scalable biocatalytic oxyfunctionalizations using heme - dependent peroxygenases. Although heme - dependent enzymes have great potential for organic synthesis, most of the processes still have to be optimized in terms of productivity for synthetic applications. However, most studies so far had mainly focused on substrate scope, neglecting stability issues which represent the major bottleneck en route to practical application. My PhD project aims at designing stable peroxygenase - based oxyfunctionalization processes. Particularly, the focus is on optimized in situ provision of  $H_2O_2$  to minimize enzyme inactivation. Eventually the practical applicability of the optimized setup is demonstrated at preparative - scale biotransformations using two liquid phase approach. A second major theme of the project deals with NAD(P)H cofactor regeneration. Two novel regeneration approaches are established, characterized, and eventually scaled - up.

#### Thesis outline

**Chapters 2, 3, 4** deal with various oxyfunctionalizations catalyzed by heme-dependent peroxygenases. To avoid the chemical degradation of the enzymes we have developed two alternative catalytic approaches for the controlled in situ  $H_2O_2$  generation from  $O_2$ . General applicability of the proposed in situ generation of  $H_2O_2$  method has been demonstrated for different peroxygenase - catalyzed biotransformations.

In *Chapter 2* a novel, photocatalytic approach for in situ  $H_2O_2$  generation has been established and applied for the CPO catalyzed sulfoxidation in two liquid phase system (2 LPS). The results in both aqueous and 2 LPS are compared. Main limitations of 2 LPS approach and possible solutions have been discussed.

In *Chapter 3* the photocatalytic approach for in situ  $H_2O_2$  generation has been combined with *Aae*APO catalyzed epoxidation and hydroxylation reactions of various substrates. Photoenzymatic oxyfunctionalization of several substrates were performed in 2 LPS and compared to biotransformations in the aqueous system. Possibilities to improve environmental impact of photocatalytic approach have been discussed.

Chapter 4 refers to the specific  $\alpha$ - or  $\beta$ -hydroxylation of fatty acid catalyzed by the cytochrome P450 peroxygenases P450Bs $\beta$  (CYP152A1) from *Bacillus subtilis* and P450Cl $\alpha$  (CYP152A2) from *Clostridium acetobutylicum*. To avoid oxidative degradation of the peroxygenases by H<sub>2</sub>O<sub>2</sub>, an alternative in situ H<sub>2</sub>O<sub>2</sub> generation method has been developed using a biomimetic nicotinamide cofactor and flavin.

Chapter 5, 6 are addressed to issues of NADH cofactor regeneration.

**Chapter 5** has been addressed to the issues of mutual inactivation between enzymes and organometallic complexes used for NADH regeneration. To overcome this issue, organometallic complexes were encapsulated into protein scaffold resulting an artificial metalloenzyme. Novel NADH regeneration approach using an artificial metalloenzyme has been established and coupled to 2-hydrohybiphenyl 3-monooxygenase (HbpA). Furthermore, the reaction has been applied in 2 LPS to obtain higher productivities

In *Chapter 6* hydrophobic formic acid esters have been established as alternative co-substrates for the formate dehydrogenase (FDH)-catalyzed regeneration of NADH. Octyl formate was demonstrated to serve as organic phase solubilizing hydrophobic reagents as well as serving as a source of reducing equivalents to enable FDH-catalyzed regeneration of NADH. This system was used to drive a HbpA-catalyzed hydroxylation reaction.

#### References

- [1] R. Sheldon, I. W. C. E. Arends, U. Hanefeld, Green Chemistry and Catalysis, *Wiley-VCH Verlag GmbH & Co. KGaA*, **2007**
- [2] M. Bordeaux, A. Galarneau, J. Drone, Catalytic, Mild, and Selective Oxyfunctionalization of Linear Alkanes: Current Challenges, *Angew. Chem. Int. Ed.*, **2012**, *51*, 10712-10723.
- [3] H. A. Wittcoff, B. G. Reuben, J. S. Plotkin, Industrial organic chemicals, 2nd ed., *John Wiley & Sons, Inc.*, **2004**
- [4] E. Roduner, W. Kaim, B. Sarkar, V. B. Urlacher, J. Pleiss, R. Glaser, W. D. Einicke, G. A. Sprenger, U. Beifuss, E. Klemm, C. Liebner, H. Hieronymus, S. F. Hsu, B. Plietker, S. Laschat, Selective Catalytic Oxidation of C-H Bonds with Molecular Oxygen, *ChemCatChem*, **2013**, *5*, 82-112.
- [5] Q. Liu, C. Guo, Theoretical studies and industrial applications of oxidative activation of inert C-H bond by metalloporphyrin-based biomimetic catalysis, *Sci. China Chem.*, 2012, 55, 2036-2053.
- [6] J. C. Lewis, P. S. Coelho, F. H. Arnold, Enzymatic functionalization of carbon-hydrogen bonds, *Chem. Soc. Rev.*, **2011**, *40*, 2003-2021.
- [7] H. G. Kulla, Enzymatic hydroxylations in industrial application, *Chimia*, **1991**, *45*, 81-85.
- [8] F. Hollmann, I. Arends, K. Buehler, A. Schallmey, B. Buhler, Enzyme-mediated oxidations for the chemist, *Green Chem.*, **2011**, *13*, 226-265.
- [9] D. Monti, G. Ottolina, G. Carrea, S. Riva, Redox Reactions Catalyzed by Isolated Enzymes, *Chem. Rev.*, **2011**, *111*, 4111-4140.
- [10] V. B. Urlacher, S. Eiben, Cytochrome P450 monooxygenases: perspectives for synthetic application, *Trends Biotechnol.*, **2006**, *24*, 324-330.
- [11] <a href="http://www.bayerpharma.com/en/index.php">http://www.bayerpharma.com/en/index.php</a>
- [12] http://www.pfizer.com/
- [13] http://www.daiichisankyo.com/
- [14] <a href="http://www.bms.com/pages/default.aspx">http://www.bms.com/pages/default.aspx</a>
- [15] M. Bordeaux, A. Galarneau, F. Fajula, J. Drone, A Regioselective Biocatalyst for Alkane Activation under Mild Conditions, *Angew. Chem. Int. Ed.*, **2011**, *50*, 2075-2079.
- [16] A. Glieder, E. T. Farinas, F. H. Arnold, Laboratory evolution of a soluble, self-sufficient, highly active alkane hydroxylase, *Nat. Biotechnol.*, **2002**, *20*, 1135-1139.
- [17] F. E. Zilly, J. P. Acevedo, W. Augustyniak, A. Deege, U. W. Hausig, M. T. Reetz, Tuning a P450 Enzyme for Methane Oxidation, *Angew. Chem. Int. Ed.*, **2011**, *50*, 2720-2724.
- [18] J. Beilen, E. Funhoff, Alkane hydroxylases involved in microbial alkane degradation, *Appl. Microbiol. Biotechnol.*, **2007**, *74*, 13-21.
- [19] J. Green, H. Dalton, Substrate specificity of soluble methane monooxygenase. Mechanistic implications, *J. Biol. Chem.*, **1989**, *264*, 17698-17703.
- [20] J. B. v. Beilen, E. G. Funhoff, Expanding the alkane oxygenase toolbox: new enzymes and applications, *Curr. Opin. Biotechnol.*, **2005**, *16*, 308-314.
- [21] H. Alonso, A. Roujeinikova, Characterization and two-dimensional crystallization of membrane component AlkB of the medium-chain alkane hydroxylase system from Pseudomonas putida GPo1, *Appl. Environ. Microbiol.*, **2012**, *78*, 7946-7953.

- [22] T. Fujii, T. Narikawa, K. Takeda, J. Kato, Biotransformation of various alkanes using the Escherichia coli expressing an alkane hydroxylase system from Gordonia sp. TF6., *Biosci. Biotechnol. Biochem.*, **2004**, *68*, 2171-2177.
- [23] M. M. Abu-Omar, A. Loaiza, N. Hontzeas, Reaction mechanisms of mononuclear non-heme iron oxygenases, *Chem. Rev.*, **2005**, *105*, 2227-2252.
- [24] E. L. Hegg, L. Que, Jr., The 2-His-1-carboxylate facial triad--an emerging structural motif in mononuclear non-heme iron(II) enzymes, *European journal of biochemistry / FEBS*, **1997**, *250*, 625-629.
- [25] L. Li, X. Liu, W. Yang, F. Xu, W. Wang, L. Feng, M. Bartlam, L. Wang, Z. Rao, Crystal Structure of Long-Chain Alkane Monooxygenase (LadA) in Complex with Coenzyme FMN: Unveiling the Long-Chain Alkane Hydroxylase, *J. Mol. Biol.*, **2008**, *376*, 453-465.
- [26] J. B. van Beilen, W. A. Duetz, A. Schmid, B. Witholt, Practical issues in the application of oxygenases, *Trends Biotechnol.*, **2003**, *21*, 170-177.
- [27] M. K. Julsing, S. Cornelissen, B. Bühler, A. Schmid, Heme-iron oxygenases: powerful industrial biocatalysts?, *Curr. Opin. Chem. Biol.*, **2008**, *12*, 177-186.
- [28] <a href="http://www.chem.gmul.ac.uk/iubmb/enzyme/">http://www.chem.gmul.ac.uk/iubmb/enzyme/</a>
- [29] I. G. Denisov, D. J. Frank, S. G. Sligar, Cooperative properties of cytochromes P450, *Pharmacol. Ther.*, **2009**, *124*, 151-167.
- [30] V. B. Urlacher, M. Girhard, Cytochrome P450 monooxygenases: an update on perspectives for synthetic application, *Trends Biotechnol.*, **2012**, *30*, 26-36.
- [31] I. G. Denisov, T. M. Makris, S. G. Sligar, I. Schlichting, Structure and chemistry of cytochrome P450, *Chem. Rev.*, **2005**, *105*, 2253-2277.
- [32] A. W. Munro, H. M. Girvan, A. E. Mason, A. J. Dunford, K. J. McLean, What makes a P450 tick?, *Trends Biochem. Sci.*, **2013**, *38*, 140-150.
- [33] F. Van Rantwijk, R. A. Sheldon, Selective oxygen transfer catalysed by heme peroxidases: Synthetic and mechanistic aspects, *Curr. Opin. Biotechnol.*, **2000**, *11*, 554-564.
- [34] S. J. Sadeghi, G. Gilardi, Chimeric P450 enzymes: Activity of artificial redox fusions driven by different reductases for biotechnological applications, *Biotechnol. Appl. Biochem.*, **2013**, *60*, 102-110.
- [35] R. Oshima, S. Fushinobu, F. Su, L. Zhang, N. Takaya, H. Shoun, Structural Evidence for Direct Hydride Transfer from NADH to Cytochrome P450nor, *J. Mol. Biol.*, **2004**, *342*, 207-217.
- [36] K. Nakahara, T. Tanimoto, K. Hatano, K. Usuda, H. Shoun, Cytochrome P-450 55A1 (P-450dNIR) acts as nitric oxide reductase employing NADH as the direct electron donor, *The Journal of biological chemistry*, 1993, 268, 8350-8355.
- [37] M. A. Noble, C. S. Miles, S. K. Chapman, D. A. Lysek, A. C. Mackay, G. A. Reid, R. P. Hanzlik, A. W. Munro, Roles of key active-site residues in flavocytochrome P450 BM3, *Biochem. J.*, 1999, 339, 371-379.
- [38] R. Fasan, Tuning P450 Enzymes as Oxidation Catalysts, ACS Catalysis, 2012, 2, 647-666.
- [39] E. T. Farinas, M. Alcalde, F. Arnold, Alkene epoxidation catalyzed by cytochrome P450 BM-3 139-3, *Tetrahedron*, **2004**, *60*, 525-528.
- [40] R. Fasan, M. M. Chen, N. C. Crook, F. H. Arnold, Engineered Alkane-Hydroxylating Cytochrome P450BM3 Exhibiting Nativelike Catalytic Properties, *Angew. Chem. Int. Ed.*, **2007**, *46*, 8414-8418.

- [41] O. Shoji, T. Fujishiro, H. Nakajima, M. Kim, S. Nagano, Y. Shiro, Y. Watanabe, Hydrogen Peroxide Dependent Monooxygenations by Tricking the Substrate Recognition of Cytochrome P450BSβ, *Angew. Chem.*, **2007**, *119*, 3730-3733.
- [42] N. Kawakami, O. Shoji, Y. Watanabe, Use of Perfluorocarboxylic Acids To Trick Cytochrome P450BM3 into Initiating the Hydroxylation of Gaseous Alkanes, *Angew. Chem. Int. Ed.*, **2011**, 50, 5315-5318.
- [43] E. G. Hrycay, S. M. Bandiera, The monooxygenase, peroxidase, and peroxygenase properties of cytochrome P450, *Arch. Biochem. Biophys.*, **2012**, *522*, 71-89.
- [44] M. Girhard, S. Schuster, M. Dietrich, P. Durre, V. B. Urlacher, Cytochrome P450 monooxygenase from Clostridium acetobutylicum: A new alpha-fatty acid hydroxylase, *Biochem. Biophys. Res. Commun.*, **2007**, *362*, 114-119.
- [45] I. Matsunaga, N. Yokotani, O. Gotoh, E. Kusunose, M. Yamada, K. Ichihara, Molecular cloning and expression of fatty acid alpha-hydroxylase from Sphingomonas paucimobilis, *The Journal of biological chemistry*, **1997**, *272*, 23592-23596.
- [46] D. S. Lee, A. Yamada, H. Sugimoto, I. Matsunaga, H. Ogura, K. Ichihara, S. Adachi, S. Y. Park, Y. Shiro, Substrate recognition and molecular mechanism of fatty acid hydroxylation by cytochrome P450 from Bacillus subtilis Crystallographic, spectroscopic, and mutational studies, J. Biol. Chem., 2003, 278, 9761-9767.
- [47] I. Matsunaga, A. Ueda, T. Sumimoto, K. Ichihara, M. Ayata, H. Ogura, Site-Directed Mutagenesis of the Putative Distal Helix of Peroxygenase Cytochrome P450, *Arch. Biochem. Biophys.*, **2001**, *394*, 45-53.
- [48] M. Girhard, E. Kunigk, S. Tihovsky, V. V. Shumyantseva, V. B. Urlacher, Light-driven biocatalysis with cytochrome P450 peroxygenases, *Biotechnol. Appl. Biochem.*, **2013**, *60*, 111-118.
- [49] T. Fujishiro, O. Shoji, N. Kawakami, T. Watanabe, H. Sugimoto, Y. Shiro, Y. Watanabe, Chiral-substrate-assisted stereoselective epoxidation catalyzed by H<sub>2</sub>O<sub>2</sub>-dependent cytochrome P450 SPα, *Chem. Asian J.*, **2012**, *7*, 2286-2293.
- [50] M. Hofrichter, R. Ullrich, Heme-thiolate haloperoxidases: versatile biocatalysts with biotechnological and environmental significance, *Appl. Microbiol. Biotechnol.*, **2006**, *71*, 276-288.
- [51] M. Hofrichter, R. Ullrich, M. J. Pecyna, C. Liers, T. Lundell, New and classic families of secreted fungal heme peroxidases, *Appl. Microbiol. Biotechnol.*, **2010**, *87*, 871–897.
- [52] J. A. Thomas, D. R. Morris, L. P. Hager, Chloroperoxidase. Classical Peroxidatic, Catalatic, and Halogenating Forms of Enzyme, *J. Biol. Chem.*, **1970**, *245*, 3129-&.
- [53] W. Sun, T. A. Kadima, M. A. Pickard, H. B. Dunford, Catalase activity of chloroperoxidase and its interaction with peroxidase activity, *Biochem. Cell Biol.*, **1994**, *72*, 321-331.
- [54] L. Casella, S. Poli, M. Gullotti, C. Selvaggini, T. Beringhelli, A. Marchesini, The chloroperoxidase-catalyzed oxidation of phenols. Mechanism, selectivity, and characterization of enzyme-substrate complexes, *Biochem.*, **1994**, *33*, 6377-6386.
- [55] E. Aranda, R. Ullrich, M. Hofrichter, Conversion of polycyclic aromatic hydrocarbons, methyl naphthalenes and dibenzofuran by two fungal peroxygenases, *Biodegrad.*, **2009**, *21*, 267-281.
- [56] K. M. Manoj, L. P. Hager, Chloroperoxidase, a Janus Enzyme, *Biochem.*, 2008, 47, 2997-3003.
- [57] C. Wannstedt, D. Rotella, J. F. Siuda, Chloroperoxidase mediated halogenation of phenols, *Bull. Environ. Contam. Toxicol.*, **1990**, *44*, 282-287.

- [58] A. Zaks, D. R. Dodds, Chloroperoxidase-catalyzed asymmetric oxidations: substrate specificity and mechanistic study, *J. Am. Chem. Soc.*, **1995**, *117*, 10419-10424.
- [59] M. Kluge, R. Ullrich, K. Scheibner, M. Hofrichter, Stereoselective benzylic hydroxylation of alkylbenzenes and epoxidation of styrene derivatives catalyzed by the peroxygenase of Agrocybe aegerita, *Green Chem.*, **2012**, *14*, 440-446.
- [60] K.-H. van Pee, Halogenating Enzymes for Selective Halogenation Reactions, *Curr. Org. Chem.*, **2012**, *16*, 2583-2597.
- [61] J. Geigert, D. J. Dalietos, S. L. Neidleman, T. D. Lee, J. Wadsworth, Peroxide oxidation of primary alcohols to aldehydes by chloroperoxidase catalysis, *Biochem. Biophys. Res. Commun.*, 1983, 114, 1104-1108.
- [62] M. P. J. van Deurzen, F. van Rantwijk, R. A. Sheldon, Chloroperoxidase-Catalyzed Oxidation of 5-Hydroxymethylfurfural, *J. Carbohydr. Chem.*, **1997**, *16*, 299-309.
- [63] M. Sundaramoorthy, J. Terner, T. L. Poulos, Stereochemistry of the chloroperoxidase active site: crystallographic and molecular-modeling studies, *Chem. Biol.*, **1998**, *5*, 461-473.
- [64] R. Ullrich, J. Nuske, K. Scheibner, J. Spantzel, M. Hofrichter, Novel haloperoxidase from the agaric basidiomycete Agrocybe aegerita oxidizes aryl alcohols and aldehydes, *Appl. Environ. Microbiol.*, **2004**, *70*, 4575-4581.
- [65] K. Piontek, R. Ullrich, C. Liers, K. Diederichs, D. A. Plattner, M. Hofrichter, Crystallization of a 45 kDa peroxygenase/peroxidase from the mushroom Agrocybe aegerita and structure determination by SAD utilizing only the haem iron, *Acta Crystallogr. F-Struct. Biol. Cryst. Commun.*, **2010**, *66*, 693-698.
- [66] F. van de Velde, N. D. Lourenço, M. Bakker, F. van Rantwijk, R. A. Sheldon, Improved operational stability of peroxidases by coimmobilization with glucose oxidase, *Biotechnol. Bioeng.*, **2000**, *69*, 286-291.
- [67] K. Seelbach, M. P. J. vanDeurzen, F. vanRantwijk, R. A. Sheldon, U. Kragl, Improvement of the total turnover number and space-time yield for chloroperoxidase catalyzed oxidation, *Biotechnol. Bioeng.*, **1997**, *55*, 283-288.
- [68] E. J. Allain, L. P. Hager, L. Deng, E. N. Jacobsen, Highly enantioselective epoxidation of disubstituted alkenes with hydrogen peroxide catalyzed by chloroperoxidase, *J. Am. Chem.* Soc., 1993, 115, 4415-4416.
- [69] R. Ullrich, M. Hofrichter, The haloperoxidase of the agaric fungus Agrocybe aegerita hydroxylates toluene and naphthalene, *FEBS Lett.*, **2005**, *579*, 6247-6250.
- [70] S. Peter, M. Kinne, X. Wang, R. Ullrich, G. Kayser, J. T. Groves, M. Hofrichter, Selective hydroxylation of alkanes by an extracellular fungal peroxygenase, *FEBS Journal*, **2011**, *278*, 3667-3675.
- [71] A. Gutiérrez, E. D. Babot, R. Ullrich, M. Hofrichter, A. T. Martínez, J. C. del Río, Regioselective oxygenation of fatty acids, fatty alcohols and other aliphatic compounds by a basidiomycete heme-thiolate peroxidase, *Arch. Biochem. Biophys.*, **2011**, *514*, 33-43.
- [72] J. B. Park, D. S. Clark, Deactivation mechanisms of chloroperoxidase during biotransformations, *Biotechnol. Bioeng.*, **2006**, *93*, 1190-1195.
- [73] B. Valderrama, M. Ayala, R. Vazquez-Duhalt, Suicide inactivation of peroxidases and the challenge of engineering more robust enzymes, *Chem. Biol.*, **2002**, *9*, 555-565.

- [74] M. P. J. Van Deurzen, K. Seelbach, F. Van Rantwijk, U. Kragl, R. A. Sheldon, Chloroperoxidase: Use of a hydrogen peroxide-stat for controlling reactions and improving enzyme performance, *Biocatal. Biotransform.*, **1997**, *15*, 1-16.
- [75] W. M. Sun, T. A. Kadima, M. A. Pickard, H. B. Dunford, Catalase activity of chloroperoxidase and its interaction with peroxidase activity, *Biochemistry and Cell Biology-Biochimie Et Biologie Cellulaire*, **1994**, *72*, 321-331.
- [76] R. Wever, H. Plat, E. Deboer, Isolation procedure and some properties of the bromoperoxidase from the seaweed Ascophyllum nodosum, *Biochim. Biophys. Acta*, **1985**, *830*, 181-186.
- [77] B. E. Krenn, M. G. M. Tromp, R. Wever, The brown alga Ascophyllum nodosum contains two different vanadium bromoperoxidases, *J. Biol. Chem.*, **1989**, *264*, 19287-19292.
- [78] E. Torres, H. Hayen, C. M. Niemeyer, Evaluation of cytochrome P450BSβ reactivity against polycyclic aromatic hydrocarbons and drugs, *Biochem. Biophys. Res. Commun.*, **2007**, *355*, 286-293.
- [79] F. van de Velde, M. Bakker, F. van Rantwijk, G. P. Rai, L. P. Hager, R. A. Sheldon, Engineering chloroperoxidase for activity and stability, *J. Mol. Catal. B-Enzym.*, **2001**, *11*, 765-769.
- [80] F. van de Velde, F. van Rantwijk, R. A. Sheldon, Selective oxidations with molecular oxygen, catalyzed by chloroperoxidase in the presence of a reductant, *J. Mol. Catal. B-Enzym.*, **1999**, *6*, 453-461.
- [81] G. P. Rai, S. Sakai, A. M. Florez, L. Mogollon, L. P. Hager, Directed evolution of chloroperoxidase for improved epoxidation and chlorination catalysis, *Adv. Synth. Catal.*, **2001**, *343*, 638-645.
- [82] Q. S. Li, J. Ogawa, S. Shimizu, Critical role of the residue size at position 87 in H2O2-dependent substrate hydroxylation activity and H2O2 inactivation of cytochrome P450BM-3, *Biochem. Biophys. Res. Commun.*, **2001**, *280*, 1258-1261.
- [83] R. Taboada-Puig, C. Junghanns, P. Demarche, M. T. Moreira, G. Feijoo, J. M. Lema, S. N. Agathos, Combined cross-linked enzyme aggregates from versatile peroxidase and glucose oxidase: Production, partial characterization and application for the elimination of endocrine disruptors, *Bioresour. Technol.*, **2011**, *102*, 6593-6599.
- [84] H. M. de Hoog, M. Nallani, J. Cornelissen, A. E. Rowan, R. J. M. Nolte, I. Arends, Biocatalytic oxidation by chloroperoxidase from Caldariomyces fumago in polymersome nanoreactors, *Org. Biomol. Chem.*, **2009**, *7*, 4604-4610.
- [85] D. I. Perez, F. van Rantwijk, R. A. Sheldon, Cross-Linked Enzyme Aggregates of Chloroperoxidase: Synthesis, Optimization and Characterization, Adv. Synth. Catal., 2009, 351, 2133-2139.
- [86] A. Petri, T. Gambicorti, P. Salvadori, Covalent immobilization of chloroperoxidase on silica gel and properties of the immobilized biocatalyst, *J. Mol. Catal. B: Enzym.*, **2004**, *27*, 103-106.
- [87] D. I. Perez, M. M. Grau, I. W. C. E. Arends, F. Hollmann, Visible light-driven and chloroperoxidase-catalyzed oxygenation reactions, *Chem Commun*, **2009**, 6848-6850.
- [88] C. Kohlmann, S. Lutz, Electroenzymatic synthesis of chiral sulfoxides, *Eng. Life Sci.*, **2006**, *6*, 170-174.
- [89] W. A. Duetz, J. B. van Beilen, B. Witholt, Using proteins in their natural environment: potential and limitations of microbial whole-cell hydroxylations in applied biocatalysis, *Curr. Opin. Biotechnol.*, **2001**, *12*, 419-425.
- [90] H. Zhao, W. A. van der Donk, Regeneration of cofactors for use in biocatalysis, *Curr. Opin. Biotechnol.*, **2003**, *14*, 583-589.

- [91] H. Chenault, G. Whitesides, Regeneration of nicotinamide cofactors for use in organic synthesis, *Appl. Biochem. Biotechnol.*, **1987**, *14*, 147-197.
- [92] Z. Shaked, G. M. Whitesides, Enzyme-catalyzed organic synthesis: NADH regeneration by using formate dehydrogenase, *J. Am. Chem. Soc.*, **1980**, *102*, 7104-7105.
- [93] F. Hildebrand, S. Luetz, Electroenzymatic synthesis of chiral alcohols in an aqueous organic two-phase system, *Tetrahedron-Asymmetry*, **2007**, *18*, 1187-1193.
- [94] F. Hollmann, K. Hofstetter, A. Schmid, Non-enzymatic regeneration of nicotinamide and flavin cofactors for monooxygenase catalysis, *Trends Biotechnol.*, **2006**, *24*, 163-171.
- [95] W. A. van der Donk, H. M. Zhao, Recent developments in pyridine nucleotide regeneration, *Curr. Opin. Biotechnol.*, **2003**, *14*, 421-426.
- [96] X. Fang, J. R. Halpert, Dithionite-supported hydroxylation of palmitic acid by cytochrome P450BM-3, *Drug metabolism and disposition: the biological fate of chemicals*, **1996**, *24*, 1282-1285.
- [97] V. Reipa, M. P. Mayhew, V. L. Vilker, A direct electrode-driven P450 cycle for biocatalysis, *Proc. Natl. Acad. Sci. U. S. A.*, **1997**, *94*, 13554-13558.
- [98] U. Schwaneberg, D. Appel, J. Schmitt, R. D. Schmid, P450 in biotechnology: zinc driven omegahydroxylation of p-nitrophenoxydodecanoic acid using P450BM-3 F87A as a catalyst, *J. Biotechnol.*, **2000**, *84*, 249-257.
- [99] X. Fang, J. R. Halpert, Dithionite-supported hydroxylation of palmitic acid by cytochrome P450BM-3, *Drug. Metab. Dispos.*, **1996**, *24*, 1282-1285.
- [100] J. Lutz, F. Hollmann, T. V. Ho, A. Schnyder, R. H. Fish, A. Schmid, Bioorganometallic chemistry: biocatalytic oxidation reactions with biomimetic NAD(+)/NADH co-factors and Cp\*Rh(bpy)H (+) for selective organic synthesis, *J. Organomet. Chem.*, **2004**, *689*, 4783-4790.
- [101] H. C. Lo, O. Buriez, J. B. Kerr, R. H. Fish, Bioorganometallic chemistry part 11. Regioselective reduction of NAD(+) models with Cp\*Rh(bpy)H (+): Structure-activity relationships and mechanistic aspects in the formation of the 1,4-NADH derivatives, *Angew. Chem. Int. Ed.*, 1999, 38, 1429-1432.
- [102] H. C. Lo, C. Leiva, O. Buriez, J. B. Kerr, M. M. Olmstead, R. H. Fish, Bioorganometallic Chemistry.

  13. Regioselective Reduction of NAD+ Models, 1-Benzylnicotinamde Triflate and β-Nicotinamide Ribose-5'-methyl Phosphate, with in Situ Generated [Cp\*Rh(Bpy)H]+: Structure–Activity Relationships, Kinetics, and Mechanistic Aspects in the Formation of the 1,4-NADH Derivatives†, *Inorg. Chem.*, 2001, 40, 6705-6716.
- [103] J. D. Ryan, R. H. Fish, D. S. Clark, Engineering Cytochrome P450 Enzymes for Improved Activity towards Biomimetic 1,4-NADH Cofactors, *ChemBioChem*, **2008**, *9*, 2579-2582.
- [104] R. E. White, M. J. Coon, Oxygen activation by cytochrome P-450, *Annu. Rev. Biochem.*, **1980**, 49, 315-356.
- [105] H. Joo, Z. L. Lin, F. H. Arnold, Laboratory evolution of peroxide-mediated cytochrome P450 hydroxylation, *Nature*, **1999**, *399*, 670-673.
- [106] P. C. Cirino, F. H. Arnold, A Self-Sufficient Peroxide-Driven Hydroxylation Biocatalyst, *Angew. Chem. Int. Ed.*, **2003**, *42*, 3299-3301.
- [107] J. W. Park, J. K. Lee, T. J. Kwon, D. H. Yi, Y. I. Park, S. M. Kang, Purification and characterization of a cytochrome p-450 from pravastatin producing Streptomyces sp Y-110, *J. Microbiol. Biotechnol.*, **2001**, *11*, 1011-1017.

- [108] W. A. Loughlin, D. B. Hawkes, Effect of organic solvents on a chloroperoxidase biotransformation, *Bioresour. Technol.*, **2000**, *71*, 167-172.
- [109] M. P. J. van Deurzen, I. J. Remkes, F. van Rantwijk, R. A. Sheldon, Chloroperoxidase catalyzed oxidations in t-butyl alcohol/water mixtures, *J. Mol. Catal. A: Chem.*, **1997**, *117*, 329-337.
- [110] C. Kohlmann, L. Greiner, W. Leitner, C. Wandrey, S. Luutz, Ionic Liquids as Performance Additives for Electroenzymatic Syntheses, *Chem. Eur. J.*, **2009**, *15*, 11692-11700.
- [111] C. Sanfilippo, N. D'Antona, G. Nicolosi, Chloroperoxidase from Caldariomyces fumago is active in the presence of an ionic liquid as co-solvent, *Biotechnol. Lett.*, **2004**, *26*, 1815-1819.
- [112] R. J. Lichtenecker, W. Schmid, Application of various ionic liquids as cosolvents for chloroperoxidase- catalysed biotransformations, *Monatsh. Chem.*, **2009**, *140*, 509-512.
- [113] K. Ryu, J. S. Dordick, How do organic solvents affect peroxidase structure and function?, *Biochem.*, **1992**, *31*, 2588-2598.
- [114] P. A. Fitzpatrick, A. M. Klibanov, How can the solvent affect enzyme enantioselectivity?, *J. Am. Chem. Soc.*, **1991**, *113*, 3166-3171.
- [115] C. Giacomo, Biocatalysis in water-organic solvent two-phase systems, *Trends Biotechnol.*, **1984**, 2, 102-106.
- [116] S. C. Maurer, K. Kühnel, L. A. Kaysser, S. Eiben, R. D. Schmid, V. B. Urlacher, Catalytic Hydroxylation in Biphasic Systems using CYP102A1 Mutants, Adv. Synth. Catal., 2005, 347, 1090-1098.
- [117] L. H. Dai, A. M. Klibanov, Peroxidase-catalyzed asymmetric sulfoxidation in organic solvents versus in water, *Biotechnol. Bioeng.*, **2000**, *70*, 353-357.
- [118] A. M. Klibanov, Asymmetric enzymatic oxidoreductions in organic solvents, *Curr. Opin. Biotechnol.*, **2003**, *14*, 427-431.
- [119] A. M. Klibanov, Improving enzymes by using them in organic solvents, *Nature*, **2001**, *409*, 241-246.
- [120] F. van de Velde, M. Bakker, F. van Rantwijk, R. A. Sheldon, Chloroperoxidase-catalyzed enantioselective oxidations in hydrophobic organic media, *Biotechnol. Bioeng.*, **2001**, *72*, 523-529.
- [121] A. Schmid, J. S. Dordick, B. Hauer, A. Kiener, M. Wubbolts, B. Witholt, Industrial biocatalysis today and tomorrow, *Nature*, **2001**, *409*, 258-268.
- [122] M. Breuer, K. Ditrich, T. Habicher, B. Hauer, M. Keßeler, R. Stürmer, T. Zelinski, Industrial Methods for the Production of Optically Active Intermediates, *Angew. Chem. Int. Ed.*, **2004**, *43*, 788-824.
- [123] R. A. Sheldon, Consider the environmental quotient, Chemtech, 1994, 24, 38-47.
- [124] R. A. Sheldon, Selective catalytic synthesis of fine chemicals: opportunities and trends, *J. Mol. Catal. A: Chem.*, **1996**, *107*, 75-83.
- [125] R. A. Sheldon, Catalysis: The Key to Waste Minimization, *J. Chem. Technol. Biotechnol.*, **1997**, *68*, 381-388.
- [126] S. L. Buchwald, R. B. Grossman, A. Gutierrez, Catalytic asymmetric reduction of ketones using metal catalysts, **1993**, *US* 5227538.
- [127] F. Balkenhohl, B. Hauer, W. Ladner, U. Pressler, U. Schnell, H. R. Staudenmaier, Lipase-catalysed acylation of alcohols with diketenes, **1998**, *EP 0716712B1*.

- [128] S. Friedrich, G. Gröbe, M. Kluge, T. Brinkmann, M. Hofrichter, K. Scheibner, Optimization of a biocatalytic process to gain (R)-1-phenylethanol by applying the software tool Sabento for ecological assessment during the early stages of development, *J. Mol. Catal. B: Enzym.*
- [129] R. A. Sheldon, Atom utilisation, E factors and the catalytic solution, *C. R. Acad. Sci. Ser. IIC Sci. Chem.*, **2000**, *3*, 541-551.
- [130] <a href="http://www.peroxicats.org/">http://www.peroxicats.org/</a>
- [131] http://cordis.europa.eu/projects/rcn/110545 en.html
- [132] S. Schulz, M. Girhard, V. B. Urlacher, Biocatalysis: Key to Selective Oxidations, *ChemCatChem*, **2012**, *4*, 1889-1895.

# Chapter 2

Increasing the productivity of peroxidase - catalyzed oxyfunctionalization - a case study on the potential of two liquid phase systems

This chapter is based on E. Churakova, I. W. C. E. Arends, F. Hollmann, *ChemCatChem*, **2013**, *5*, 565-568

# Chapter 2

Increasing the productivity of peroxidase - catalyzed oxyfunctionalization – a case study on the potential of two liquid phase systems

# Introduction

Peroxidases (E.C.1.11.1.) bear an enormous potential for organic oxyfunctionalization chemistry  $^{[1]}$ . Especially the heme - thiolate peroxidases (peroxygenases) combine P450 monooxygenase reactivity with independence from costly and instable nicotinamide cofactors  $^{[2]}$ . Instead, peroxidases regenerate their catalytically active oxyferryl - species using hydrogen peroxide ( $H_2O_2$ )  $^{[2-4], [Chapter \, 1]}$ . The chloroperoxidase from *Caldariomyces fumago* (CPO) represents the most widely used and best-characterized peroxidase for catalytic sulfoxidation and oxyfunctionalization  $^{[1]}$ .

However the  $H_2O_2$ -related suicide inhibition of CPO limits its practical application <sup>[5-6]</sup>. To achieve high productivities, various approaches on CPO immobilization <sup>[7-13]</sup> or protein engineering <sup>[8, 14]</sup> has been examined. However the catalytic activity of CPO in terms of total turnover number (TTN, mole product / mole of enzyme) in most of the cases remained low, although there are outstanding examples (vide infra).

Alternatively, the enzyme stability can be improved by maintaining a low hydrogen peroxide concentration via its stepwise or continuous addition <sup>[15-16]</sup>. For example, a sensor-controlled method, wherein the  $H_2O_2$  concentration is adjusted according to the progress of the reaction has proved to be efficient for CPO - catalyzed oxidations <sup>[15-16]</sup>. Thus a TTN of 850\*10<sup>3</sup> was obtained for indole oxidation in a sensor controlled fed - batch reaction <sup>[15]</sup>. Also the TTN in the oxidation of thioanisole was increased to 148 \*10<sup>3</sup> by sensor - controlled oxidation in aqueous buffer solution containing 30% (v/v) tert-butyl alcohol <sup>[1]</sup>.

However sensor-controlled addition of hydrogen peroxide forms so called 'hot spots' containing locally high concentrations of  $H_2O_2$  that lead to enzyme inactivation <sup>[4]</sup>. This can be circumvented by in situ  $H_2O_2$  generation from  $O_2$  via chemical <sup>[17-19]</sup>, electrochemical <sup>[20-22]</sup> and enzymatic approaches <sup>[9, 23-24]</sup>. All systems share the possibility to control the  $H_2O_2$  generation rate thus balancing the rates of peroxidase - activity and - inactivation, which both inversely depend on the in situ concentration of  $H_2O_2$  <sup>[1-2]</sup>. For example, one of the highest TTN of 250\*10<sup>3</sup> for oxidation of thioanisole (a commonly used model substrate for CPO-catalysis) was obtained in the presence of CPO coimmobilized with glucose oxidase on polyurethane foam for in situ  $H_2O_2$  generation <sup>[9]</sup>.

To avoid the suicidal inactivation of CPO by  $H_2O_2$  we applied a photocatalytic system for in situ  $H_2O_2$  generation <sup>[19]</sup>. Here, visible-light exited flavins such as flavin adenine mononucleotide (FMN) oxidizes simple and abundant electron donors such as EDTA (ethylenediaminetetracetic acid disodium salt dihydrate). The resulting reduced flavin (FMNH<sub>2</sub>) rapidly reacts with molecular oxygen (from ambient atmosphere) yielding the re-oxidized flavin and hydrogen peroxide, which is utilized by the peroxidase to promote oxyfunctionalization chemistry (Scheme 1).

Scheme 1. Schematic representation of the proposed photocatalytic in situ  $H_2O_2$  generation approach. CPO: Chloroperoxidase from *Caldariomyces fumago*, hv: visible light.

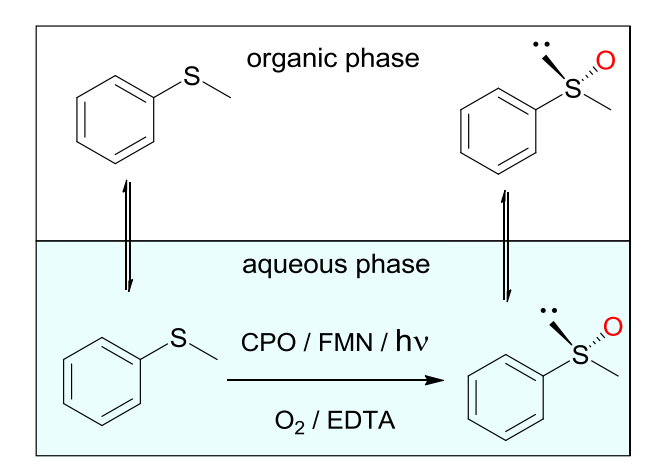
Another concern of peroxidase - catalysis, and of biocatalysis for organic chemistry in general, is based on the hydrophobic nature of most synthetically important substrates and products. Interestingly, the apparent incompatibility with aqueous reaction media has so far not raised great concern amongst researchers and the majority of publications deals with substrate loadings in the range of a few millimolar. Such low concentrations require the use of high volumes of aqueous reaction mixture in order to produce a given amount of product.

Notably, also the solubility of molecular oxygen in aqueous media is also very poor (approx. 0.25 mM). Hence, in case of reductive  $H_2O_2$  generation from  $O_2$ , this 'co - substrate' quickly becomes limiting and overall rates are determined by  $O_2$  diffusion rather than other factors.

To overcome such solubility issues, researchers have evaluated various water - miscible co - solvents <sup>[25]</sup>, e.g. *tert* - butanol <sup>[26]</sup>, acetone <sup>[27]</sup> or ionic liquids <sup>[28-30]</sup>. However, presence of organic co - solvents can impair both the enzyme activity <sup>[31]</sup> and selectivity <sup>[25, 32]</sup>.

Alternatively, the substrate can be supplied via a second water-immiscible phase using the two liquid - phase concept, where the organic phase serves as a substrate reservoir and a product sink <sup>[33-35]</sup>. The use of the two liquid phase system (2 LPS) ensures that the substrate and products are concentrated in an organic phase, simultaneously preventing enzyme inhibition by high concentrations of substrate/product.

Inspired by the report by Park and Clark [36] who utilized the liquid organic substrate itself as a substrate reservoir and product sink we decided applying the 2LPS concept on the oxygenation of thioanisole (Scheme 2).



Scheme 2. Schematic representation of the proposed two liquid phase system for the photoenzymatic approach. CPO: Chloroperoxidase from *Caldariomyces fumago*, FMN: flavin mononucleotide, hv: visible light, EDTA: ethylenediaminetetraacetic acid.

## **Results and discussions**

# The benchmark - monophasic reactions

In order to establish the benchmark conditions we further investigated the monophasic sulfoxidation system. A correlation of the initial sulfoxidation rate on the light distance was observed (Figure 1), which we attribute to the light intensity, as thermal effect can be excluded (reaction was performed in the thermostate at  $30^{\circ}$ C). Furthermore, we assume the light intensity directly corresponds to the in situ concentration of photoexcited FMN<sup>‡</sup> (flavin mononucleotide, FMN).

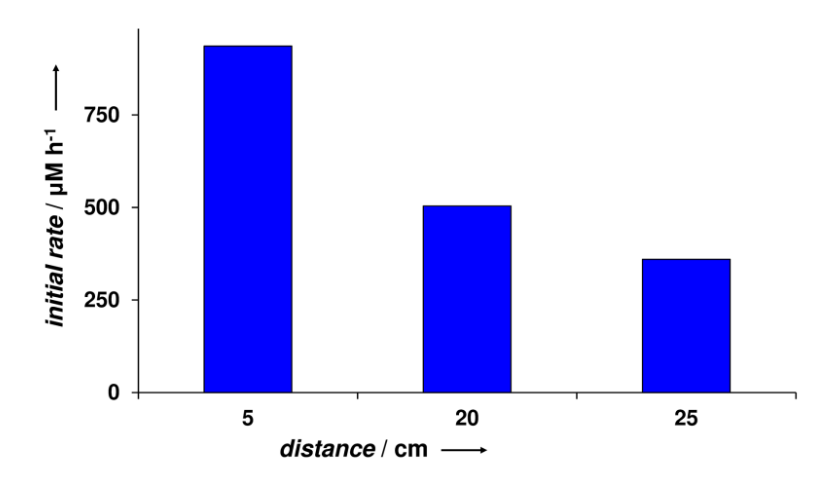


Figure 1. Influence of distance of the light source on the initial rate of the photoenzymatic sulfoxidation. Conditions: [CPO] = 4  $\mu$ M, [FMN] = 50  $\mu$ M, [EDTA] = 5 mM, [thioanisole] = 5 mM, T = 30°C. The results of duplicate experiments are shown; the deviation was always less than 10%.

As the in situ concentration of photoexcited FMN<sup>‡</sup> should also correlate with the overall FMN concentration we also systematically varied this parameter. To our surprise, a saturation - type dependence of the initial rate on the photocatalyst concentration was found (Figure 2).

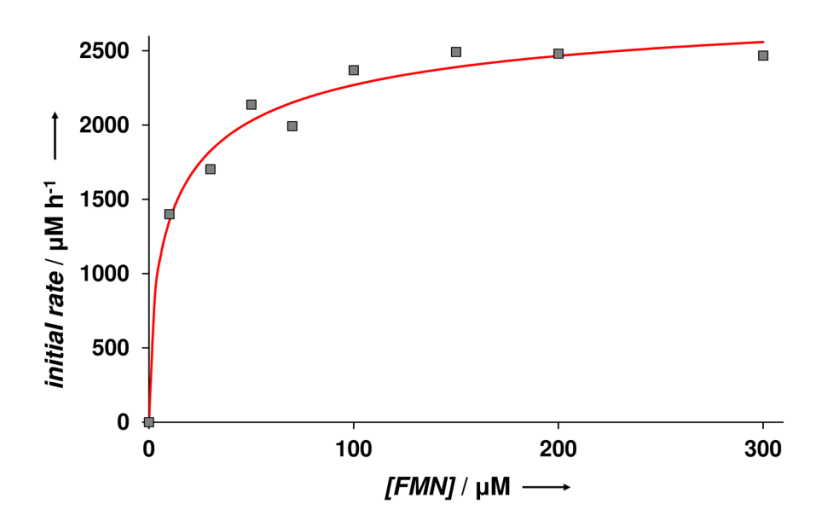


Figure 2. Influence of photocatalyst concentration on the rate of the photoenzymatic sulfoxidation in aqueous medium. Conditions: [CPO] = 4  $\mu$ M, [EDTA] = 5 mM, [thioanisole] = 5 mM, methanol 1% (v/v); T = 30°C. The results of duplicate experiments are shown; the deviation was always less than 5%.

It is noteworthy that 'half saturation rate' was obtained at approximately 10  $\mu$ M FMN. Under these conditions CPO turnover frequency (TF) was in the range of 10 min<sup>-1</sup> thereby falling back behind the reported Vmax of 960 min<sup>-1</sup> by orders of magnitude <sup>[1]</sup>.

We attribute this saturation - type behaviour to a fast depletion of dissolved  $O_2$  in the reaction medium leading to diffusion of atmospheric  $O_2$  becoming overall - rate limiting. Heterogeneous intake of  $O_2$  (e.g. by bubbling air into the reaction medium) was not feasible due to fast inactivation of the biocatalyst caused by the mechanical force from the gas stream. Furthermore, the monophasic system was severely limited by evaporation of the starting material (typically, the mass balance was less than 50%, Figure 3  $\diamond$ ). Hence, we decided to evaluate the 2LPS to overcome both challenges mentioned above.

## Two liquid phase reactions

Indeed, adding thioanisole as a second organic phase to a typical monophasic reaction resulted in a significant prolonging of the reaction time from approximately 2h to at least 24h of linear accumulation of (R)-methyl phenyl sulfoxide (ee 97%) under otherwise identical conditions (Figure 3 •). Furthermore, overoxidation towards methylphenylsulfone was not observed (in none of the experiments).

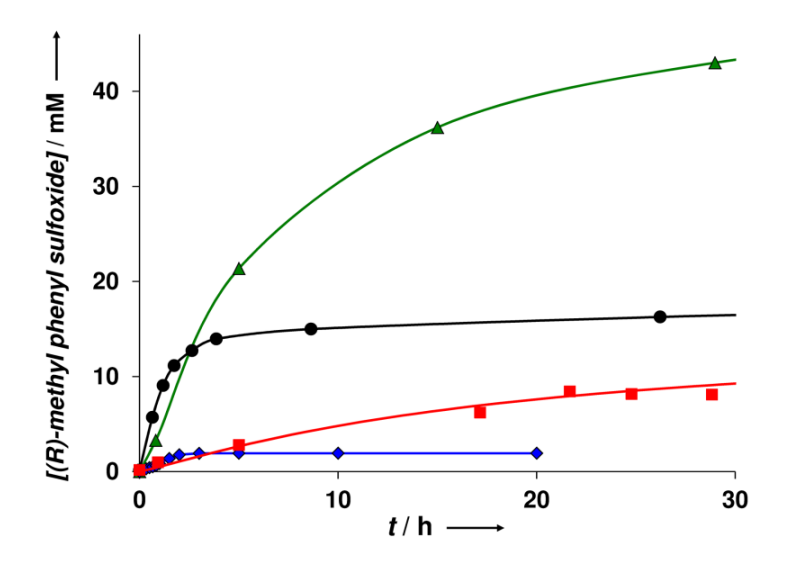


Figure 3. Comparison of photoenzymatic sulfoxidations with general conditions of 50 mM sodium acetate buffer (pH 5.1), [CPO] = 4  $\mu$ M, [FMN] = 50 $\mu$ M, T = 30°C, light distance 1 cm, and the following variable conditions: initial conditions of an aqueous reaction system: [EDTA] = 5 mM, [thioanisole] = 5 mM, methanol 1% (v/v), V = 20 ml ( $\spadesuit$ ); 2LPS with clearly defined phases: low mechanical stress; [EDTA] = 5 mM, V thioanisole = V aq. phase = 15 ml ( $\blacksquare$ ); 2 LPS obtained by mechanical stirring: emulsion obtained by high mechanical stress; [EDTA] = 5 mM, V thioanisole = V aq. phase = 10 ml ( $\bullet$ ); surfactant - stabilized 2 LPS: emulsion obtained by low mechanical stress; 0.4% (w/v) Aerosol OT, [EDTA] = 50 mM, V thioanisole = V aq. phase = 5 ml ( $\blacktriangle$ ).

We attribute this significant prolongation of the productivity time to the constant supply of CPO with thioanisole from the organic phase. Interestingly, the initial rates in both monophasic and biphasic set up were identical (within experimental error). We suspected diffusion limitation to account for this apparently very poor catalytic activity of the photoenzymatic sulfoxidation system. Repeating the reaction under identical conditions albeit forming an emulsion (by vigorous mechanical stirring) resulted in an 8-fold increased initial rate (Figure 3 ◆) supporting the assumption of diffusion limitation being overall rate limiting. The robustness of this emulsion reaction, however, was rather poor and the sulfoxidation reaction ceased after 2 - 3h. Possibly CPO was rapidly inactivated under the mechanically demanding reaction. We therefore evaluated the use of sodium dioctyl sulfosuccinate (Aerosol AOT) as surfactant (Figure 4) enabling formation of a stable emulsion at significantly reduced mechanical stress. As a result, the reaction rate was somewhat decreased but allowed for much longer reaction times (Figure 3 ▲). Overall, more than 45 mM of enantioenriched (>96% ee) (R)-methyl phenyl sulfoxide was obtained using this procedure.

Figure 4. Sodium dioctyl sulfosuccinate. Commercial name Aerosol® OT surfactant.

We re-evaluated the influence of [FMN] on the rate of the photoenzymatic sulfoxidation reaction, this time under the conditions of the surfactant - stabilized emulsion (Figure 5).

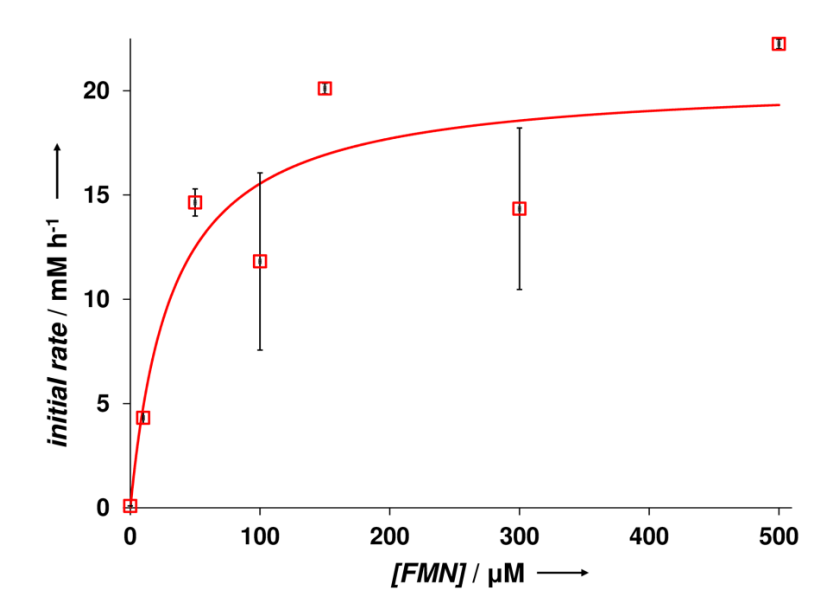


Figure 5. Influence of [FMN] on the rate of the photoenzymatic sulfoxidation under 2LPS conditions. Conditions: 50 mM sodium acetate buffer (pH 5.1), [CPO] = 4  $\mu$ M, [EDTA] = 50 mM, [FMN] = 0 - 300  $\mu$ M; 0.4% (w/v) Aerosol OT; V <sub>thioanisole</sub> = V <sub>aq. phase</sub> = 1 ml; T = 30°C; light distance 1 cm. The experiments were performed as triplicate.

It should be mentioned here the reproducibility of these experiments was rather poor as seen by the large error bars in Figure 5. The present emulsion remains to be optimized as the droplet size presumably depended on stirrer speed and phase separation occurred quickly upon stopping the stirring.

Nevertheless, compared to the initial monophasic reaction system (Figure 2) the maximal rate was increased almost 10-fold. Also the half-saturation concentration of FMN increased to approximately 30  $\mu$ M, which we attribute to an increased  $O_2$  transfer rate to the aqueous reaction medium. This assumption is supported by the observation that the initial rate was largely independent of the biocatalyst concentration applied. Hence, lowering [CPO] from 8  $\mu$ M to 60 nM hardly affected the initial (R)-methyl phenyl sulfoxide generation rate (Figure 6). Hence, the nominal TF (CPO) increased to up to 470 min<sup>-1</sup> and TTNs up to 126000 have been observed. However, especially at low biocatalyst concentrations product accumulation ceased quickly, which we attribute to CPO inactivation. Here also enantioselectivity at low CPO concentration was impaired over 24 hours e.g. resulting ee 85% at 2  $\mu$ M of CPO. We attribute the decrease in enantioselectivity to non – enzymatic photooxidation of thioanisole (vide infra).

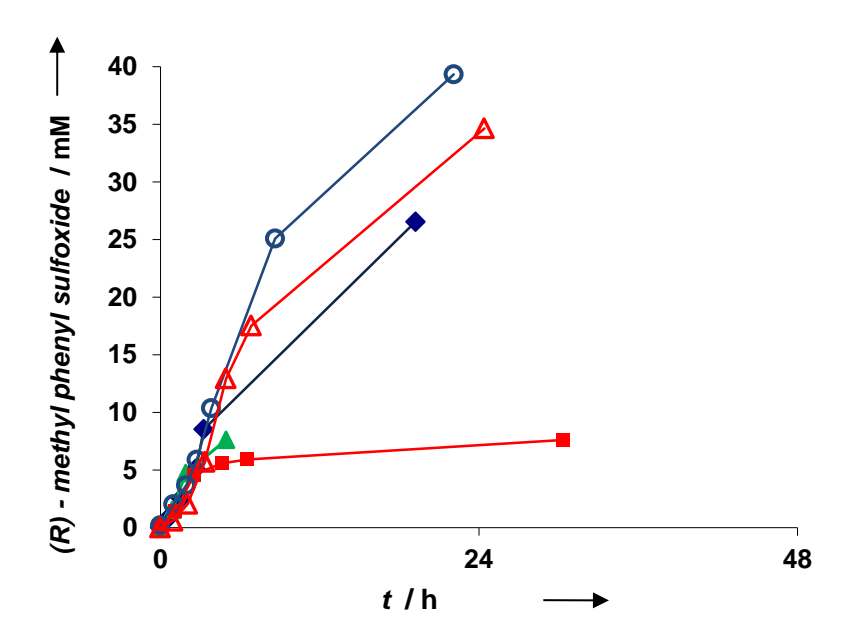


Figure 6. [CPO] - dependence of the initial rate in the photobiocatalytic sulfoxidation reaction under 2LPS conditions. General conditions: surfactant - stabilized 2LPS, V <sub>thioanisole</sub> = V <sub>aq. phase</sub>, 50mM sodium acetate buffer (pH 5.1), 0.4% (w/v) Aerosol OT, [CPO] = O: 4  $\mu$ M,  $\triangle$ : 2  $\mu$ M,  $\triangle$ : 0.5  $\mu$ M,  $\triangle$ : 0.1  $\mu$ M,  $\square$ : 0.06  $\mu$ M, [FMN] = 50  $\mu$ M, [EDTA] = 5 mM, T = 30°C, light distance = 1 cm.

Control experiments incubating CPO in the emulsion in the absence of a  $H_2O_2$  generation system let us estimate a half life time of 5 h under these conditions at low CPO concentration (0.5  $\mu$ M) (Figure 7). Possibly the remaining mechanical stress and/or direct contact of the biocatalyst with the hydrophobic phase may account for this. Further studies will clarify the nature of this inactivation. Using immobilized CPO may be a viable approach to overcome this inactivation limitation [10, 37-39].

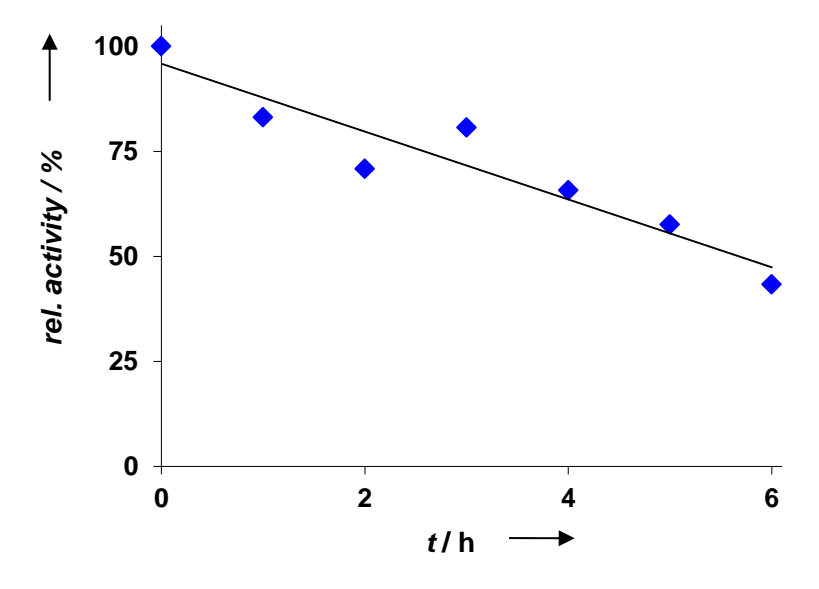


Figure 7. Stability of CPO under the conditions of a 2LPS applied in this study. General conditions: surfactant - stabilized 2LPS, V <sub>thioanisole</sub> = V <sub>aq. phase</sub> = 5 ml, 50 mM sodium acetate buffer (pH 5.1), 0.4% (w/v) Aerosol OT, [CPO] = 0.5  $\mu$ M, [EDTA] = 5 mM, T = 30°C, light distance = 1cm.

An influence of light on the stability/activity of CPO cannot be ruled out presently. Thus the photoinactivation of catalase, a heme containing enzyme, was previously reported by Grotjohann et al.  $^{[40]}$  In our hands, no significant difference was observed when performing CPO - catalyzed sulfoxidation reaction upon the external  $H_2O_2$  addition under illumination or in the darkness (Figure 8); however identical experiments, but in the emulsion, over longer reaction period remain to be elucidated.

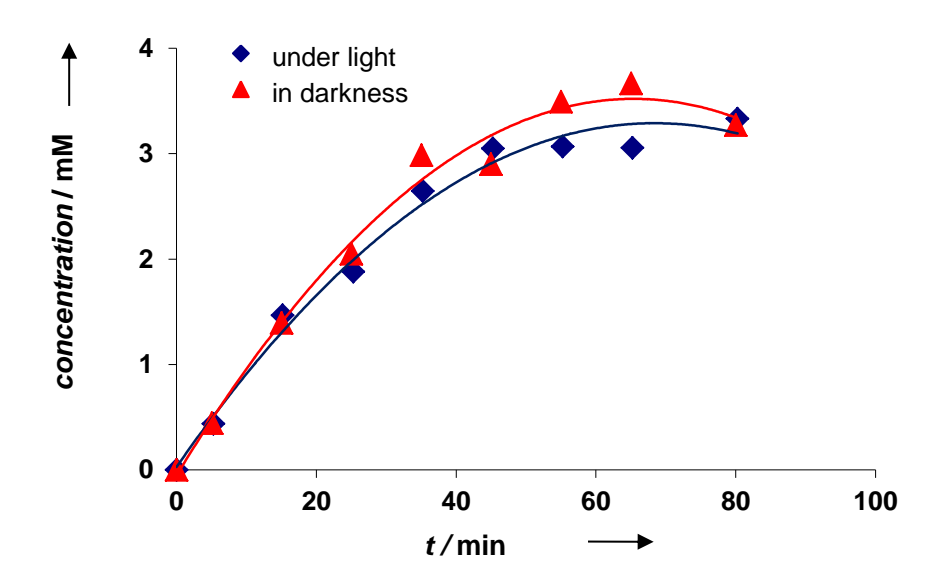


Figure 8. Thioanisole oxidation catalyzed by CPO upon  $H_2O_2$  addition; blue – under illumination; red – in darkness. General conditions: V = 3 ml; [thioanisole] = 5 mM; CPO = 4  $\mu$ M; 50 mM sodium acetate buffer (pH 5.1); methanol 1% (v/v); 36°C; aliquots (10  $\mu$ L) of aqueous  $H_2O_2$  solution (162.5 mM) were added at indicated time points to the final  $[H_2O_2] = 0.5$  mM.

Furthermore, we performed several control experiments in order to elucidate the possible background chemical activity under photocatalytic conditions in the emulsion. Reactions without CPO<sup>1</sup> and in the darkness<sup>2</sup> gave expected results (Table 1, entries 2-3).

Interestingly, sluggish sulfoxidation (ee 34% (R)) was observed in the absence of photocatalyst (Table 1, entry 4). The spontaneous oxidation of the sulfides to sulfoxides is possibly due to the presence of adventitious impurities in the reaction mixture. Thus, it is known that catalytic amounts of acid or metal oxide can enhance the oxidation of sulfides to sulfoxides <sup>[26]</sup>. In addition, sluggish thioanisole oxidation catalyzed by CPO, using  $O_2$  as an oxidant in the presence of reductant (EDTA), might occur and thus would explain the low enantioselectivity observed <sup>[41-42]</sup> (Table 1, entry 4). Light exposure seems to play a crucial role for these background reactions, as no conversion was observed in darkness.

41

<sup>&</sup>lt;sup>1</sup> Thermally inactivated CPO was used (see experimental section). The background chemical activity is due to thioanisole oxidation by  $H_2O_2$  formed photocatalytically.

<sup>&</sup>lt;sup>2</sup> No H<sub>2</sub>O<sub>2</sub> was formed, therefore no conversion was observed

Table 1. Background activity in the photoenzymatic approach. Standard conditions (1): 50 mM sodium acetate buffer (pH 5.1), [CPO] = 4  $\mu$ M, [FMN] = 50  $\mu$ M, [EDTA] = 50 mM 0.4% (w/v) Aerosol OT, V <sub>thioanisole</sub> = V <sub>aq. phase</sub> = 5 ml, T = 30°C, light distance 1 cm. Control experiments were performed under standard conditions omitting one of the mentioned reaction components (entries 2-6).

Entry	Experiment	Initial rate, n	nM/h (%)ª	[R+S] <sup>b</sup> , 1	mM (%) <sup>c</sup>	ee, (R) %
1	Standard conditions	4.27	(100)	43.8	(100)	96
2	No light	0	(0)	0	(0)	0
3	No CPO	0.1	(2.5)	2.5	(6)	0
4	No FMN	0.05	(1)	1.2	(3)	34
5	No EDTA (AOT)	1.26	(31)	14.4	(33)	66
6	No EDTA, no AOT	0.68	(17)	7	(16)	22

<sup>&</sup>lt;sup>a</sup> Calculated as the ratio of the initial rate in the control experiment to the initial rate of the standard reaction (Figure  $3 \triangle$ ) over 24 h. <sup>b</sup> Sum of (R) - and (S) – methyl phenyl sulfoxide after reaction period of 24 h; <sup>c</sup> calculated as the ratio of the final product concentration in the control experiment to the final product concentration in the standard reaction (Figure  $3 \triangle$ ) over 24 h.

Unexpectedly, the significant formation of the (R) – methyl phenyl sulfoxide (ee 66% (R)) was also observed in the absence of electron donor (EDTA) (Figure 9) (Table 1, entry 5). Thioanisole photooxidation by oxygen in the presence of flavin was recently described by Dad'ova et al  $^{[43]}$ . However the enantioselectivity observed in our experiment implies that the sulfoxidation occurs in a chiral environment, i.e. in the active site of CPO. We assume the inherent impurities in the reaction mixture could serve the equivalents for FMN reduction, resulting in production of  $H_2O_2$  for the peroxidase catalytic cycle. Thus dioctyl sulfosuccinate (surfactant) may play the role of reductant (Figure 4); moreover commercial Aerosol OT solution often contains impurities  $^{[44]}$ . Indeed performing the control experiment without EDTA and surfactant showed decrease in enantioselectivity (final ee 22% (R)) over reaction period (Table 1, entry 6) (Figure 9). The decreased enantioselectivity implies that the non - enzymatic thioanisole photooxidation becomes predominant in the absence of any reducing agents.

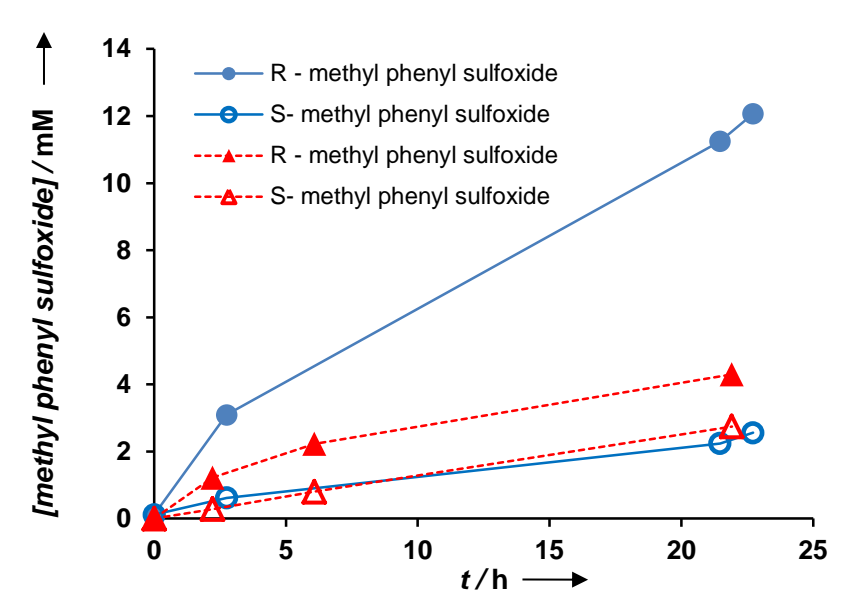


Figure 9. Time - course of thioanisole photoxidation in the organic aqueous emulsion: (solid line) - supplemented with surfactant 0.4% (w/v) sodium dioctyl sulfosuccinate; (dashed line) - without surfactant. General conditions: 50 mM sodium acetate buffer (pH 5.1), V <sub>thioanisole</sub> = V <sub>aq. phase</sub> = 5 ml, [CPO] = 4  $\mu$ M, [FMN] = 50  $\mu$ M, T = 30°C, light distance 1 cm.

Previously two mechanism of sulfides photooxidation has been observed: photooxidation promoted by singlet oxygen ( ${}^{1}O_{2}$ ) and electron transfer (ET) mechanism involving formation of superoxide anion ( $O_{2}^{-}$ ) from triplet oxygen  ${}^{[45]}$  (Figure 10, Figure 11). Singlet oxygen pathway is known to be promoted by protic solvents  ${}^{[46]}$ . Dad'ova et al proved the thioanisole photooxidation in the presence of flavin in methanol takes place via singlet oxygen pathway, although the contribution of ET mechanism cannot be excluded in other solvents  ${}^{[43]}$ .

$${}^{3}O_{2} \xrightarrow{} {}^{1}O_{2}$$

$${}^{1}O_{2} + R_{2}S \xrightarrow{} R_{2}S^{+} - O - O^{-}$$

$$R_{2}S^{+} - O - O^{-} + R_{2}S \xrightarrow{} 2 R_{2}S^{+} - O^{-}$$

Figure 10. Singlet oxygen mechanism of sulfides oxidation mediated by a flavin (FI) [43].

Sens\* + 
$$R_2S$$
  $\longrightarrow$  Sens +  $R_2S$   $\stackrel{\cdot}{}$ 

Sens +  $O_2$   $\longrightarrow$  Sens +  $O_2$ 
 $O_2$ 
 $O_2$ 
 $O_3$ 
 $O_4$ 
 $O_2$ 
 $O_4$ 
 $O_2$ 
 $O_4$ 
 $O_2$ 

Figure 11. Mechanism of electron transfer sulfides oxidation mediated by a sensitizer [43].

Currently we can only speculate on the thioanisole photooxidation mechanism. Nevertheless we consider the aforementioned non - enzymatic thioanisole oxidation reactions become uncompetitive

in the overall photoenzymatic approach. Therefore, the photoenzymatic thioanisole oxidation in 2LPS results in (*R*)-methyl phenyl sulfoxide at great enantioselectivity (ee 96%).

# **Conclusions and outlook**

Overall, comparably small changes to the initial production system, i.e. application of a surfactant - stabilized two – liquid - phase system, have led to very substantial improvements of the performance of the photobiocatalytic sulfoxidation system. Both, initial rate and robustness of the system could be enhanced significantly leading to an increase of the final product concentration by more than one order of magnitude. Diffusion limitation represents the major challenge to be addressed to achieve optimized reaction conditions with maximized biocatalyst activity and stability.

Further optimization should aim at more advanced emulsions (e.g. thermodynamically stable microemulsions). Medium engineering based on identification of the optimal ratio between organic substrate (solvent) / enzyme/ surfactant has to be elaborated.

Alternatively to surfactants, microgel stabilized emulsion represent an attractive tool for biocatalysis [47]. These microgels are based on polyacrylamide polymers (i.g. poly(N-isopropylacrylamide-co-N-isopropylmethacrylamide) copolymer), which are known to be good emulsion stabilizers depending on temperature and pH value. Consequently, microgel - stabilized smart emulsion can be simply broken via temperature or pH change.

For better understanding of the biocatalysis in emulsion we should clarify various aspects as 1) droplet size distribution, 2) localization of the enzyme, 3) partitioning of a substrate and product between organic and aqueous phase in the presence of surfactant. Moreover for the downstream processes, the emulsion has to be reproducible, stable, and breakable under enzyme optimal conditions.

Obviously enzyme stability represents a challenge for implementation of organic - aqueous emulsion (Figure 7), although the photocatalyst (FMN) stability under the conditions chosen remains to be elucidated. We assume one of the following reasons may explain CPO inactivation: remaining distortion at the organic - aqueous interphase (Figure 7), or certain interaction between CPO and surfactant combined with remained shear force and oxidative influence of  $H_2O_2$ . Additional studies are needed to clarify CPO inactivation. The control of  $H_2O_2$  generation rate based on the optimized ratio between CPO and photocatalyst may result in improved stability and consequently, even better productivities. Also current setup has to be elaborated in order to provide high oxygen concentration for in situ generation of  $H_2O_2$ . Nevertheless simple oxygen saturation of organic phase prior reaction might be a good - enough solution.

Finally it would be interesting to investigate the mechanistic aspects of photosulfoxidations in order to obtain higher productivity without loss of enantioselectivity. Thus the light effect on CPO in organic - aqueous emulsion supplemented with surfactant would be interesting to investigate. Also the control experiment of thioanisole photooxidation mediated by flavin (in the absence of CPO and EDTA) remains to be done. Understanding whether singlet oxygen  $^{1}O_{2}$  or electron transfer mechanism is predominant under the conditions studied may provide ideas how to suppress / regulate undesirable background reactions.

# **Experimental**

## **Chemicals**

All chemicals were purchased from Sigma-Aldrich or Fluka in the highest purity available and used as received. Chloroperoxidase from *Caldariomyces fumago* (E.C. 1.11.1.10) was purchased from Fluka as suspension in 0.1 M sodium phosphate, pH 4 and used as received. The concentration of the enzyme solution was determined specrophotometrically by using  $\epsilon_{400}$  = 91200 M<sup>-1</sup>cm<sup>-1</sup> [48] and contained 13.6 – 31 mg/ml (500-735  $\mu$ M) of protein. CPO specific activity was ~2900 U/ml. One unit forms 1.0 mg of purpurogallin from pyrogallol in 20 seconds at pH 6.0 at 20°C.

#### **Reaction conditions**

Unless mentioned otherwise reactions were performed at 30°C and ambient atmosphere in organic/aqueous emulsion (phase ratio = 1:1 (v/v), working volume 3 - 20 ml), consisting of thioanisole and sodium acetate buffer (50 mM, pH 5.1) containing [FMN] =  $10-250\,\mu\text{M}$ , [CPO] = 0.06 -  $8.00\,\mu\text{M}$ , and 50 mM EDTA. The reaction mixture was exposed to visible light (white light bulb, Philips 7748XHP 200W) and illuminated for  $0.5-30\,\text{h}$  under aerobic conditions and stirred gently (Figure 12). The reaction vessel was made of transparent borosilicate glass (Schott Duran). At intervals, aliquots were withdrawn, centrifuged to separate water and organic phase, extracted with ethyl acetate (containing 5 mM anisole as internal standard) and analyzed via gas chromatography.

Initial rates were determined via the accumulation of (R)-methyl phenyl sulfoxide over time as analyzed by (chiral) gas chromatography. At least three data points were used for the calculation.

It should be mentioned here that all experiments has been performed in triplicates (unfortunately not always sampling at identical times). Therefore, no error bars are given in the figures. Nevertheless, the deviation between the single experiments was maximally 5 - 10% unless mentioned otherwise.

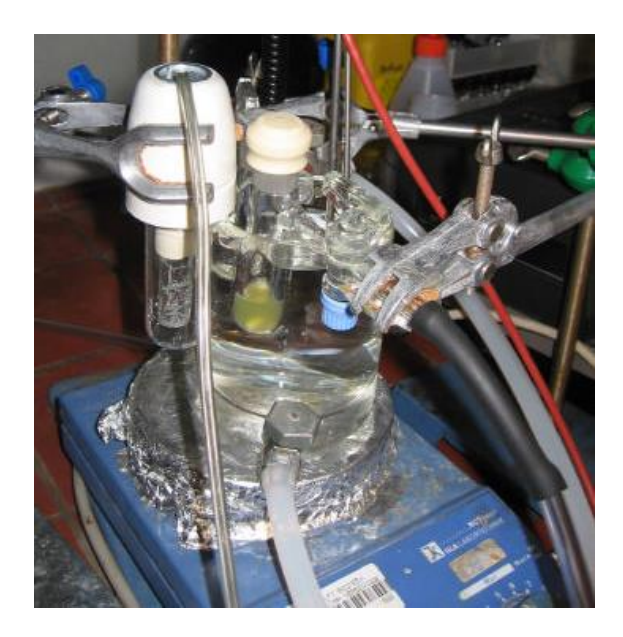


Figure 12. Picture of the experimental setup used in this study.

All control experiments omitting flavin, EDTA, or in darkness were performed under aforementioned conditions. The control experiment using thermally inactivated CPO (4  $\mu$ M) was performed upon CPO incubation at 90°C for 1.5 h.

# Peroxidase activity assay

UV analysis of enzyme activity was performed in disposable UV cuvettes (polystyrene) at 20° C on a Shimadzu UV-2401 PC spectrophotometer with Julabo F12 Refrigerated/Heating Circulator. Peroxidase activity was measured using pyrogallol activity assay following by the increase in absorbance per minute at 420 nm  $^{[49]}$ . The reaction was initiated by the addition of 100  $\mu$ L of CPO solution (ca. 0.7 U/mL) in KPi buffer (100 mM, pH = 6) to a cuvette containing 2.1 ml of MilliQ water, 0.32 ml potassium phosphate buffer solution (100 mM, pH = 6), 0.32 ml pyrogallol water solution (5% w/v) and 0.16 ml of hydrogen peroxide solution (0.5% w/w).

## **Analytical details**

The progress of the reactions was measured by chiral GC and the final concentrations were calculated based on calibration equations using external standards. Chiral GC analysis was performed on a Shimadzu GC 17A with AOC-201 automatic injector using a chiraldex G-TA column ( $50m*0.25mm*0.12~\mu m$ ) that was run at  $120^{\circ}$  C for 4 minutes and at  $175^{\circ}$  C for 8.75 min (column flow: 1.07 ml/min; split ratio: 1/60). Retention times were 3.8 min for thioanisole, 8.44 min for (R) - methyl phenyl sulfoxide, 9.22 min for (S) - methyl phenyl sulfoxide, 13.17 min for methyl phenyl sulfone and 2.45 min for anisole (assigned by authentic standards). The data were processed using GC solution software. A representative chromatogram of a photobiocatalytic sulfoxidation reaction is shown in Figure 13:

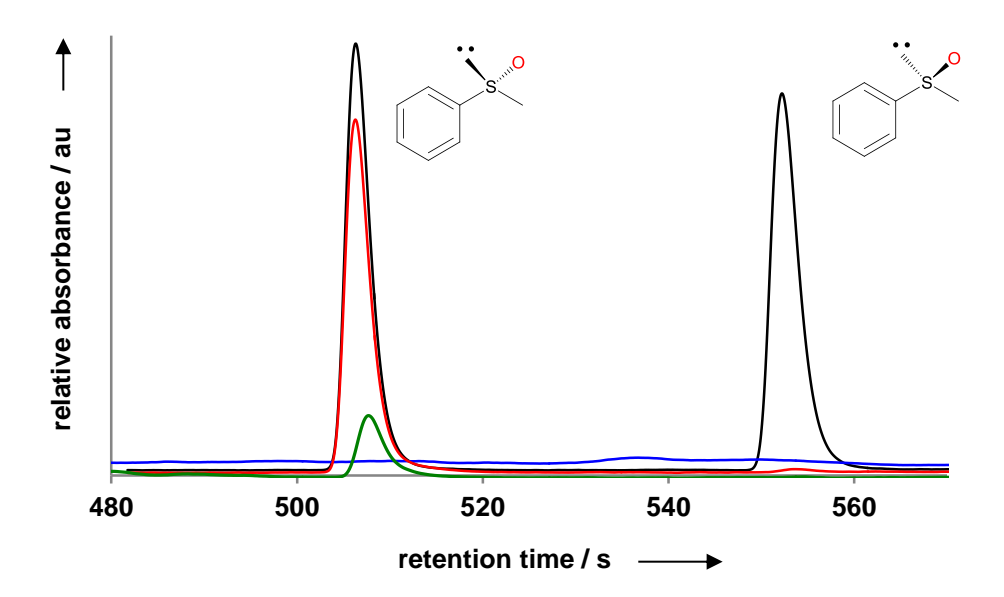


Figure 13. Representative chromatograms of a photobiocatalytic oxyfunctionalization reaction of thioanisol. **Black**: racemic methyl phenyl sulfoxide, **blue**: sample taken at t0, green: sample taken after 50 minutes; **red**: sample taken after 5h.

Enantiomeric excesses (ee,%) were determined as difference in yields between enantiomers:

$$ee, \% = \frac{[(R) - enatiomer] - [(S) - enantiomer]}{[(R) - enatiomer] + [(S) - enantiomer]} \times 100$$

# References

- [1] F. Van Rantwijk, R. A. Sheldon, Selective oxygen transfer catalysed by heme peroxidases: Synthetic and mechanistic aspects, *Curr. Opin. Biotechnol.*, **2000**, *11*, 554-564.
- [2] M. Hofrichter, R. Ullrich, M. J. Pecyna, C. Liers, T. Lundell, New and classic families of secreted fungal heme peroxidases, *Appl. Microbiol. Biotechnol.*, **2010**, *87*, 871–897.
- [3] A. T. Smith, N. C. Veitch, Substrate binding and catalysis in heme peroxidases, *Curr. Opin. Chem. Biol.*, **1998**, *2*, 269-278.
- [4] J. H. Dawson, M. Sono, Cytochrome P-450 and chloroperoxidase: thiolate-ligated heme enzymes. Spectroscopic determination of their active-site structures and mechanistic implications of thiolate ligation, *Chem. Rev.*, **1987**, *87*, 1255-1276.
- [5] B. Valderrama, M. Ayala, R. Vazquez-Duhalt, Suicide inactivation of peroxidases and the challenge of engineering more robust enzymes, *Chem. Biol.*, **2002**, *9*, 555-565.
- [6] J. B. Park, D. S. Clark, Deactivation mechanisms of chloroperoxidase during biotransformations, *Biotechnol. Bioeng.*, **2006**, *93*, 1190-1195.
- [7] H. M. de Hoog, M. Nallani, J. Cornelissen, A. E. Rowan, R. J. M. Nolte, I. Arends, Biocatalytic oxidation by chloroperoxidase from Caldariomyces fumago in polymersome nanoreactors, *Org. Biomol. Chem.*, **2009**, *7*, 4604-4610.
- [8] F. van de Velde, M. Bakker, F. van Rantwijk, G. P. Rai, L. P. Hager, R. A. Sheldon, Engineering chloroperoxidase for activity and stability, *J. Mol. Catal. B-Enzym.*, **2001**, *11*, 765-769.

- [9] F. van de Velde, N. D. Lourenço, M. Bakker, F. van Rantwijk, R. A. Sheldon, Improved operational stability of peroxidases by coimmobilization with glucose oxidase, *Biotechnol. Bioeng.*, **2000**, *69*, 286-291.
- [10] D. I. Perez, F. van Rantwijk, R. A. Sheldon, Cross-Linked Enzyme Aggregates of Chloroperoxidase: Synthesis, Optimization and Characterization, Adv. Synth. Catal., 2009, 351, 2133-2139.
- [11] A. Petri, T. Gambicorti, P. Salvadori, Covalent immobilization of chloroperoxidase on silica gel and properties of the immobilized biocatalyst, *J. Mol. Catal. B: Enzym.*, **2004**, *27*, 103-106.
- [12] V. Trevisan, M. Signoretto, S. Colonna, V. Pironti, G. Strukul, Microencapsulated Chloroperoxidase as a Recyclable Catalyst for the Enantioselective Oxidation of Sulfides with Hydrogen Peroxide, *Angew. Chem.*, **2004**, *116*, 4189-4191.
- [13] F. van de Velde, M. Bakker, F. van Rantwijk, R. A. Sheldon, Chloroperoxidase-catalyzed enantioselective oxidations in hydrophobic organic media, *Biotechnol. Bioeng.*, **2001**, *72*, 523-529.
- [14] G. P. Rai, S. Sakai, A. M. Florez, L. Mogollon, L. P. Hager, Directed evolution of chloroperoxidase for improved epoxidation and chlorination catalysis, *Adv. Synth. Catal.*, **2001**, *343*, 638-645.
- [15] K. Seelbach, M. P. J. vanDeurzen, F. vanRantwijk, R. A. Sheldon, U. Kragl, Improvement of the total turnover number and space-time yield for chloroperoxidase catalyzed oxidation, *Biotechnol. Bioeng.*, **1997**, *55*, 283-288.
- [16] M. P. J. Van Deurzen, K. Seelbach, F. Van Rantwijk, U. Kragl, R. A. Sheldon, Chloroperoxidase: Use of a hydrogen peroxide-stat for controlling reactions and improving enzyme performance, *Biocatal. Biotransform.*, **1997**, *15*, 1-16.
- [17] S. K. Karmee, C. Roosen, C. Kohlmann, S. Lutz, L. Greiner, W. Leitner, Chemo-enzymatic cascade oxidation in supercritical carbon dioxide/water biphasic media, *Green Chem.*, **2009**, *11*, 1052-1055.
- [18] F. Hollmann, A. Schmid, Towards Cp\*Rh(bpy)(H2O)(2+)-promoted P450 catalysis: Direct regeneration of CytC, *J. Inorg. Biochem.*, **2009**, *103*, 313-315.
- [19] D. I. Perez, M. M. Grau, I. W. C. E. Arends, F. Hollmann, Visible light-driven and chloroperoxidase-catalyzed oxygenation reactions, *Chem Commun*, **2009**, 6848-6850.
- [20] T. Krieg, S. Huttmann, K.-M. Mangold, J. Schrader, D. Holtmann, Gas diffusion electrode as novel reaction system for an electro-enzymatic process with chloroperoxidase, *Green Chem.*, 2011, 13, 2686-2689.
- [21] C. Kohlmann, S. Lutz, Electroenzymatic synthesis of chiral sulfoxides, *Eng. Life Sci.*, **2006**, *6*, 170-174.
- [22] S. Lütz, K. Vuorilehto, A. Liese, Process development for the electroenzymatic synthesis of (R)-methylphenylsulfoxide by use of a 3-dimensional electrode, *Biotechnol. Bioeng.*, **2007**, *98*, 525-534.
- [23] R. Taboada-Puig, C. Junghanns, P. Demarche, M. T. Moreira, G. Feijoo, J. M. Lema, S. N. Agathos, Combined cross-linked enzyme aggregates from versatile peroxidase and glucose oxidase: Production, partial characterization and application for the elimination of endocrine disruptors, *Bioresour. Technol.*, **2011**, *102*, 6593-6599.
- [24] H. Uyama, H. Kurioka, S. Kobayashi, Novel bienzymatic catalysis system for oxidative polymerization of phenols, *Polymer Journal*, **1997**, *29*, 190-192.

- [25] W. A. Loughlin, D. B. Hawkes, Effect of organic solvents on a chloroperoxidase biotransformation, *Bioresour. Technol.*, **2000**, *71*, 167-172.
- [26] M. P. J. van Deurzen, I. J. Remkes, F. van Rantwijk, R. A. Sheldon, Chloroperoxidase catalyzed oxidations in t-butyl alcohol/water mixtures, *J. Mol. Catal. A: Chem.*, **1997**, *117*, 329-337.
- [27] E. J. Allain, L. P. Hager, L. Deng, E. N. Jacobsen, Highly enantioselective epoxidation of disubstituted alkenes with hydrogen peroxide catalyzed by chloroperoxidase, *J. Am. Chem. Soc.*, **1993**, *115*, 4415-4416.
- [28] C. Kohlmann, L. Greiner, W. Leitner, C. Wandrey, S. Luutz, Ionic Liquids as Performance Additives for Electroenzymatic Syntheses, *Chem. Eur. J.*, **2009**, *15*, 11692-11700.
- [29] C. Sanfilippo, N. D'Antona, G. Nicolosi, Chloroperoxidase from Caldariomyces fumago is active in the presence of an ionic liquid as co-solvent, *Biotechnol. Lett.*, **2004**, *26*, 1815-1819.
- [30] R. J. Lichtenecker, W. Schmid, Application of various ionic liquids as cosolvents for chloroperoxidase- catalysed biotransformations, *Monatsh. Chem.*, **2009**, *140*, 509-512.
- [31] K. Ryu, J. S. Dordick, How do organic solvents affect peroxidase structure and function?, *Biochem.*, **1992**, *31*, 2588-2598.
- [32] P. A. Fitzpatrick, A. M. Klibanov, How can the solvent affect enzyme enantioselectivity?, *J. Am. Chem. Soc.*, **1991**, *113*, 3166-3171.
- [33] S. Wenda, S. Illner, A. Mell, U. Kragl, Industrial biotechnology-the future of green chemistry?, *Green Chem.*, **2011**, *13*, 3007-3047.
- [34] E. Kiljunen, L. T. Kanerva, Chloroperoxidase-catalysed oxidation of alcohols to aldehydes, *J. Mol. Catal. B: Enzym.*, **2000**, *9*, 163-172.
- [35] G. Zhu, P. Wang, Novel interface-binding chloroperoxidase for interfacial epoxidation of styrene, *J. Biotechnol.*, **2005**, *117*, 195-202.
- [36] J. B. Park, D. S. Clark, New reaction system for hydrocarbon oxidation by chloroperoxidase, *Biotechnol. Bioeng.*, **2006**, *94*, 189-192.
- [37] W. Wang, Y. Xu, D. I. C. Wang, Z. Li, Recyclable Nanobiocatalyst for Enantioselective Sulfoxidation: Facile Fabrication and High Performance of Chloroperoxidase-Coated Magnetic Nanoparticles with Iron Oxide Core and Polymer Shell, J. Am. Chem. Soc., 2009, 131, 12892-12893.
- [38] C. Roberge, D. Amos, D. Pollard, P. Devine, Preparation and application of cross-linked aggregates of chloroperoxidase with enhanced hydrogen peroxide tolerance, *J. Mol. Catal. B: Enzym.*, **2009**, *56*, 41-45.
- [39] D. Jung, M. Paradiso, D. Wallacher, A. Brandt, M. Hartmann, Formation of Cross-Linked Chloroperoxidase Aggregates in the Pores of Mesocellular Foams: Characterization by SANS and Catalytic Properties, *ChemSusChem*, **2009**, *2*, 161-164.
- [40] N. Grotjohann, A. Janning, R. Eising, In VitroPhotoinactivation of Catalase Isoforms from Cotyledons of Sunflower (Helianthus annuusL.), *Arch. Biochem. Biophys.*, **1997**, *346*, 208-218.
- [41] F. van de Velde, F. van Rantwijk, R. A. Sheldon, Selective oxidations with molecular oxygen, catalyzed by chloroperoxidase in the presence of a reductant, *J. Mol. Catal. B-Enzym.*, **1999**, *6*, 453-461.
- [42] P. Pasta, G. Carrea, E. Monzani, N. Gaggero, S. Colonna, Chloroperoxidase-catalyzed enantioselective oxidation of methyl phenyl sulfide with dihydroxyfumaric acid oxygen or ascorbic acid oxygen as oxidants, *Biotechnol. Bioeng.*, **1999**, *62*, 489-493.

- [43] J. Dad'ova, E. Svobodova, M. Sikorski, B. Konig, R. Cibulka, Photooxidation of Sulfides to Sulfoxides Mediated by Tetra-O-Acetylriboflavin and Visible Light, *ChemCatChem*, **2012**, *4*, 620-623.
- [44] P. L. Luisi, Enzymes Hosted in Reverse Micelles in Hydrocarbon Solution, *Angew. Chem. Int. Ed. Engl.*, **1985**, *24*, 439-450.
- [45] E. Baciocchi, T. D. Giacco, F. Elisei, M. F. Gerini, M. Guerra, A. Lapi, P. Liberali, Electron Transfer and Singlet Oxygen Mechanisms in the Photooxygenation of Dibutyl Sulfide and Thioanisole in MeCN Sensitized by N-Methylquinolinium Tetrafluoborate and 9,10-Dicyanoanthracene. The Probable Involvement of a Thiadioxirane Intermediate in Electron Transfer Photooxygenations, *J. Am. Chem. Soc.*, **2003**, *125*, 16444-16454.
- [46] S. M. Bonesi, A. Albini, Effect of Protic Cosolvents on the Photooxygenation of Diethyl Sulfide, *J. Org. Chem*, **2000**, *65*, 4532-4536.
- [47] S. Wiese, A. C. Spiess, W. Richtering, Microgel-stabilized smart emulsions for biocatalysis, *Angew. Chem. Int. Ed. Engl.*, **2013**, *52*, 576-579.
- [48] E. Gonzalezvergara, D. C. Ales, H. M. Goff, A simple, rapid, high yield isolation and purification procedure for chloroperoxidase isoenzymes, *Prep. Biochem.*, **1985**, *15*, 335-348.
- [49] B. Chance, A. C. Maehly, The assay of catalases and peroxidases, *Methods Enzymol.*, **1955**, *2*, 764-775.

# Chapter 3

# Specific photobiocatalytic oxyfunctionalization reactions

This chapter is based on E. Churakova, M. Kluge, R. Ullrich, I. Arends, M. Hofrichter, F. Hollmann,

Angew. Chem. Int. Ed., 2011, 50, 10716-10719

# Chapter 3

# Specific photobiocatalytic oxyfunctionalization reactions

# Introduction

Specific oxyfunctionalization chemistry requires a delicate balance between reactivity and selectivity and therefore still represents a major challenge in organic chemistry [1-2]. Transition metal catalysis is widely applied for selective oxidation of non-activated C-H bonds, benzylic hydroxylation and epoxidation reactions [3-7]. The disadvantage of these processes is the use environmentally problematic heavy metals, stoichiometric amount of oxidants and harsh reaction conditions that often affect the preparation of labile products. Moreover the selectivity of these catalysts often remains below the requirements for pharmaceuticals or fine chemicals, although there are successful examples in asymmetric epoxidation [8].

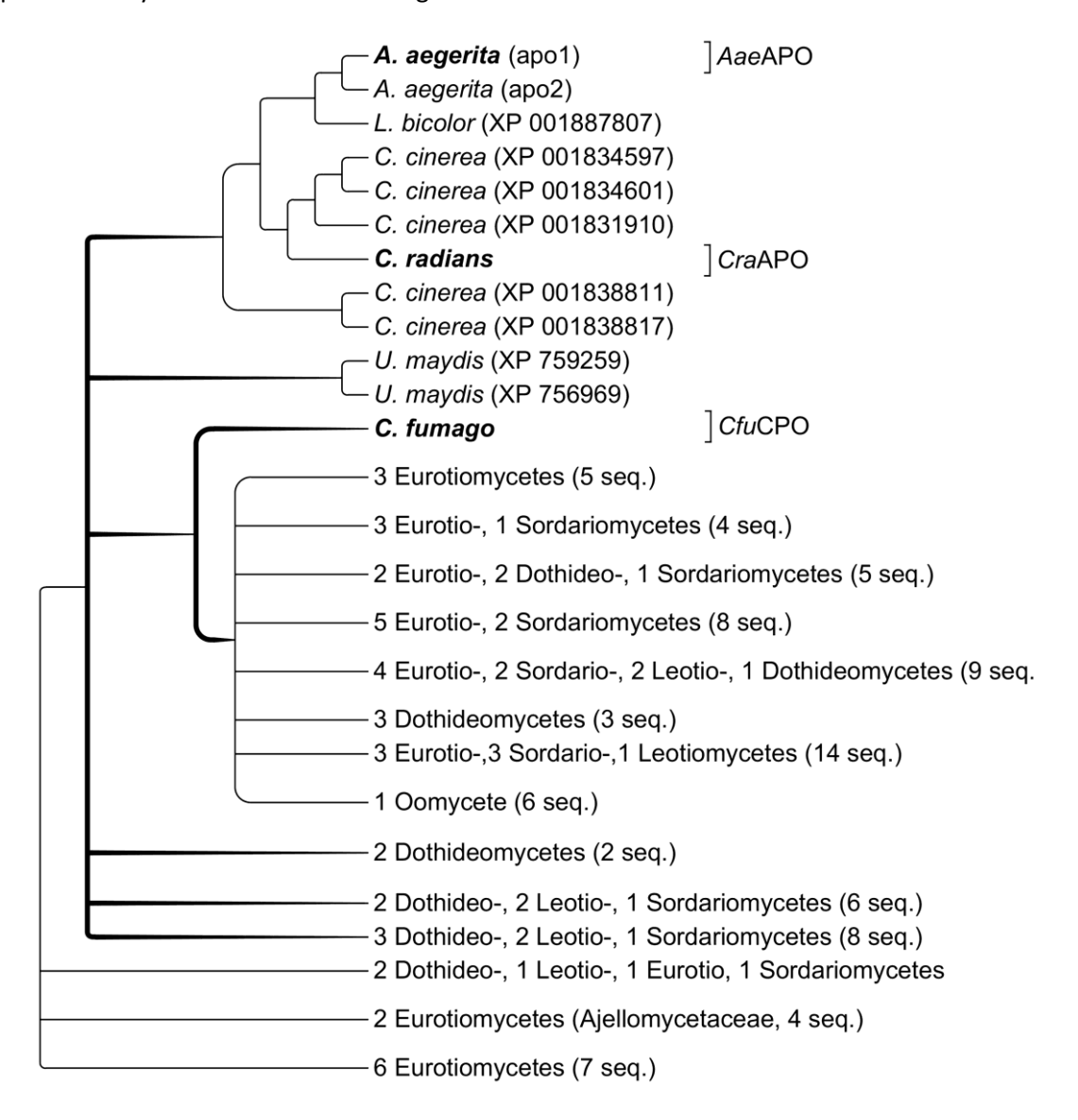
In recent years, biocatalytic transformation became more popular in the field of oxyfunctionalizations due to their high specificities and lower environmental impact. Cytochrome P450 monooxygenases (P450s) are widely considered as catalysts of choice in enzymatic oxyfunctionalization reactions. Here, the reactive oxo - ferryl species (Compound I) is embedded in the defined three dimensional protein structure enabling regio-, chemo-, and enantioselective oxyfunctionalization reactions even on non-activated hydrocarbons [Chapter 1], [9-12]. Their practical application, however, is limited to whole-cell biotransformations due to their cofactor dependency and their complex molecular architecture [Chapter 1], [Chapter 5], [13-14]. But microbial transformations are not always straight-forward to perform and might suffer from intrinsic disadvantages such as reactant metabolization and – toxicity and often low productivities.

Great hope has been placed on the protein superfamily of heme - thiolate peroxidases to solve both challenges, the cofactor dependency as well as the complicated molecular architecture of P450s by using the hydrogen peroxide shunt  $^{[15-17]}$ . Here, the catalytically active oxo - ferryl species are formed directly from  $H_2O_2$  instead of reductive activation of  $O_2$ . This allows a simple circumvention of the above - mentioned challenges and enables practical oxyfunctionalization procedures. Chloroperoxidase (CPO) from *Caldariomyces fumago* (*Leptoxyphium fumago*) represents the archetype of such heme - thiolate peroxidases  $^{[18-20]}$ .

Unfortunately, CPO is active in sulfoxidation reactions only whereas its performance in hydroxylation of C-H bonds and epoxidation reactions drops by several orders of magnitude <sup>[15-17]</sup>. Generally, CPO only performs a few hundred to thousands turnovers prior to loss of catalytic activity (vide infra).

Non-activated hydrocarbons such as cyclohexane are not converted by CPO at all <sup>[15-17]</sup>. Obviously, this disqualifies CPO as a broadly applicable catalyst for oxyfunctionalization chemistry.

Nowadays, with more and more genome sequences becoming available, today more than 100 putative heme-thiolate CPO-analogues can be found in nucleotide databases (Scheme 1) [16-17]. Hence, there is a wealth of potential alternatives to CPO with potentially more suitable catalytic properties in oxyfunctionalization waiting to be discovered!

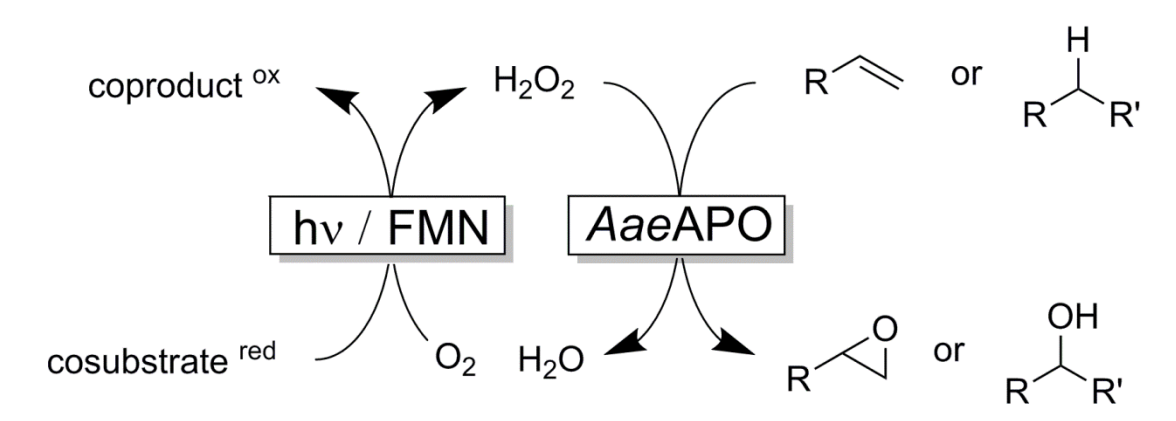


Scheme 1. Simplified phylogenetic tree of the heme - thiolate peroxygenase superfamily. The names highlighted in bold refer to fungal species whose heme - thiolate enzymes have been purified and characterized. The other terms belong to taxonomic units of the fungal kingdom with putative CPO-/AaePO-like proteins found in databases [17].

Recently, a novel peroxidase from the basidomycetous fungus *Agrocybe aegerita* (*Aae*APO - *Agrocybe aegerita* aromatic peroxygenase) has been isolated and characterized <sup>[21-27]</sup>. *Aae*APO specifically converts aromatic hydrocarbons into the corresponding phenols and has been classified as 'unspecific peroxygenase' in the E.C. nomenclature (E.C.1.11.2.1).

Here we report that *Aae*APO is an active and versatile catalyst for enantioselective hydroxylation and epoxidation reactions. Furthermore, we demonstrate that *Aae*APO, in contrast to CPO, can also hydroxylate non-activated C-H bonds.

Since AaeAPO, like all heme-dependent enzymes, is easily inactivated by  $H_2O_2$  (vide infra), strict control over the  $H_2O_2$  concentration is essential. Therefore, we chose to provide  $H_2O_2$  using our recently developed photochemical in situ  $H_2O_2$  generation system [Chapter 2]. Overall, a photobiocatalytic oxyfunctionalization system was set up (Scheme 2).



Scheme 2. Photoenzymatic oxyfunctionalization. *Aae*APO: *Agrocybe aegerita* aromatic peroxygenase; FMN: flavin mononucleotide; hv: visible light

#### Results and discussion

Enantiopure  $\alpha$ -hydroxyalkylbenzenes are of great importance for the production of fine chemicals and drug precursors <sup>[8]</sup>. Therefore, the substrate scope for the light-driven and AaeAPO-mediated hydroxylation reactions was investigated.

In a first set of experiments we investigated the AaeAPO-catalyzed hydroxylation of ethylbenzene. We chose flavin adenine mononucleotide (FMN, 50  $\mu$ M) as a photocatalyst. Unless stated otherwise, EDTA (1 - 10 mM) served as stoichiometric source of reducing equivalents (co-substrate). Upon illumination with visible light the photoexcited flavin oxidizes EDTA; the reduced flavin is then reoxidized by molecular oxygen (from ambient atmosphere) forming  $H_2O_2$  which is utilized by AaeAPO (40 nM) for oxyfunctionalization (Scheme 2).

Rewardingly, a high degree of regio- enantio- and chemoselectivity was observed: (*R*)-1-phenylethanol was obtained in greater than 97% optical purity as the sole product (Table 1, entry 1). Further oxidation to acetophenone was observed only after complete depletion of ethylbenzene. Noteworthy, the second oxidation step proceeded at significantly decreased rate (less than 5% of the initial hydroxylation rate, Table 1, entry 1).

Compared to stoichiometric use of  $H_2O_2$ , the photochemical in situ  $H_2O_2$  generation method yielded somewhat lower rates (approx. one third, Table 1, entry 2). This was compensated by the increased robustness of the enzymatic hydroxylation reaction: while AaeAPO lost more than 75% of its initial activity already in the first 10 minutes using stoichiometric amounts of  $H_2O_2$ , stable activity was observed for at least 5 hours with in situ  $H_2O_2$  generation.

Table 1. Photoenzymatic hydroxylation reactions.

	Product	TF(AaeAPO) [min <sup>-1</sup> ] <sup>[a]</sup>	TN(AaeAPO)	ee(R) [%] <sup>[b]</sup>	Substrate [mM]
1	ÕН	494 (14)	18080	> 97	10
<b>2</b> <sup>[c]</sup>		1252 (138)	6000	97	10
3	QH -	270 (6)	6430	93	1
4	H <sub>3</sub> CO QH	385 (18)	17260	90	1
5	CI	303 (12)	11500	> 99	1
6	QH	366 (6)	17520	85	1
7	ОН	105 (25)	10700		5
8 <sup>[d]</sup>		180 (15)	39200	-	2 LPS
9	OH	182 (17)	17900	-	5
10	OH §	8.4 (0.6)	1040	n.d.	5

[a] Values in parentheses denote overoxidation rates observed upon complete conversion of the starting materials; [b] Determined by chiral GC or HPLC; [c] results from stoichiometric use of  $H_2O_2$ ; [d] results from the conversion in biphasic setup; 2 LPS – two liquid phase system; n.d. – not determined, TF – turnover frequency, TN - turnover number.

We additionally characterized the influence of the single reaction components on the rate of the photoenzymatic hydroxylation reaction. As expected, increasing the light intensity as well as FMN concentration increased the overall reaction rate, whereas [EDTA] had only a negligible effect. This supports the assumption that the concentration of in situ generated photoexcited FMN is overall rate limiting. It should be noted that beyond a FMN concentration of ca. 0.05 mM no significant increase

of the hydroxylation rate was observed (Figure 1). This can be attributed to fast depletion of dissolved molecular oxygen. The phase-transfer of  $O_2$  into the reaction phase then becomes overall rate limiting.

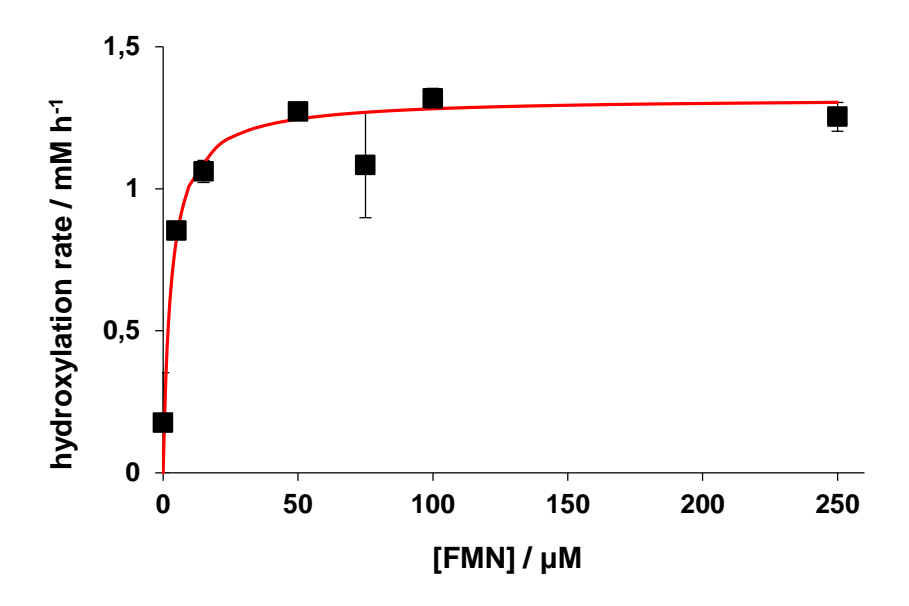


Figure 1. Influence of [FMN] on the (initial) rate of the photobiocatalytic hydroxylation system (at the example of using ethylbenzene as substrate). General conditions: [ethylbenzene] = 1 mM, [AaeAPO] = 0.04  $\mu$ M; [ascorbic acid] = 10 mM (vide infra); [acetonitrile] = 10% (v/v); KP<sub>i</sub> buffer 50 mM, pH = 7; V=5 mL; T = 30°C.

Like ethylbenzene, a range of derivatives was also converted at similarly high rate and selectivity (Table 1 entries 3 - 7). In any case alkyl benzenes were converted smoothly in the benzylic position with good to excellent enantioselectivities. The overoxidation rate to the corresponding ketones was negligibly slow and was observed only upon almost full consumption of the initial substrate. The exemplary time course of 1-chloro-4-ethylbenzene hydroxylation is shown on Figure 2.

In case of toluene, slow accumulation of the aldehyde product and traces of benzoic acid were observed upon full consumption of the starting material. Also *p*-cresol and *o*-cresol were found as side products demonstrating the aromatic hydroxylation activity of *Aae*APO. Benzene derivatives with longer side chain were exclusively attacked at the benzylic carbon.

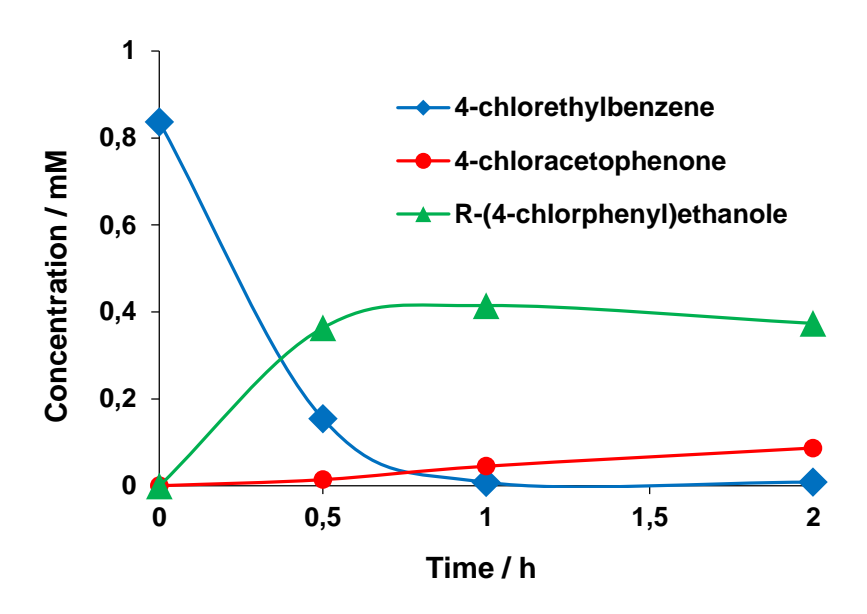


Figure 2. Time course of 1-chloro-4-ethylbenzene hydroxylation. General conditions: [1-chloro-4-ethylbenzene] = 1 mM,  $[AaeAPO] = 0.04 \mu M$ ;  $[FMN] = 50 \mu M$ , [EDTA] = 1 mM; light; phosphate buffer 50mM, pH = 7; [acetonitrile] = 10% (v/v);  $T = 30^{\circ} C$ 

More interestingly, also non-activated alkanes such as cyclohexane and n-octane were converted by AaeAPO (Table 1, entries 9 - 10). Cyclohexane was hydroxylated at approximately 50% of the rate of alkylbenzenes with a slightly increased relative overoxidation rate (approx. 9% of the initial hydroxylation rate), which again only occurred at almost full consumption of the initial starting material. In contrast, n-octane was converted rather sluggishly with decreased regioselectivity. We could ascertain the formation of 2-octanol, traces of 2-octanone and one unidentified product. These results are in good agreement with recent report for AaeAPO catalyzed octane hydroxylation with the formation of (R)-2-octanol (51% ee) and (R)-3-octanol (99.9% ee)  $^{[28]}$ .

Interestingly, although ethylbenzene was exclusively converted to (*R*)-1-phenylethanol, *Aea*APO did not show selectivity for the oxidation of the racemic mixture of 1-phenylethanol. I.e. both enantiomers were converted to acetophenone at the same rate (Figure 3). The control experiment under identical conditions in the absence of the biocatalyst did not show any conversion of 1-phenylethanol. Currently, we are lacking a plausible explanation for this non-selective activity of *Aae*APO. Further experiments involving mechanistic studies and computer simulations (the docking of the 1-phenylethanol to the enzyme active site) may clarify this observation.

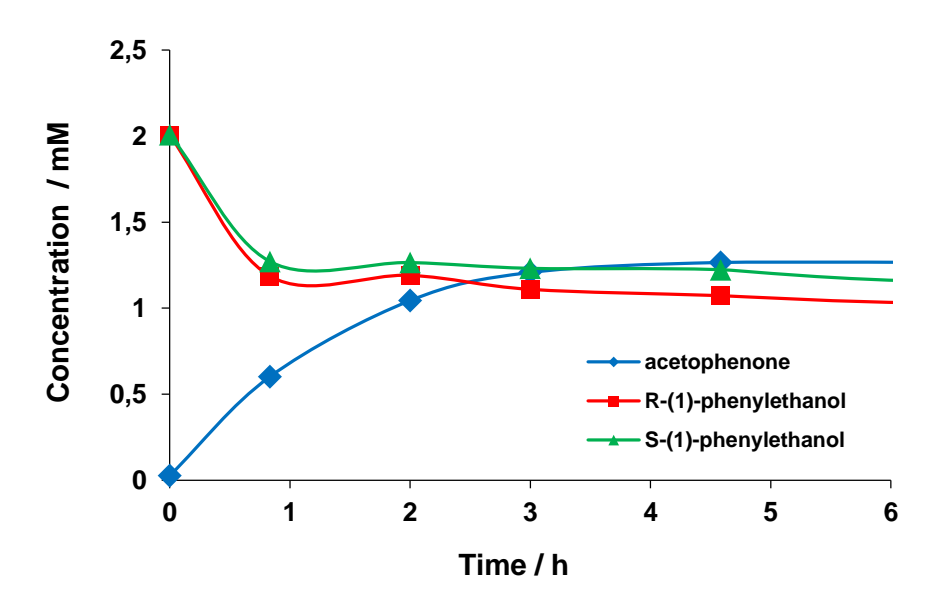


Figure 3. 1 - Phenylethanol oxidation by AaeAPO in photoenzymatic approach. General conditions: [1 - phenylethanol] = 5 mM, [AaeAPO] = 0.04  $\mu$ M; [FMN] = 50  $\mu$ M, [EDTA] = 5 mM; light; V = 10 mL; phosphate buffer 50 mM, pH=7; [acetonitrile] = 10% (v/v); T = 30 °C

Next, we evaluated the performance of the photoenzymatic system in epoxidation reactions. As model substances we chose styrene and its derivatives. As shown in Table 2, there was a distinct dependency of activity and selectivity on the substitution pattern of the C=C-double bond. Terminal alkenes were converted at reasonable rates albeit poor enantioselectivity. *Cis*-ß-methyl styrene was converted efficiently while its *trans*-isomer was converted at less than 1% of the rate of the *cis*-isomer. Steric repulsion between the methyl group of *trans*-ß-methyl styrene and porphyrin plane, which makes the coordination less favourable, was reported by Grove and co-authors <sup>[29]</sup>. Recent studies of Hofrichter and co-authors reported the oxidation of *trans*-ß-methyl styrene by *Aae*APO preferably at the terminal position and only in poor extent <sup>[30]</sup>. This implies that *trans*-ß-methyl styrene is restricted entering *Aae*APO active site in a way to facilitate the contact of the alkene bond and Compound I. It is worth mentioning here, that styrene oxides were the only products detectable in our experiments.

Aliphatic alkenes were converted less specifically. For example, cyclohexene was converted to corresponding epoxide and allylic alcohol at a ratio of approximately 2 to 1 (Table 2). Similarly, conversion of (R)-limonene and 1-octene yielded complex product mixtures. Here the allylic hydroxylation and/or epoxidation combined with hydrolysis products is likely to give rise to these (undesired) side products. Recently, Hofrichter and co-authors reported a distinct selectivity for (S)-enantiomer in epoxidation of several linear 1-alkenes, although allylic hydroxylation also was observed. Thus 1-octene oxidation yielded 55% of (S)-1,2-epoxyoctane (S)-1,2-epoxyoctane (S)-1,2-epoxyolimonene (S)-1,2-epoxylimonene (S)-1,2-epoxylimonen

ratio 154:1), (+)-8,9-epoxylimonene and (+)-mentha-6,8-dien-2-ol (*cis:trans* ratio 6:1) for (*R*)-limonene oxidation with a products ratio of 1.9:1.25:1 [31].

Table 2. Photoenzymatic epoxidation reactions.

	Product	TF(AaeAPO) [min <sup>-1</sup> ]	TN(AaeAPO)	ee [%]	Substrate [mM]
1	Tro O	92	10390	4.6 (n.d.)	10
2	r <sub>O</sub>	28	1830	40 (n.d.)	1
3		<5	<100	50 (n.d.)	1
4	<u>o</u>	228	4730	>99% (n.d.)	1
5	OH SH	181 / 80	3970 / 1980	- / n.d.	1

Under the non-optimized conditions we determined a TNs of at least 10000 for AaeAPO in hydroxylations of ethylbenzene derivatives. In comparison, the TNs determined for CPO generally are 1-2 orders of magnitude lower in hydroxylation and epoxidation reactions <sup>[15, 20, 32]</sup>. Few thousands of TNs for CPO in epoxidation reactions were achieved only under optimized conditions <sup>[33-34]</sup>. For example, 12000 TNs were obtained for styrene epoxidation in a two liquid phase system <sup>[34]</sup>. Substituting AaeAPO with CPO in our hands did not yield any product formation neither for ethylbenzene hydroxylation nor styrene epoxidation. It should be mentioned here, that we used CPO in the same concentration as AaeAPO (40 nM) whereas the CPO-based epoxidation methods generally utilized more than 100-fold higher CPO concentrations (1-10  $\mu$ M) <sup>[19, 35]</sup>. Furthermore, to the best of our knowledge, no CPO-catalyzed oxidation of non-activated alkanes such as cyclohexane or octane has been reported yet.

In contrast to CPO, AaeAPO was not a very efficient sulfoxidation catalyst. Using thioanisole as substrate, a TF (AaeAPO) of only 35 min<sup>-1</sup> with decreased enantioselectivity (ee < 70%) was observed.

Such a striking difference in the oxygenation/hydroxylation activity between *Aae*APO and CPO might be due to the significant difference in the substrate positioning/binding in the enzyme active site or the difference in redox potentials of heme - thiolate proteins. Recent studies showed similarity of *Aae*APO and CPO around the active site, but also considerable difference in the heme channel and its amino acids <sup>[21]</sup>. *Aae*APO structural studies revealed the funnel shaped tunnel leading from the protein surface to the active site. This tunnel contains several phenylalanine and other apolar residues that make it favorable for hydrophobic substrates. This molecular architecture may explain the failure of converting hydrophilic substrates as hydroxymethylfurfural.

In spite of high TNs, preparative application of *Aae*APO catalyzed transformation is limited by very poor solubility and high volatility of organic substrate. To overcome this restriction we performed photoenzymatic oxyfunctionalization of several substrates in two liquid phase system (2 LPS). Here the enzyme, photocatalyst (FMN) and electron donor are dissolved in the aqueous phase, while the hydrophobic substrate is present at high concentration in the organic phase. As a second organic phase we applied pure substrate avoiding the supplementary co-solvent in the system. The overall system was complemented with dioctyl sulfosuccinate surfactant. This approach has been successfully applied previously, e.g. for styrene and thioanisole oxifunctionalizations catalyzed by CPO [Chapter 2], [34].

Toluene conversion in 2 LPS was promising compared to monophasic set up as both, initial rate and TNs were enhanced (Table 1, entry 8). However aromatic hydroxylation became more pronounced in 2 LPS yielding considerable amount of *o*- and *p*-cresol together with benzyl alcohol. Similarly epoxidation of *cis*-ß-methyl styrene in 2LPS yielded twice as high TNs in comparison to the monophasic system without loss of enantioselectivity. However, the product formation ceased in less than 1 hour.

More than 200000 turnovers for *Aae*APO were achieved in the two phase system for ethylbenzene hydroxylation over 5 hours, however enantioselectivity was significantly impaired resulting in racemic 1-phenylethanol. Moreover, the overoxidation became more pronounced in the two phase system yielding acetophenone as a dominant product. This result can be expected as the aqueous solubility of the product – 1-phenylethanol is higher than the solubility of ethylbenzene. Therefore 1-phenylethanol becomes the more accessible substrate for further biotransformation.

The loss of enantioselectivity in ethylbenzene/buffer biphasic system however is not clear. Most probably the enzyme changes its conformation upon exposure to hydrophobic substrate losing its stereospecificity. Preliminary results using immobilized *Aae*APO in sol-gel indicate that the

enantioselectivity in 2 LPS might be significantly improved resulting in (R)-1-phenylethanol with optical purity of 70% (ee), although acetophenone remains as a main product.

Finally, we evaluated some alternatives to EDTA as the sacrificial electron donor. So far EDTA has been our preferred co-substrate since it is commercially available and simple to apply. From an environmental point of view however, EDTA is somewhat questionable since it is oxidized to toxic co-products - formaldehyde and amines. Therefore, we evaluated a range of alternative sacrificial electron donors to promote *Aae*APO-catalyzed hydroxylation of ethylbenzene (Table 3). The enantioselectivity of *Aae*APO was not impaired by any of the sacrificial electron donors. However, reaction rates (expressed as photocatalyst turnover frequencies) differed significantly. Further studies elucidating the electron transfer mechanism will be necessary to clarify the rate-dependency. Nevertheless, substituting EDTA with ascorbic acid seems attractive considering the availability of vitamin C together with the formation of a harmless, if not valuable by-product (Table 3).

Table 3. Photoenzymatic hydroxylation of ethylbenzene using alternative sacrificial electron donors. General conditions: [substrate] = 1 mM, [FMN] = 50  $\mu$ M, [co-substrate] = 1 mM, [AaeAPO] = 40 nM, phosphate buffer (50 mM, pH 7), T = 25°C, reaction time: 3h

	co-substrate	co-products <sup>a</sup>	TF (FMN) [h <sup>-1</sup> ]	ee [%]
1	EDTA	ethylene diamine + 4 eq CO <sub>2</sub> & CH <sub>2</sub> O	19.2	97
2	ascorbic acid	dehydro ascorbic acid	21.8	97
3	NaHCO <sub>2</sub>	CO <sub>2</sub>	3.3	>99
4	hydrazine	$H_2N_2/N_2$	0.5	>99
5	HPO <sub>3</sub>	HPO <sub>4</sub> <sup>2-</sup>	1.2	>99

<sup>&</sup>lt;sup>a</sup> We assume these co-products are formed during the reaction, however we did not establish analytical methods to confirm it.

# **Conclusions and outlook**

Overall, we have demonstrated that the peroxygenase from *Agrocybe aegerita* (*Aae*APO) is a versatile oxyfunctionalization catalyst. Its performance in hydroxylation is unparalleled by chemical catalysts <sup>[2-7]</sup>. In epoxidation, activity and selectivity strongly depend on the substitution pattern of

the C=C-double bond. Nevertheless, *Aae*APO appears to be an interesting tool for the asymmetric epoxidation of alkenes.

In situ production of  $H_2O_2$  via photochemical  $O_2$ -reduction proved to be beneficial to sustain robust oxyfunctionalization activity over several hours. Already under non-optimized reaction conditions enzyme turnover numbers exceed those of comparable systems (P450s and CPO) by several orders of magnitude. Furthermore, preliminary results indicate that hundreds of thousands of turnovers can be achieved after reaction engineering. Therefore, we are convinced that AaeAPO is a preparatively very valuable catalyst that might give a fresh impetus to biocatalytic oxyfunctionalization chemistry.

Further studies will be necessary to substantiate *Aae*APO's full potential for preparative organic chemistry. In this context the application of *Aae*APO catalysis in biphasic system seems attractive. Preliminary studies show the enantioselectivity markedly depends on the solvent. To understand this phenomenon additional experiments using wide range of the solvents have to be done.

Also the full characterization and optimization of the proposed in situ  $H_2O_2$  generation system coupled to biocatalytic transformations in biphasic system are necessary. Thus optimized ratio of flavin /biocatalyst may result in higher reaction rates and better productivities. Furthermore in situ generation of  $H_2O_2$  for preparative applications require high oxygen concentrations. Engineering measures to overcome this technical limitation of the present reaction setup have to be implemented. Bubble free aeration using oxygen-permeable membranes can be one of the solutions to avoid enzyme inactivation by mechanical forces during external oxygen intake [36].

In order to extend the biocatalyst life-time different immobilization techniques would be interesting to test. Hopefully an immobilized catalyst would permit its recycling for even higher TNs, opening doors to industrial applications.

Finally, it would be very interesting to explore further 'new' peroxidases for organic synthesis (Scheme 1) and to rationalize the structural basis for the striking difference in activity between CPO and AaeAPO.

# **Experimental**

## **Materials**

Enzymes: AaeAPO was produced from Agrocybe aegerita following a previously reported purification protocol <sup>[37]</sup>. The stock solution used for all experiments contained AaeAPO (2.8 mg/mL, 60  $\mu$ M) (detected by Bradford assay). CPO (163  $\mu$ M) was purchased from BioChemika and used as received.

Chemicals: All chemicals were purchased from Sigma-Aldrich, Fluka or Acros in the highest purity available and used as received. cis- $\beta$ -methylstyrene oxide,  $\alpha$ -methylstyrene oxide and octene oxide were produced as racemate from corresponding styrenes using m-CPBA by the following procedure. m-CPBA (60 mmol), diethyl ether (100 mL), olefin (58 mmol) were mixed in a flask and stirred on ice for 24h. The reaction mixture was first washed with 10% NaOH solution and then with water until the pH was neutral. The organic phase was separated from the aqueous phase and dried over MgSO<sub>4</sub>. MgSO<sub>4</sub> was filtered off, and mixture of racemic epoxides in diethyl ether was directly used to establish gas chromatography analysis.

#### **General procedure**

Reactions were performed at ambient temperature and ambient atmosphere in 100 mM potassium phosphate buffer pH 7. Unless mentioned otherwise, the reaction mixture contained 1 mM of EDTA (Ethylenedinitrilotetraacetic acid, as sacrificial electron donor), 50 µM FMN (Riboflavin 5'-phosphate, as photocatalyst), and 40 nM AaeAPO. After substrate addition (generally from a 10 mM stock solution in acetonitrile to achieve a final concentration of 1 mM) the reaction mixture was exposed to visible light (Philips 7748XHP 200W, white light bulb) and stirred gently. The experimental setup is shown in [Chapter 2. CPO]. At intervals, aliquots were taken, extracted with ethyl acetate (containing 5 mM anisole as internal standard), dried over MgSO<sub>4</sub> and analyzed by GC or HPLC (vide infra). Styrene/ styrene derivatives, octene and corresponding epoxides were extracted by diethylether (containing 5 mM anisole as internal standard). Cyclohexane, cyclohexanole and cyclohexanone were extracted by octane (containing dodecane as internal standard). Cyclohexene and cyclohexene oxide were extracted by dichlormethane (containing anisole as internal standard). Propylbenzene, 4-chlorethylbenzene, tetralin and corresponding products were extracted by heptane (containing anisole as internal standard).

Reactions in two phase system consisted of organic phase (toluene, ethylbenzene, cis- $\beta$ -methylstyrene) and potassium phospahte buffer (50 mM, pH 7) (phase ratio = 1:1, working volume 10.42 ml), containing aqueous concentrations of [FMN] = 50  $\mu$ M (flavin mononucleotide), [AaeAPO] = 0.04  $\mu$ M, and EDTA = 5 mM as sacrificial electron donor. At intervals, aliquots of aqueous-organic emulsion were taken, extracted with ethyl acetate (containing 5 mM anisole as internal standardand centrifuged for phase separation; organic phase was dried over MgSO<sub>4</sub> and analyzed by GC.

The experimental setup chosen for these experiments suffered for significant evaporation of the starting materials and products. Typically after 2-3 hours all starting material was consumed and only

the (less volatile) products could be observed. Therefore, we decided to express the catalyst performance as turnover numbers (TN) and - frequencies (TF):

$$TN = \frac{mol(product)}{mol(catalyst)} \left[ mol * mol^{-1} \right]$$

$$TF = \frac{TN}{time}$$
 [h<sup>-1</sup>]; time period corresponds to the linear reaction rate

It should be mentioned here that the given TNs do not reflect the actual catalyst (*Aae*APO or FMN) lifetime or stability under these conditions. As mentioned above, evaporation typically limited the reaction time and product formation. Thus, TNs and TOFs are based on a conservative estimation. Under more controlled reaction conditions, these numbers are likely to be higher.

# **Analytical procedures**

The reaction progress as well as the optical purity of the products was determined using chiral GC or chiral HPLC.

For ethylbenzene, octane, cyclohexane, cyclohexene, limonene, styrene, styrene derivatives, toluene and thioanisole oxidation, chiral GC analysis was performed on a Shimadzu GC 17A with AOC-201 automatic injector using a chiraldex G-TA column ( $50m \times 0.25mm \times 0.12$  um). The data was processed using GC solution (Table 4).

Table 4: Details for the GC analysis.

Compound	Retention time [min]	Method <sup>[a]</sup>	flow [ml×min <sup>-1</sup> ]	split ratio
S	2.20	А	1.2	1/60
S.,, (R)	7. 88	А	1.2	1/60
(5)	10.60	А	1.2	1/60
	3.58	В	0.6	1/50
	12.67	В	0.6	1/50

OH (S)	14.68	В	0.6	1/50
OH (R)	15.52	В	0.6	1/50
	4.05	В	0.6	1/50
(5)	10.54	В	0.6	1/50
(R)	11.98	В	0.6	1/50
	6.06	В	0.6	1/50
	11.04 12.21	В	0.6	1/50
	5.21	В	0.6	1/50
[b]	10.47 12.84	В	0.6	1/50
	12.19	С	0.7	1/100
[b]	46.59 47.92	С	0.7	1/100
\\\\\\\\\\\\\\\\\\\\\\\\\\\\\\\\\\\\\\	2.89	D	0.8	1/20
0	7.84	D	0.8	1/20
OH [c]	8.01	D	0.8	1/20
	2.54	D	0.8	1/20

—он	6.84	D	0.8	1/20
~он	7.73	D	0.8	1/20
=0	7.97	D	0.8	1/20
	2.54	E	0.8	1/20
0	5.35	E	0.8	1/20
	3.07	F	0.6	1/50
	7.29	F	0.6	1/50
ОН	14.10	F	0.6	1/50
ОН	15.47	F	0.6	1/50
но	15.96	F	0.6	1/50

[a] Temperature profiles: A: isothermal at 160 °C for 12.5 minutes followed by increase to 170 °C at 2 °C min<sup>-1</sup>; B: isothermal at 100 °C for 18 minutes followed by increase to 170 °C at 50 °C min<sup>-1</sup>; C: isothermal at 70 °C for 50 minutes followed by increase to 170 °C at 50 °C min<sup>-1</sup>; D: isothermal at 75 °C for 5 minutes followed by increase to 110 °C at 30 °C min<sup>-1</sup>, isothermal for 4 min followed by increase to 170 °C at 30 °C min<sup>-1</sup>; E: isothermal at 75 °C for 6 minutes followed by increase to 170 °C at 30 °C min<sup>-1</sup>; F: isothermal at 100 °C for 14 minutes followed by increase to 170 °C at 70 °C min<sup>-1</sup>. [b] absolute configuration is unknown. [c] enantiomers could not be separated.

For propylbenzene, 4-chlorethylbenzene, tetralin, 4-ethylanisole, toluene oxidation chiral HPLC analysis was performed on a Waters HPLC system (515 pump 486 UV detector 410 RI detector) using a Chiralcel OD column (4.6×250 mm, Daicel 10  $\mu$ m). The temperature was controlled by a Chrompack SpH-99 column oven (Table 5). The eluent was heptane/2-propanol (98/2). Benzoic acid measurements were performed on a Shimadzu LC-20 system with a Shimadzu mSPD-20A Photo Diode Array detector using Xterra column (Rp18 3.5  $\mu$ M, 4.6×150 mm). The eluent was acetonitrile/water (45/55) (Table 5).

Table 5: Details for the HPLC analysis.

Compound	Retention time [min]	Compound	Retention time [min]
	4.68		8.02
	7.38	C O	11.25
OH (R)	12.24	OH (R)	13.58
OH (5)	13.52	OH (S)	16.80
CI	4.77	H <sub>3</sub> CO	4.90
CI	8.63	H <sub>3</sub> CO	10.73
OH (R)	30.82	OH H <sub>3</sub> CO	24.22
OH (S)	33.69	H <sub>3</sub> CO OH	26.03
	4.89	ОН	9.1

#### **Encapsulation of** *Aae***APO within sol - gel matrix**

Encapsulation of *Aae*APO in sol-gel matrix was done following a previously reported protocol <sup>[38]</sup>. Sol was prepared by mixing acidic water (1.38 mL, pH 2.85 adjusted by addition of HCl), methyltrimethoxysilane (MTMS, 98%, Aldrich, 2.19 mL), tetramethoxysilane (TMOS, 98%, Aldrich; 8.89 mL) and distilled water (10.4 mL) in a 100 mL round bottom flask until a homogenous mixture was obtained. Methanol formed during hydrolysis of MTMS and TMOS was continuously removed under vacuum. Then the mixture was cooled to 0 °C on ice and distilled water was added to the initial

volume. Next sol and enzyme as an aqueous solution (1.25 mL of 0.16  $\mu$ M) were mixed in proportion 1:1 (v/v) for enzyme encapsulation. The mixture was stirred for 20 seconds. Magnetic bar was removed and the gel was formed (approx. 5 min). 2 mL of potassium phosphate buffer (50 mM, pH 7) were added and gel with encapsulated proteins was aged at 4°C for 24 hours.

Ethylbenzene hydroxylation using AaeAPO encapsulated in sol-gel (2.5 mL of 0.08  $\mu$ M) was performed in 2LP system consisted of ethylbenzene and potassium phosphate buffer (50 mM, pH 7) (phase ratio = 1:1, working volume 2.5 ml), containing aqueous concentrations of [FMN] = 50  $\mu$ M and 35 mM ascorbic acid as sacrificial electron donor. At intervals, aliquots of aqueous-organic emulsion were taken, extracted with ethyl acetate (containing 5 mM anisole as internal standard) and centrifuged for phase separation; organic phase was dried over MgSO<sub>4</sub> and analyzed by GC.

#### References

- [1] E. Gonzalezvergara, D. C. Ales, H. M. Goff, A simple, rapid, high yield isolation and purification procedure for chloroperoxidase isoenzymes, *Prep. Biochem.*, **1985**, *15*, 335-348.
- [2] D. Monti, G. Ottolina, G. Carrea, S. Riva, Redox Reactions Catalyzed by Isolated Enzymes, *Chem. Rev.*, **2011**, *111*, 4111-4140.
- [3] K. Schröder, B. Join, A. J. Amali, K. Junge, X. Ribas, M. Costas, M. Beller, A Biomimetic Iron Catalyst for the Epoxidation of Olefins with Molecular Oxygen at Room Temperature, *Angew. Chem. Int. Ed.*, **2011**, *50*, 1425-1429.
- [4] B. A. Arndtsen, R. G. Bergman, Unusually Mild and Selective Hydrocarbon C-H Bond Activation with Positively Charged Iridium(III) Complexes, *Science*, **1995**, *270*, 1970-1973.
- [5] S. E. Bromberg, H. Yang, M. C. Asplund, T. Lian, B. K. McNamara, K. T. Kotz, J. S. Yeston, M. Wilkens, H. Frei, R. G. Bergman, C. B. Harris, The mechanism of a C-H bond activation reaction in room-temperature alkane solution, *Science*, **1997**, *278*, 260-263.
- [6] L. Que, W. B. Tolman, Biologically inspired oxidation catalysis, *Nature*, **2008**, *455*, 333-340.
- [7] E. M. McGarrigle, D. G. Gilheany, Chromium and Manganese-salen Promoted Epoxidation of Alkenes, *Chem. Rev.*, **2005**, *105*, 1563-1602.
- [8] M. Breuer, K. Ditrich, T. Habicher, B. Hauer, M. Keßeler, R. Stürmer, T. Zelinski, Industrial Methods for the Production of Optically Active Intermediates, *Angew. Chem. Int. Ed.*, **2004**, *43*, 788-824.
- [9] F. E. Zilly, J. P. Acevedo, W. Augustyniak, A. Deege, U. W. Hausig, M. T. Reetz, Tuning a P450 Enzyme for Methane Oxidation, *Angew. Chem. Int. Ed.*, **2011**, *50*, 2720-2724.
- [10] V. Urlacher, R. D. Schmid, Biotransformations using prokaryotic P450 monooxygenases, *Curr. Opin. Biotechnol.*, **2002**, *13*, 557-564.
- [11] V. B. Urlacher, M. Girhard, Cytochrome P450 monooxygenases: an update on perspectives for synthetic application, *Trends Biotechnol.*, **2012**, *30*, 26-36.
- [12] S. Schulz, M. Girhard, V. B. Urlacher, Biocatalysis: Key to Selective Oxidations, *ChemCatChem*, **2012**, *4*, 1889-1895.
- [13] F. Hollmann, I. W. C. E. Arends, K. Buehler, Biocatalytic Redox Reactions for Organic Synthesis: Nonconventional Regeneration Methods, *ChemCatChem*, **2010**, *2*, 762-782.

- [14] F. Hollmann, I. Arends, K. Buehler, A. Schallmey, B. Buhler, Enzyme-mediated oxidations for the chemist, *Green Chem.*, **2011**, *13*, 226-265.
- [15] F. Van Rantwijk, R. A. Sheldon, Selective oxygen transfer catalysed by heme peroxidases: Synthetic and mechanistic aspects, *Curr. Opin. Biotechnol.*, **2000**, *11*, 554-564.
- [16] M. Hofrichter, R. Ullrich, Heme-thiolate haloperoxidases: versatile biocatalysts with biotechnological and environmental significance, *Appl. Microbiol. Biotechnol.*, **2006**, *71*, 276-288.
- [17] M. Hofrichter, R. Ullrich, M. J. Pecyna, C. Liers, T. Lundell, New and classic families of secreted fungal heme peroxidases, *Appl. Microbiol. Biotechnol.*, **2010**, *87*, 871–897.
- [18] S. H. Hu, L. P. Hager, Highly enantioselective propargylic hydroxylations catalyzed by chloroperoxidase, *J. Am. Chem. Soc.*, **1999**, *121*, 872-873.
- [19] J. T. Groves, S. J. Crowley, K. V. Shalyaev, Paramagnetic 1H-NMR relaxation probes of stereoselectivity in metalloporphyrin catalyzed olefin epoxidation, *Chirality*, 1998, 10, 106-119.
- [20] A. Zaks, D. R. Dodds, Chloroperoxidase-catalyzed asymmetric oxidations: substrate specificity and mechanistic study, *J. Am. Chem. Soc.*, **1995**, *117*, 10419-10424.
- [21] K. Piontek, R. Ullrich, C. Liers, K. Diederichs, D. A. Plattner, M. Hofrichter, Crystallization of a 45 kDa peroxygenase/peroxidase from the mushroom Agrocybe aegerita and structure determination by SAD utilizing only the haem iron, *Acta Crystallogr. F-Struct. Biol. Cryst. Commun.*, **2010**, *66*, 693-698.
- [22] M. Kinne, C. Zeisig, R. Ullrich, G. Kayser, K. E. Hammel, M. Hofrichter, Stepwise oxygenations of toluene and 4-nitrotoluene by a fungal peroxygenase, *Biochem. Biophys. Res. Commun.*, **2010**, *397*, 18-21.
- [23] E. Aranda, R. Ullrich, M. Hofrichter, Conversion of polycyclic aromatic hydrocarbons, methyl naphthalenes and dibenzofuran by two fungal peroxygenases, *Biodegrad.*, **2009**, *21*, 267-281.
- [24] R. Ullrich, C. Dolge, M. Kluge, M. Hofrichter, Pyridine as novel substrate for regioselective oxygenation with aromatic peroxygenase from Agrocybe aegerita, *FEBS Lett.*, **2008**, *582*, 4100-4106.
- [25] M. Kinne, M. Poraj-Kobielska, S. A. Ralph, R. Ullrich, M. Hofrichter, K. E. Hammel, Oxidative Cleavage of Diverse Ethers by an Extracellular Fungal Peroxygenase, *J. Biol. Chem.*, **2009**, *284*, 29343-29349.
- [26] M. Kinne, M. Poraj-Kobielska, E. Aranda, R. Ullrich, K. E. Hammel, K. Scheibner, M. Hofrichter, Regioselective preparation of 5-hydroxypropranolol and 4'-hydroxydiclofenac with a fungal peroxygenase, *Bioorg. Med. Chem. Lett.*, **2009**, *19*, 3085-3087.
- [27] M. Kinne, R. Ullrich, K. E. Hammel, K. Scheibner, M. Hofrichter, Regioselective preparation of (R)-2-(4-hydroxyphenoxy)propionic acid with a fungal peroxygenase, *Tetrahedron Lett.*, **2008**, *49*, 5950-5953.
- [28] V. Reipa, M. P. Mayhew, V. L. Vilker, A direct electrode-driven P450 cycle for biocatalysis, *Proc. Natl. Acad. Sci. U. S. A.*, **1997**, *94*, 13554-13558.
- [29] J. T. Groves, S. J. Crowley, K. V. Shalyaev, Paramagnetic H-1-NMR relaxation probes of stereoselectivity in metalloporphyrin catalyzed olefin epoxidation, *Chirality*, **1998**, *10*, 106-119.

- [30] M. Kluge, R. Ullrich, K. Scheibner, M. Hofrichter, Stereoselective benzylic hydroxylation of alkylbenzenes and epoxidation of styrene derivatives catalyzed by the peroxygenase of Agrocybe aegerita, *Green Chem.*, **2012**, *14*, 440-446.
- [31] D. E. T. Pazmino, M. Winkler, A. Glieder, M. W. Fraaije, Monooxygenases as biocatalysts: Classification, mechanistic aspects and biotechnological applications, *J. Biotechnol.*, **2010**, 146, 9-24.
- [32] S. Colonna, N. Gaggero, C. Richelmi, P. Pasta, Recent biotechnological developments in the use of peroxidases, *Trends Biotechnol.*, **1999**, *17*, 163-168.
- [33] F. van de Velde, N. D. Lourenço, M. Bakker, F. van Rantwijk, R. A. Sheldon, Improved operational stability of peroxidases by coimmobilization with glucose oxidase, *Biotechnol. Bioeng.*, **2000**, *69*, 286-291.
- [34] J. B. Park, D. S. Clark, New reaction system for hydrocarbon oxidation by chloroperoxidase, *Biotechnol. Bioeng.*, **2006**, *94*, 189-192.
- [35] F. Jensen, A. Greer, E. L. Clennan, Reaction of Organic Sulfides with Singlet Oxygen. A Revised Mechanism, *J. Am. Chem. Soc.*, **1998**, *120*, 4439-4449.
- [36] Y. Liu, S.-Y. Jung, C. P. Collier, Shear-Driven Redistribution of Surfactant Affects Enzyme Activity in Well-Mixed Femtoliter Droplets, *Anal. Chem.*, **2009**, *81*, 4922-4928.
- [37] J. R. Kanofsky, Singlet oxygen production by chloroperoxidase-hydrogen peroxide-halide systems, *J. Biol. Chem.*, **1984**, *259*, 5596-5600.
- [38] L. Veum, U. Hanefeld, A. Pierre, The first encapsulation of hydroxynitrile lyase from Hevea brasiliensis in a sol-gel matrix, *Tetrahedron*, **2004**, *60*, 10419-10425.

## Chapter 4

# A novel approach to utilize cytochrome P450 peroxygenases

## Chapter 4

### A novel approach to utilize cytochrome P450 peroxygenases

#### Introduction

The cytochrome P450 monooxygenases belong to a diverse group of heme - thiolate enzymes widely involved in the metabolism of plants, bacteria, and mammals. They catalyze chemo-, regio-, stereoselective oxidations of non - activated C - H bonds, thus realizing chemical transformations that represent a significant challenge for synthetic organic chemistry [Chapter 1], [1]. P450 catalysis involves activation of molecular oxygen, which requires sequential electron transfer from pyridine cofactors NADH or NADPH via flavoproteins or/and iron - sulfur redox partners [Chapter 1], [2]. The complex electron transport chain and NAD(P)H cofactor dependency are the major obstacles for the synthetic application of P450 monooxygenases.

The cytochrome P450 peroxygenases P450Sp $\alpha$  (CYP152B1) from *Sphingomonas paucimobilis*, P450Bs $\beta$  (CYP152A1) from *Bacillus subtilis*, and P450Cl $\alpha$  (CYP152A2) from *Clostridium acetobutylicum* are atypical enzymes in the P450 monooxygenases superfamily <sup>[Chapter 1]</sup>, [3-4]. Unlike many P450 monooxygenases, they do not rely on the NADH as a cofactor for oxygen activation, but utilize  $H_2O_2$  in the hydrogen peroxide shunt pathway to catalyze the specific  $\alpha$ - or  $\beta$ - hydroxylation of fatty acids and fatty acid methyl esters <sup>[Chapter 1]</sup>, [5-6]. Recently, the substrate scope of P450Bs $\beta$  and P450Sp $\alpha$  was also extended towards some non - natural substrates, such as styrene and ethylbenzene in the presence of carboxylic acids as decoy molecules <sup>[7-8]</sup>. P450Bs $\beta$  also exhibited activity towards polycyclic aromatic hydrocarbons <sup>[9]</sup>.

The main challenge encountered in the catalysis of P450 peroxygenases, and peroxygenases in general, is the irreversible inactivation of the prosthetic heme group even by low  $H_2O_2$  concentrations <sup>[5, 9]</sup>. As an alternative to hydrogen peroxide, organic peroxides were also used, however the stability of P450 peroxygenases was not significantly improved <sup>[9]</sup>. Additionally, the activity of P450Cl $\alpha$  and P450Bs $\beta$  also could be reconstituted in the monooxygenase pathway using different flavoproteins from *E. coli*, *B. megaterium* and *C. acetobutylicum* as redox partners and NADPH as an electron donor <sup>[5, 10]</sup>. However, for synthetic application this approach is restricted by its complexity.

The stability and overall productivity of heme-dependent peroxygenases can be significantly improved using chemical, electrochemical, or enzymatic in situ generation of hydrogen peroxide [11-12]. Recently, Urlacher and co-workers obtained promising results applying light-driven in situ

generation of  $H_2O_2$  to promote hydroxylation of the range of fatty acids using P450Cl $\alpha$  and P450Bs $\beta$  <sup>[13]</sup>. Inspired by their results, we have developed an alternative in situ  $H_2O_2$  generation method by applying a synthetic nicotinamide cofactor 1 - benzyldihydronicotinamide (mNADH) for the reduction of flavins. The resulting reduced flavins such as flavin mononucleotide (FMNH<sub>2</sub>) react with molecular oxygen to eventually yield the re - oxidized FMN and hydrogen peroxide ( $H_2O_2$ ). The overall reaction cascade coupled to hydroxylation of myristic acid by P450Bs $\beta$  and P450Cl $\alpha$  is shown on Scheme 1.

$$\begin{array}{c} \begin{array}{c} \begin{array}{c} \begin{array}{c} \begin{array}{c} \\ \\ \\ \end{array} \end{array} \end{array}$$

Scheme 1. Hydroxylation of myristic acid catalyzed by P450Bs $\beta$  or P450Cl $\alpha$  using in situ generation of H<sub>2</sub>O<sub>2</sub>. 1- mNADH, 2 - FMN; P450 - P450Bs $\beta$  or P450Cl $\alpha$ 

#### **Results and discussion**

#### Hydrogen peroxide production

As a starting point, we validated our hypothesis of using mNADH as an electron donor for in situ  $H_2O_2$  generation catalyzed by FMN.  $H_2O_2$  formation envisioned in Scheme 1 occurs via a two-step reaction: (1) reduction of FMN by mNADH; (2) aerobic re - oxidation of the reduced flavin (Figure 1).

$$mNADH + FMN + H^{+} = FMNH_{2} + mNAD^{+}$$
 (1)

$$FMNH_2 + O_2 = FMN + H_2O_2$$
 (2)

Figure 1. Hydrogen peroxide formation catalyzed by FMN using mNADH as a reductant under aerobic conditions.

According to reactions (1) and (2) the amount of hydrogen peroxide produced can be indirectly measured by the amount of mNADH depleted or oxygen consumed. Initially, we estimated the  $H_2O_2$  production rate by measuring the mNADH depletion rate using UV-Vis spectroscopy. Incubating mNADH (100  $\mu$ M, 10 equivalents) in the presence of catalytic amounts of FMN (10  $\mu$ M) under aerobic conditions revealed a steady decrease in the characteristic mNADH absorption at 360 nm

caused by the oxidation of mNADH (Figure 2). From these measurements we could estimate the initial depletion rate for mNADH of 0.36 mM/h that should correlate with the  $H_2O_2$  production rate.

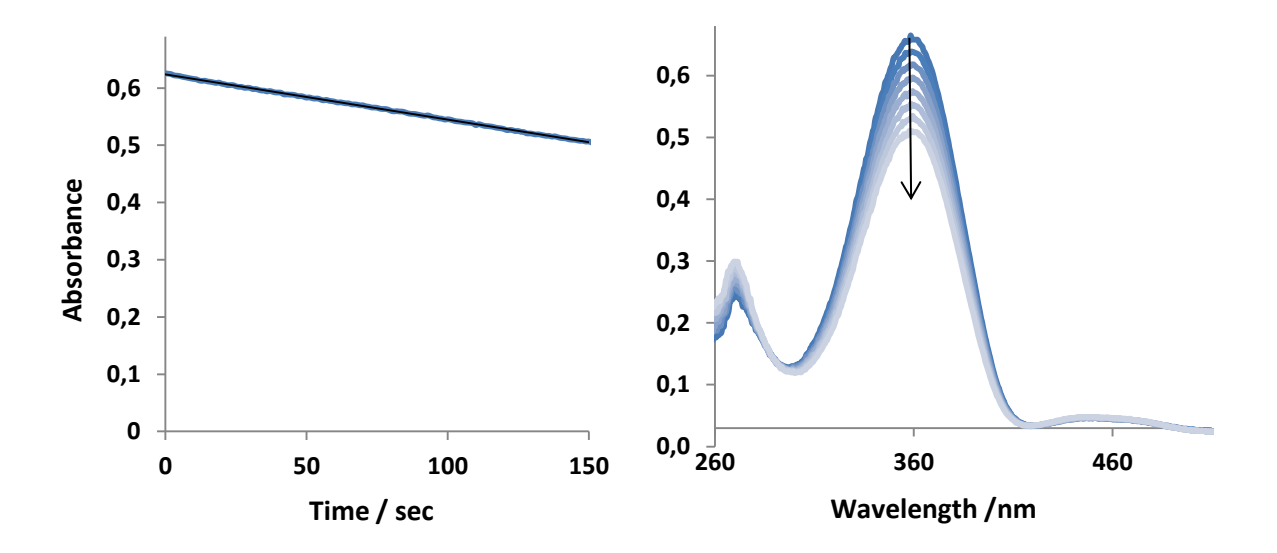


Figure 2. The decrease of the characteristic UV - absorbance band of mNADH at 360 nm (right). General conditions: [mNADH] = 100  $\mu$ M, [FMN] = 10  $\mu$ M, 50 mM TRIS - HCl buffer, pH = 7.7; T = 30 °C

Further we measured the initial mNADH depletion rate varying the concentration of mNADH or FMN alternately (Figure 3). These studies showed the initial depletion rate linearly depends on both FMN and mNADH concentrations. Thus, in comparison with initial setup (Figure 2) the initial  $H_2O_2$  production rate could be accelerated by one order of magnitude (up to approximately 3 mM/h) upon increasing both mNADH and FMN concentrations (Figure 3, left).

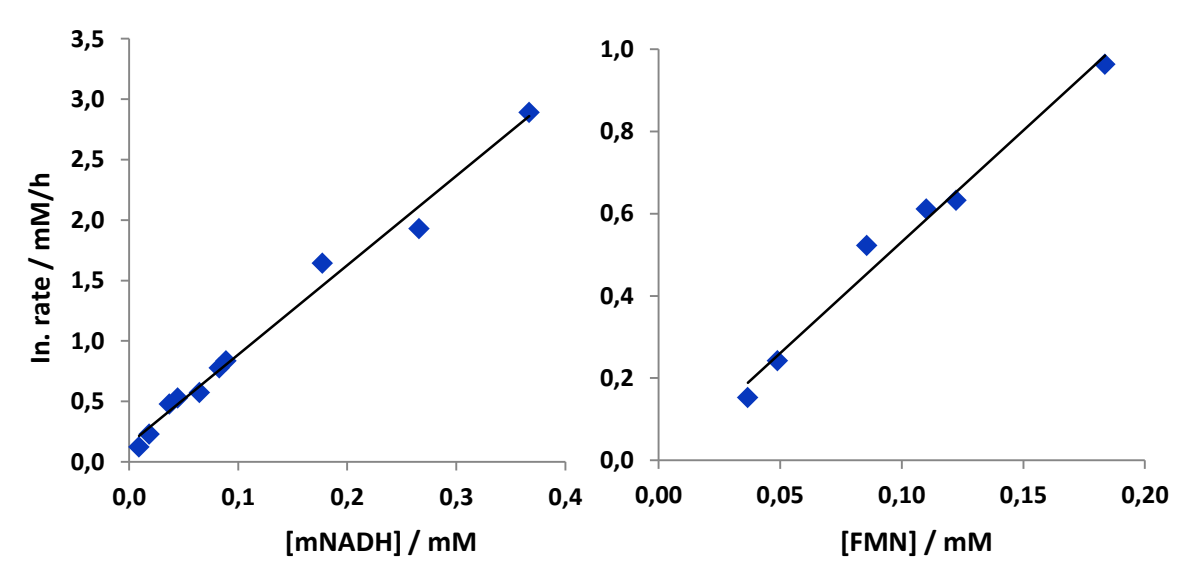


Figure 3. Initial depletion rate of mNADH depending on: mNADH concentration (left); or on FMN concentration (right). General conditions: 50 mM TRIS - HCl buffer, pH = 7.7; 360 nm; T = 30  $^{\circ}$ C; left: [FMN] = 120  $\mu$ M, [mNADH] = 10 – 370  $\mu$ M; right: [mNADH] = 85  $\mu$ M, [FMN] = 40 – 210  $\mu$ M; All experiments were performed in triplicates with standard deviation less than 15%.

Although an increase of FMN and mNADH concentration leads to higher reaction rates, the overall catalytic activity of FMN remained rather sluggish, e.g. reaching only 25 h<sup>-1</sup> using 0.4 mM of mNADH concentrations (Figure 3, left). In comparison up to 300 h<sup>-1</sup> for FMN could be obtained in hydride transfer from native NADH to FMN under light illumination, which is known to activate FMN <sup>[14]</sup>. In the same way, the catalytic activity of FMN might be improved by light activation in future experiments.

Additionally, we estimated the  $H_2O_2$  production rate measuring oxygen consumption rates at different FMN concentrations using the Clark electrode. These experiments showed the linear dependence of the oxygen consumption rate on the FMN concentration (Figure 4). Incubating mNADH (100  $\mu$ M, 10 equivalents) in the presence of catalytic amounts of FMN (10  $\mu$ M) revealed an oxygen consumption rate of 0.24 mM/h that correlates with mNADH depletion rate measured by UV-Vis in the range of experimental error. It is worth mentioning that a side mNADH oxidation by oxygen occurs, which contributes up to 15% to the overall mNADH depletion rate at catalytic amount of FMN (10  $\mu$ M). Nevertheless, the side aerobic oxidation rate of mNADH becomes negligible with increase of FMN concentration, e.g. mNADH aerobic oxidation contributes only 5% to overall reaction rate at 50  $\mu$ M of FMN.

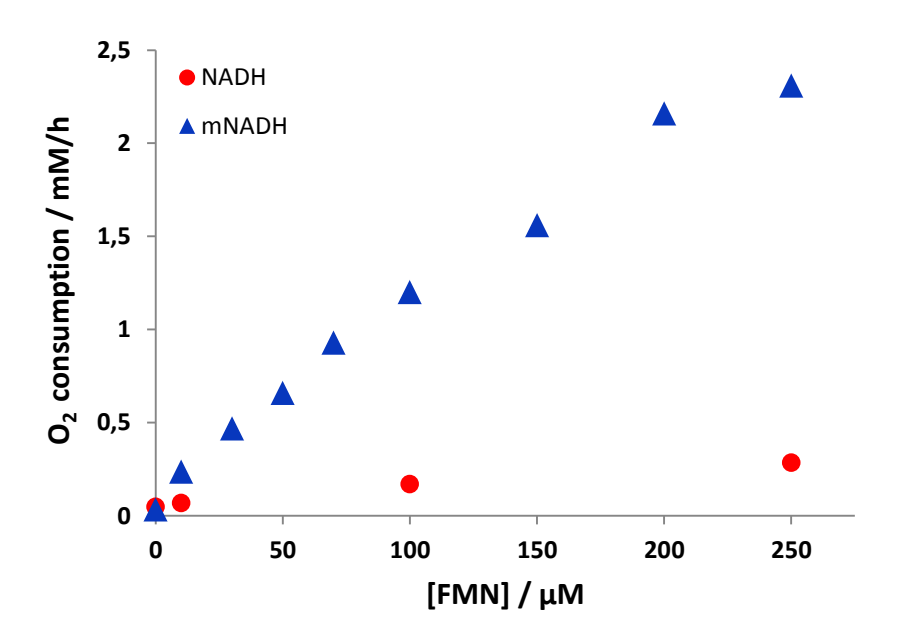


Figure 4. Oxygen consumption rate depending on flavin concentration. General conditions: 100 mM phosphate buffer, pH = 7; T =  $25^{\circ}$ C; [mNADH] = 100  $\mu$ M, [FMN] = 0 – 250  $\mu$ M. phosphate buffer was saturated with oxygen before experiment for 15 min. All experiments were performed in triplicates with standard deviation less than 15%.

Interestingly, substituting mNADH by native NADH showed poor activity, reaching only 15% of initial reaction rates obtained with mNADH (Figure 4). This finding emphasizes a higher activity of synthetic mNADH over native NADH. Furthermore, the significant difference in initial rates implies that the

reduction of FMN by pyridine cofactors (Figure 1, reaction 1) is a rate limiting step in the hydrogen peroxide production, and reduced FMN is quickly re-oxidized under aerobic conditions (Figure 1, reaction 2).

#### Hydroxylation of myristic acid

Furthermore, we investigated the applicability of the novel in situ  $H_2O_2$  generation concept to promote the hydroxylation of myristic acid catalyzed by P450Cl $\alpha$  and P450Bs $\beta$  peroxygenases. Pleasingly, the hydroxylation of myristic acid proceeded smoothly, leading to 75% and 92% yields for P450Cl $\alpha$  and P450Bs $\beta$  respectively over 20 minutes under arbitrarily chosen reaction conditions (Figure 5). We assume the incomplete conversions are most likely due to the enzymes' inactivation under conditions studied, although product inhibition cannot be excluded. Nevertheless, the previously reported conversion of myristic acid catalyzed by P450Cl $\alpha$  reached only 40% in the presence of 200  $\mu$ M  $H_2O_2$  and enzyme was inactivated within 2 - 4 minutes <sup>[5]</sup>. Therefore, in situ formation of  $H_2O_2$  might be advantageous to the use of stoichiometric amount of  $H_2O_2$ .

Interestingly, both enzymes exhibited similar catalytic activities in terms of turnover frequencies (TF): myristic acid was converted to  $\alpha$ - and  $\beta$ -hydroxymyristic acid with TF of 22 and 28 min<sup>-1</sup> for P450Cl $\alpha$  and P450Bs $\beta$  respectively. The ratio of  $\alpha$ : $\beta$  hydroxylated products were 1:1.7 for P450Bs $\beta$  and 24:1 for P450Cl $\alpha$  (see experimental). Using in situ generation of  $H_2O_2$ , the catalytic activity of both P450Cl $\alpha$  and P450Bs $\beta$  significantly fell far behind reported TF values (200 min<sup>-1</sup> [5] and 1200 min<sup>-1</sup> [15], respectively). Girhard et al. reported that high concentration of  $H_2O_2$  was needed for high catalytic activity of peroxygenases, although it led to the rapid enzyme inactivation [5]. Therefore, the comparable slow catalytic activities of P450Cl $\alpha$  and P450Bs $\beta$  in our experiments can be attributed to low in situ concentration of  $H_2O_2$ , implying the  $H_2O_2$  generation is the rate-limiting step of the overall system.

Additionally, FMN reached TF of 22 and 27 h<sup>-1</sup> for P450Cl $\alpha$  and P450Bs $\beta$  respectively, which are in a good agreement with spectrophotometric studies under equal reaction conditions. Therefore, FMN catalytic potential was fully exploited in the coupled reaction. Interesting, a TF of approx. 1 h<sup>-1</sup> for FMN was reported for myristic acid hydroxylation catalyzed by P450Cl $\alpha$  and P450Bs $\beta$  adding the excess of NADPH and NADH mixture <sup>[13]</sup>. These findings show an advantage of synthetic mimics over native NAD(P)H cofactors.

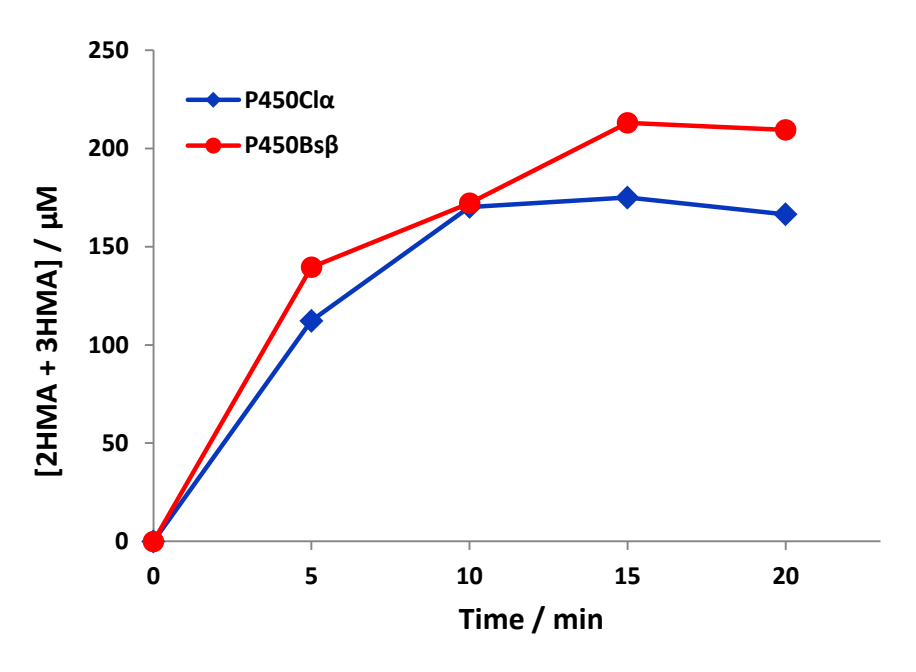


Figure 5. Time - course of myristic acid hydroxylation using in situ  $H_2O_2$  generation. General conditions: 50 mM TRIS - HCl buffer, pH 7.7, T = 30 °C, [myristic acid] = 210  $\mu$ M, [mNADH] = 600  $\mu$ M, [FMN] = 60  $\mu$ M; [P450Cl $\alpha$ ] = 1  $\mu$ M; [P450Bs $\beta$ ] = 1  $\mu$ M; 2HMA - 2-hydroxymyristic acid; 3HMA - 3-hydroxymyristic acid

As spectrophotometric studies showed, the  $H_2O_2$  formation rate can be enhanced upon increase of flavin and mNADH concentrations. Therefore we further investigated the influence of different mNADH and FMN concentrations on the hydroxylation rate of myristic acid. We observed a saturation type dependence of the initial hydroxylation rate when varying the mNADH concentration at fixed FMN concentration (60  $\mu$ M) (Figure 6). Thus the overall reaction rate was enhanced with increase of the mNADH concentration up to 400  $\mu$ M, and a maximum TF of approx. 30 min<sup>-1</sup> was reached for both P450Cl $\alpha$  and P450Bs $\beta$  (Figure 6). Furthermore, we obtained the saturation type dependence of initial hydroxylation rate on FMN concentration with an apparent maximum TF of approx. 25 min<sup>-1</sup> for P450Cl $\alpha$  (Figure 7). The influence of both mNADH and FMN concentrations on the reaction rate with comparable TF supports the assumption the  $H_2O_2$  generation is the rate determining step of the reaction.

We assume that the saturation type-behavior of the initial rate at elevated FMN and mNADH concentrations is due to the fast depletion of dissolved oxygen due to its low solubility in the aqueous solution ( $\sim$ 0.25 mM). Therefore, oxygen diffusion to the aqueous medium may become the major limitation of the system, especially at elevated substrate concentrations. Previously, we obtained similar results for thioanisole oxidation using photocatalytic in situ generation of  $H_2O_2$  in an aqueous system [Chapter 2]. However, 10 - fold increase of maximal thioanisole oxidation rate could be obtained in a two liquid - phase system consisting of a buffer and thioanisole due to increased  $O_2$  solubility in organic medium [Chapter 2]. Therefore, medium engineering might be one of the

possibilities to address the oxygen diffusion limitation for myristic acid hydroxylation. External oxygen supply would be another option to overcome the rate transfer limitations.

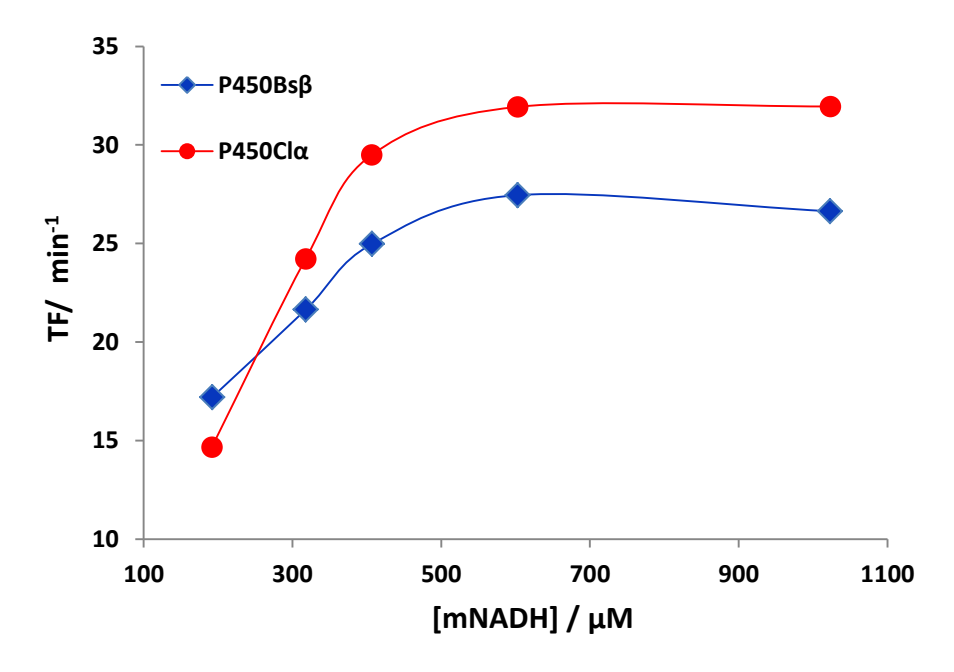


Figure 6. Initial rates for total product formation at different mNADH concentrations for P450Bs $\beta$  and P450Cl $\alpha$ . General conditions: 50 mM TRIS - HCl buffer; pH 7.7, [myristic acid] = 210  $\mu$ M, [FMN] = 60  $\mu$ M, [P450Bs $\beta$ ] = [P450Cl $\alpha$ ] = 1  $\mu$ M, [mNADH] = 190-1020  $\mu$ M; T = 30 °C; Initial rates were measured after 5 minutes at each mNADH concentration

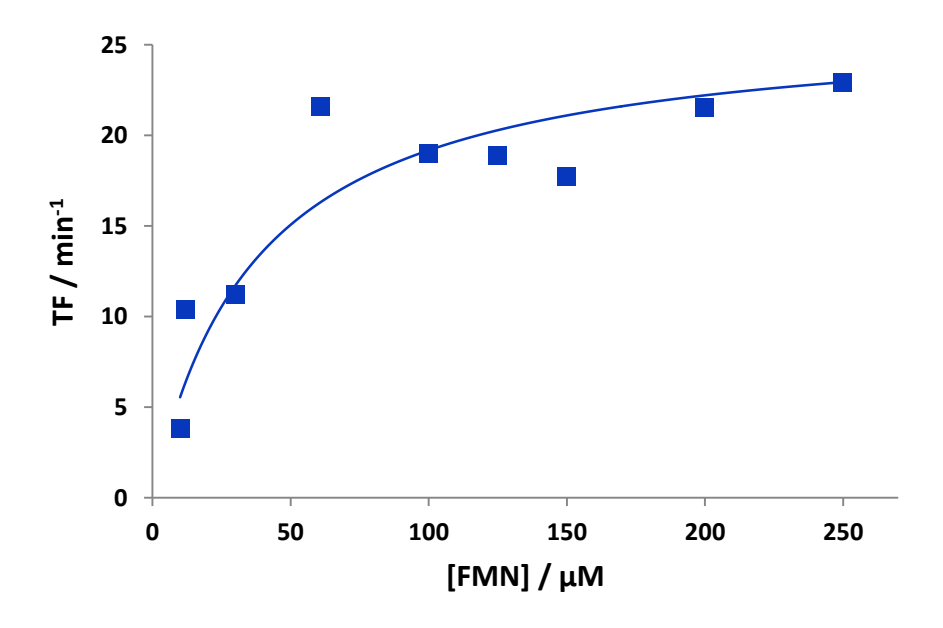


Figure 7. Initial rates at different FMN concentrations for P450Cl $\alpha$ . General conditions: 50 mM TRIS - HCl buffer, pH 7.7, [myristic acid] = 210  $\mu$ M, [FMN] = 10 - 1225  $\mu$ M, [P450Cl $\alpha$ ] = 1  $\mu$ M, [mNADH] = 600  $\mu$ M; T = 30 °C; Initial rates were measured after 5 minutes at each FMN concentration

#### **Up-scaling**

Encouraged by the promising results, we scaled up P450Cl $\alpha$  - catalyzed hydroxylation of myristic acid at a concentration of 10 mM  $^1$ . Despite the low solubility of mNADH and myristic acid, we avoided using co - solvents that are toxic to enzyme and performed the reaction as a suspension of the aqueous buffer and the insoluble substrates. However, the reaction yielded only 4% of the products over a reaction period of 70 h. Although the system might be limited by the solubility of the reagents in the aqueous reaction system leading to the sluggish reaction rates, we assume the low productivity is most likely due to the enzyme instability. In this respect, it is important to find an appropriate balance between the rates of in situ  $H_2O_2$  generation and enzyme stability. Further studies are necessary to clarify the aspects of P450 peroxygenases stability and putative inactivation at elevated (co) - substrates concentrations.

#### **Control experiments**

In addition, we performed several control experiments in order to elucidate the possible background activity. As expected we did not observe any conversion performing described experiments in the absence of P450s. Interestingly, omitting mNADH or FMN from the reaction mixture led to considerable product formation (Figure 8). The catalytic activity without mNADH is probably due to the presence of inherent electron donors like native NAD(P)H in the enzymes' crude extract, which might reduce FMN with sequential formation of  $H_2O_2$  in sufficient amount for hydroxylation of low concentration of myristic acid. Similarly, hydroxylation without addition of FMN might occur due to availability of flavins in the enzymes crude extract.

Furthermore, we performed aforementioned standard experiment adding catalase as a rapid scavenger of  $H_2O_2$  suppressing peroxygenase activity (Figure 9). Remarkably, reaction yield dropped to less than 20% confirming that peroxygenase pathway is predominant under reaction conditions. However, we cannot exclude the contribution of the classical P450 monooxygenase catalytic cycle. In this case, P450 catalysis may occur via sequential electron transfer to heme-iron for oxygen activation. Thus, we conceive of heme-iron reduction by the reduced FMN or flavoproteins, which may present in the crude extract. This assumption can be confirmed by the previous studies, where besides peroxygenase activity P450Cl $\alpha$  exhibited monooxygenase activity in reconstituted systems containing either flavodoxin and flavodoxin reductase or the diflavin reductase as electron transport partners <sup>[5, 10]</sup>.

<sup>&</sup>lt;sup>1</sup> Reaction condition: 50 mM TRIS-HCl buffer, pH 7.7, [myristic acid] = 10 mM, [FMN] = 60 μM, [P450Clα] = 1 μM, [mNADH] = 50 mM; T = 30 °C; t = 70 hours

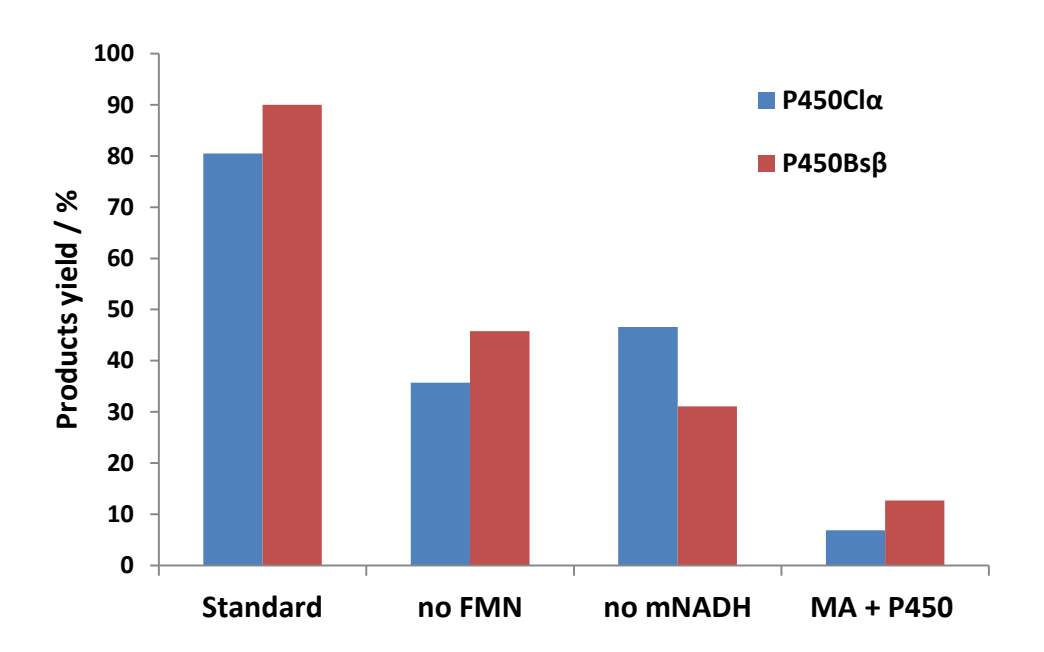


Figure 8. Myristic acid conversion catalyzed by P450Cl $\alpha$  and P450Bs $\beta$  in control experiments. Standard conditions: 50 mM TRIS - HCl buffer, pH 7.7, T = 30 °C; (blue) - [P450Cl $\alpha$ ] = 1  $\mu$ M, [myristic acid] = 200  $\mu$ M, [FMN] = 10  $\mu$ M, mNADH = 600  $\mu$ M, 90 min; (red) – [P450Bs $\beta$ ] = 1.0  $\mu$ M, [myristic acid] = 60  $\mu$ M, [FMN] = 60  $\mu$ M, [mNADH] = 600  $\mu$ M, 20 min; MA – myristic acid

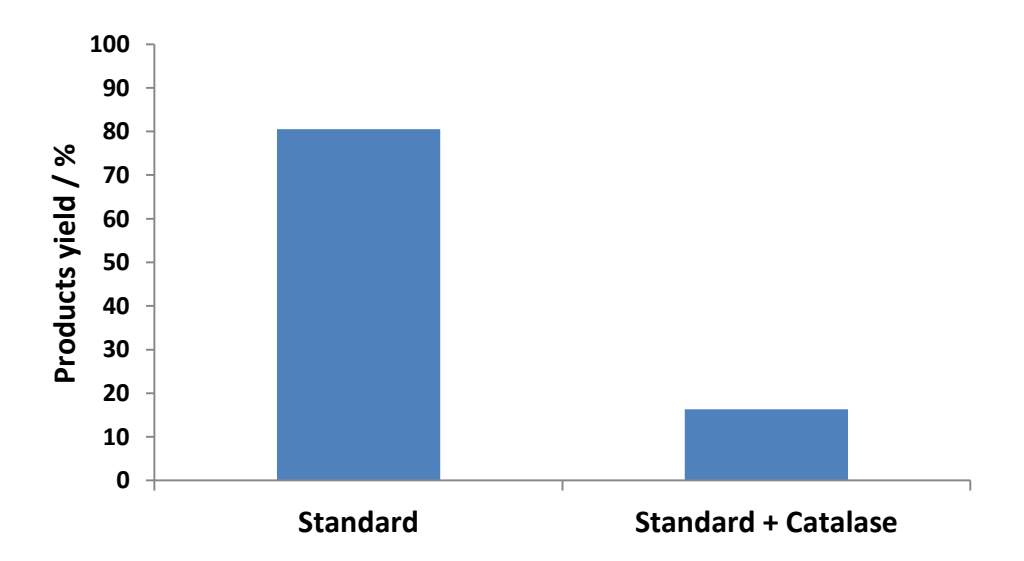


Figure 9. Myristic acid conversion catalyzed by P450Cl $\alpha$ . Standard conditions: 50 mM TRIS - HCl buffer, pH 7.7, T = 30 °C; [P450Cl $\alpha$ ] = 1  $\mu$ M, [myristic acid] = 200  $\mu$ M, [FMN] = 10  $\mu$ M, [mNADH] = 600  $\mu$ M; [catalase] = 300 U/mL; V = 1 mL; Samples were taken after 90 minutes

The direct electron transfer from mNADH to the heme - iron also cannot be excluded, although the direct reduction of heme - iron and subsequent oxygen activation represent a challenging task in the absence of electron transfer partners [16]. Additional experiments should be performed using purified

enzymes to clarify current results and to elucidate the putative contribution of monooxygenase pathway via direct reduction of heme - iron whether by mNADH or FMNH<sub>2</sub>.

#### **Conclusions and outlook**

Overall, we demonstrated the novel in situ  $H_2O_2$  generation is a promising approach to promote P450 peroxygenases catalysis. Thus, final productivity could be enhanced due to higher enzymes operational stability at low  $H_2O_2$  concentrations. The  $H_2O_2$  generation represented the rate - limiting step, however it could be easily controlled via both FMN and mNADH concentrations. Further characterization should result in an optimized ratio of flavin/mNADH/biocatalyst enabling high reaction rates while minimizing  $H_2O_2$  - related inactivation of the enzyme.

It was shown previously that synthetic mimics of NADH can substitute the natural NADH for catalysis of P450cam from *Pseudomonas putida* in the presence of electron transfer partners  $^{[17]}$ . Here we extended the application of the synthetic mNADH for in situ  $H_2O_2$  generation to promote P450 peroxygenase catalysis. The hydroxylation mainly proceeded via the peroxygenase pathway. However, the significant conversion in the presence of catalase may suggest also the contribution of the classical P450 monooxygenase catalytic cycle. Additional studies will clarify the putative direct electron transfer (from the reduced flavin or mNADH) to heme iron in monooxygenase pathway. Nevertheless, we believe that novel in situ  $H_2O_2$  system has a great potential and its future application can be extended to more biocatalytic systems.

#### **Experimental**

#### **Materials**

Crude extracts of P450Cl $\alpha$  and P450Bs $\beta$  were provided by Prof. V.B. Urlacher, Düsseldorf University. The concentration of the enzyme solution (17.3  $\mu$ M) was determined by CO - difference spectral assay with  $\epsilon_{450-490}$  = 91 mM<sup>-1</sup>cm<sup>-1</sup> [18]. Catalase (2100 U/mg) from bovine liver was purchased from Sigma - Aldrich. Myristic acid, lauric acid, 2-hydroxy myristic acid, FMN, diethyl ether, hydrochloric acid, 2-amino-2-(hydroxymethyl)-1,3-propanediol (TRIS), ethyl acetate, dimethyl sulfoxide, and N,O-bis(trimethylsilyl) trifluoroacetamide (BSTFA) containing trimethylchlorosilane (99:1) were purchased from Sigma-Aldrich in analytical pure grade. 1-Benzyldihydronicotinamide (mNADH) was provided by Hogeschool Rotterdam, Rotterdam, The Netherlands.

The following buffers and stock solutions were used: TRIS - HCl buffer (50 mM, pH 7.7), FMN (1mM aqueous solution), myristic acid (20 mM in DMSO), lauric acid (20 mM in DMSO). Stock solution of mNADH (10 - 100 mM) was freshly prepared in methanol before each use. TRIS - HCl buffer solution

was prepared by dissolving TRIS (3.00 gram, 25 mmol) in deionized water (500 mL) and pH was adjusted by addition of hydrochloric acid (37% w/w).

#### **Reaction conditions**

Unless otherwise mentioned the reactions were performed in polystyrene tubes (V = 2 mL) at 30°C, ambient atmosphere. The reaction mixture contained TRIS - HCl buffer (50 mM, pH 7.7; V = 1 mL), myristic acid (200  $\mu$ M), FMN (40 – 250  $\mu$ M), mNADH (200 - 600  $\mu$ M), P450Cl $\alpha$  (1  $\mu$ M) or P450Bs $\beta$  (1  $\mu$ M), DMSO (1% v/v), MeOH (1% v/v). The reaction assays were mixed at 1200 rpm for 5 - 20 minutes. Reaction was stopped at indicated time - points by adding HCl (40  $\mu$ L, 37% w/w) followed by the addition of lauric acid (10  $\mu$ L) as internal standard. The reaction mixtures were extracted twice with 1mL diethyl ether. After evaporation of diethyl ether the remaining reagents were dissolved in BSTFA (200  $\mu$ L) and incubated for 30 minutes at 80 °C mixing at 1200 rpm. After cooling down to room temperature the samples were transferred to the glass GC - vials and GC or GC-MS analysis was performed.

All control experiment were performed identically excluding one of the reaction components. To confirm the peroxygenase activity standard reaction assay was performed upon addition of catalase from bovine liver (2100 U/mg).

#### **Analytical details**

The reaction progress was determined by gas chromatography analysis and the final concentrations were calculated based on calibration equations using an external standard. GC-MS analysis was performed on a Shimadzu GCMS-QP2010S with AOC-20i auto injector (230°C) using a Factor four VF-1 MS column (25 m x 0.25 mm x 0.4  $\mu$ m) with helium as a carrier gas. Column oven temperature was increased from 50 °C to 212 °C with the rate 60 °C min<sup>-1</sup> and kept at 212 °C for 8 minutes, then increased from 212 °C to 325 °C with the rate 60 °C min<sup>-1</sup> and kept at 325 °C for 5 minutes (total time 17.58 min). Column flow was 37 cm/sec; split ratio: 5. Characteristic mass fragmentation patterns were obtained from the EI-MS using ion source (200 °C); scan mode with an m/z range 40-600 in 0.5 sec.

Myristic (ret. time 5.54 min), lauric (ret. time 4.25 min) and 2-hydroxymyristic acid (ret. time 7.45 min) were also assigned by authentic standards. Peak at 7.69 min represents 3-hydroxymyristic acid (identified by mass fragmentation pattern). A representative chromatogram of a myristic hydroxylation reaction is shown in Figure 10 and Figure 11. The regioselectivity for  $\alpha$ : $\beta$  hydroxylation were 1:1.7 for P450Bs $\beta$  and 24:1 for P450Cl $\alpha$ .

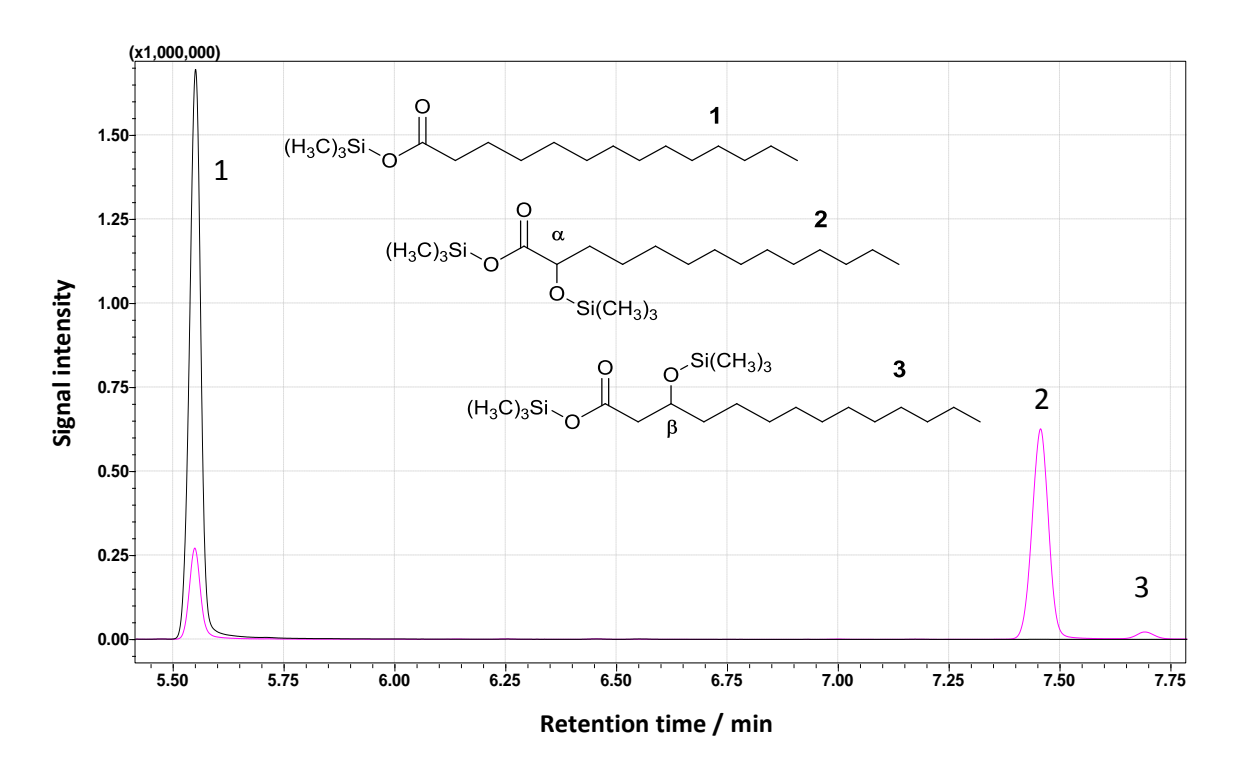


Figure 10. Representative GC-MS chromatograms of a myristic acid hydroxylation catalyzed by P450Cl $\alpha$  using in situ generation of H<sub>2</sub>O<sub>2</sub>. General conditions: 50 mM TRIS - HCl buffer, pH 7.7, [Myristic acid] = 200  $\mu$ M, [FMN] = 10  $\mu$ M, [P450Cl $\alpha$ ] = 1  $\mu$ M, [mNADH] = 600  $\mu$ M. Black: sample taken at t=0 containing myristic acid, pink: sample taken after 5 minutes.

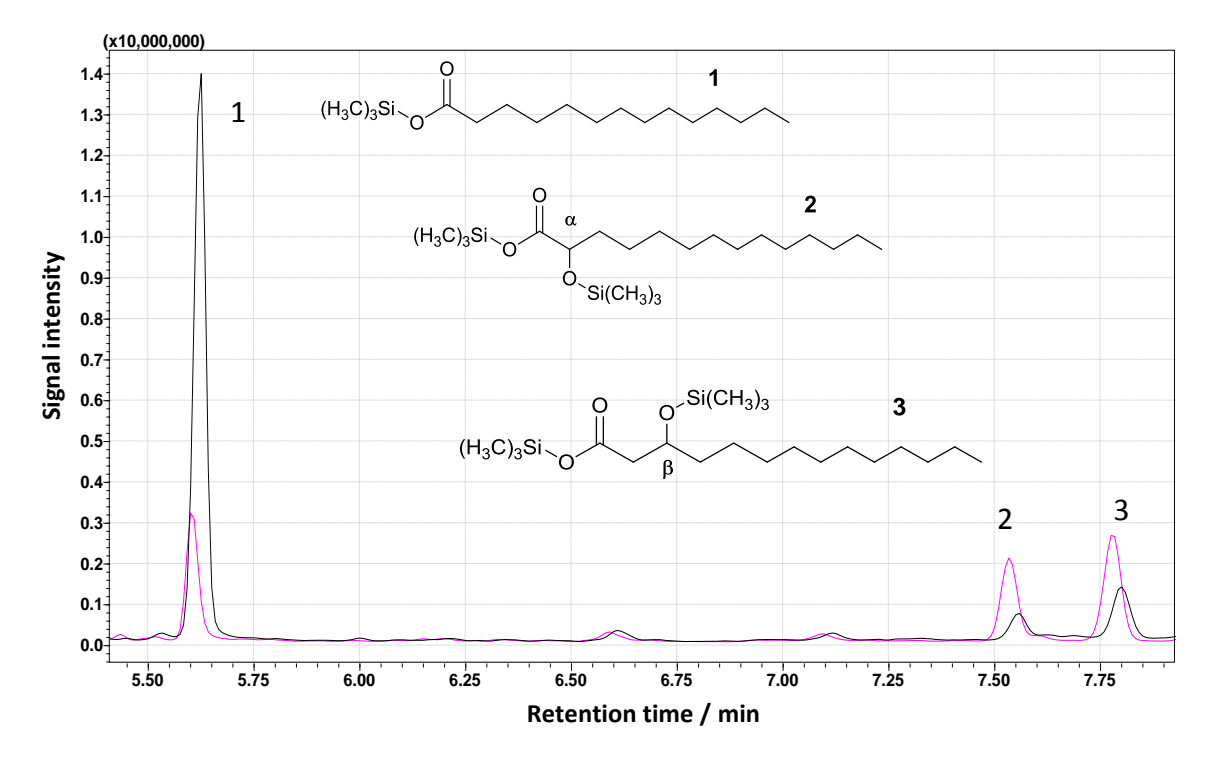


Figure 11. Representative GC-MS chromatograms of a myristic acid hydroxylation catalyzed by P450Bs $\beta$  using in situ generation of H<sub>2</sub>O<sub>2</sub>. General conditions: 50 mM TRIS - HCl buffer, pH 7.7, [Myristic acid] = 200  $\mu$ M, [FMN] = 60  $\mu$ M, [P450Bs $\beta$ ] = 1  $\mu$ M, Black: sample taken after 5 minutes using [mNADH] = 200  $\mu$ M; pink: sample taken after 5 minutes using [mNADH] = 600  $\mu$ M.

The common fragment ion at m/z = 73 results from the cleavage of the TMS group. The fragment ions at m/z = 233, 257 and 271 represent typical fragmentations indicated in the corresponding structures (Figure 12). The fragment ion at m/z = 147, might correspond to polysilylated compound, formed by interaction of TMS group with TMS ester group followed by the loss of a methyl group.

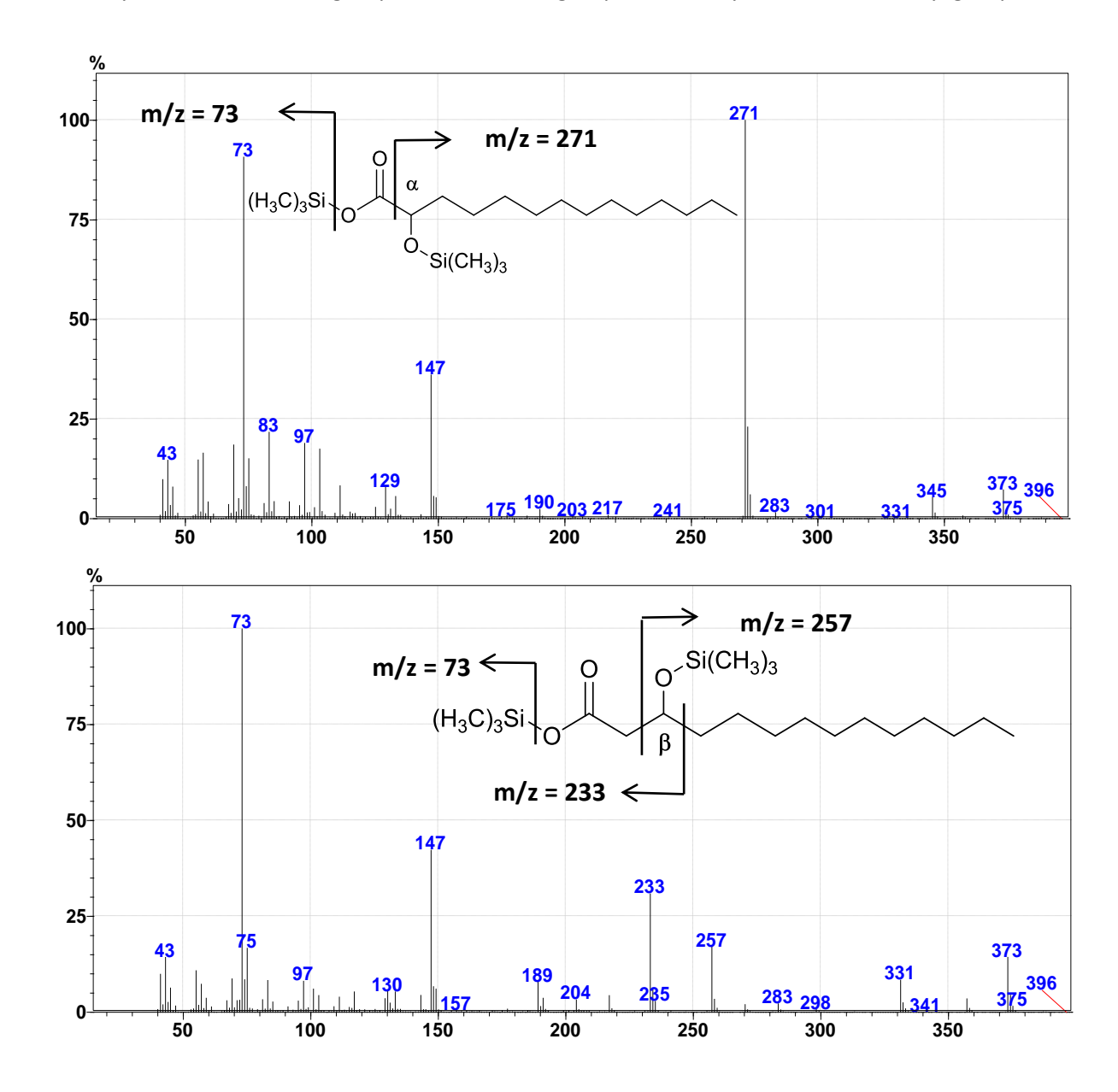


Figure 12. Mass spectra of trimethylsiloxyl (TMS) esters of (up)  $\alpha$ -hydroxy myristic acid and (down)  $\beta$ -hydroxy myristic acid.

#### **UV-Vis**

mNADH depletion rate was determined spectrophotometrically following the decrease of the characteristic UV-absorbance band of mNADH at 360nm. The experiments were performed in disposable UV cuvettes (polystyrene, 1.5 mL) at 30° C on a Shimadzu UV-2401 PC spectrophotometer with Julabo F12 Refrigerated/Heating Circulator. mNADH stock solution was diluted in buffer to final

concentration of  $10-400~\mu M$ , and the samples were incubated for 5 minutes at  $30^{\circ} C$ . The reactions were initiated by the addition of FMN solution to final concentration of  $10-250~\mu M$ .

#### Oxygen electrode

Oxygen consumption was measured on Strathkelvin 782 2-Channel oxygen system using Strathkelvin 1302 Clark - type microcathode oxygen electrodes. The measurement was done in the water-jacketed respiration chamber made from precision bore glass covered by aluminium foil (to prevent flavin illumination by light); water jacket was connected to pumped source of water at 25° C. The chamber was placed on the magnetic stirrer. Electrode was calibrated prior measurement.

The following buffers and stock solutions were used: phosphate buffer (KPi) (50 mM, pH 7.0), mNADH (1 mM in methanol), FMN (1 - 25 mM aqueous solution). Buffer was saturated with oxygen prior usage by bubbling air for 15 minutes. mNADH was diluted in buffer to final concentration of 100  $\mu$ M and pipetted into the chamber containing a magnetic stirring bar. The reactions were initiated by the addition of FMN solution to final concentration of  $10-250~\mu$ M, and electrode holder was immersed into the chamber immediately. Oxygen consumption was followed by the decrease in oxygen concentration using Strathkelvin software.

#### References

- [1] A. W. Munro, H. M. Girvan, A. E. Mason, A. J. Dunford, K. J. McLean, What makes a P450 tick?, *Trends Biochem. Sci.*, **2013**, *38*, 140-150.
- [2] V. B. Urlacher, M. Girhard, Cytochrome P450 monooxygenases: an update on perspectives for synthetic application, *Trends Biotechnol.*, **2012**, *30*, 26-36.
- [3] E. G. Hrycay, S. M. Bandiera, The monooxygenase, peroxidase, and peroxygenase properties of cytochrome P450, *Arch. Biochem. Biophys.*, **2012**, *522*, 71-89.
- [4] I. N. A. Van Bogaert, S. Groeneboer, K. Saerens, W. Soetaert, The role of cytochrome P450 monooxygenases in microbial fatty acid metabolism, *FEBS Journal*, **2011**, *278*, 206-221.
- [5] M. Girhard, S. Schuster, M. Dietrich, P. Durre, V. B. Urlacher, Cytochrome P450 monooxygenase from Clostridium acetobutylicum: A new alpha-fatty acid hydroxylase, *Biochem. Biophys. Res. Commun.*, **2007**, *362*, 114-119.
- [6] D. S. Lee, A. Yamada, H. Sugimoto, I. Matsunaga, H. Ogura, K. Ichihara, S. Adachi, S. Y. Park, Y. Shiro, Substrate recognition and molecular mechanism of fatty acid hydroxylation by cytochrome P450 from Bacillus subtilis Crystallographic, spectroscopic, and mutational studies, J. Biol. Chem., 2003, 278, 9761-9767.
- [7] O. Shoji, T. Fujishiro, H. Nakajima, M. Kim, S. Nagano, Y. Shiro, Y. Watanabe, Hydrogen Peroxide Dependent Monooxygenations by Tricking the Substrate Recognition of Cytochrome P450BSβ, *Angew. Chem.*, **2007**, *119*, 3730-3733.
- [8] T. Fujishiro, O. Shoji, N. Kawakami, T. Watanabe, H. Sugimoto, Y. Shiro, Y. Watanabe, Chiral-substrate-assisted stereoselective epoxidation catalyzed by H<sub>2</sub>O<sub>2</sub>-dependent cytochrome P450 SPα, *Chem. Asian J.*, **2012**, *7*, 2286-2293.

- [9] E. Torres, H. Hayen, C. M. Niemeyer, Evaluation of cytochrome P450BSβ reactivity against polycyclic aromatic hydrocarbons and drugs, *Biochem. Biophys. Res. Commun.*, **2007**, *355*, 286-293.
- [10] S. Honda Malca, M. Girhard, S. Schuster, P. Dürre, V. B. Urlacher, Expression, purification and characterization of two Clostridium acetobutylicum flavodoxins: Potential electron transfer partners for CYP152A2, *Biochimica et Biophysica Acta Proteins and Proteomics*, **2011**, *1814*, 257-264.
- [11] S. K. Karmee, C. Roosen, C. Kohlmann, S. Lutz, L. Greiner, W. Leitner, Chemo-enzymatic cascade oxidation in supercritical carbon dioxide/water biphasic media, *Green Chem.*, **2009**, *11*, 1052-1055.
- [12] C. Kohlmann, S. Lutz, Electroenzymatic synthesis of chiral sulfoxides, *Eng. Life Sci.*, **2006**, *6*, 170-174.
- [13] M. Girhard, E. Kunigk, S. Tihovsky, V. V. Shumyantseva, V. B. Urlacher, Light-driven biocatalysis with cytochrome P450 peroxygenases, *Biotechnol. Appl. Biochem.*, **2013**, *60*, 111-118.
- [14] S. Gargiulo, I. Arends, F. Hollmann, A Photoenzymatic System for Alcohol Oxidation, *ChemCatChem*, **2011**, *3*, 338-342.
- [15] I. Matsunaga, A. Ueda, T. Sumimoto, K. Ichihara, M. Ayata, H. Ogura, Site-Directed Mutagenesis of the Putative Distal Helix of Peroxygenase Cytochrome P450, *Arch. Biochem. Biophys.*, **2001**, *394*, 45-53.
- [16] F. Hollmann, A. Schmid, Towards [Cp\*Rh(bpy)(H<sub>2</sub>O)]<sup>2+</sup>-promoted P450 catalysis: Direct regeneration of CytC, *J. Inorg. Biochem.*, **2009**, *103*, 313-315.
- [17] J. D. Ryan, R. H. Fish, D. S. Clark, Engineering Cytochrome P450 Enzymes for Improved Activity towards Biomimetic 1,4-NADH Cofactors, *ChemBioChem*, **2008**, *9*, 2579-2582.
- [18] T. Omura, R. Sato, The carbon monoxide-binding pigment of liver microsomes: I. evidence for its hemoprotein nature *J. Biol. Chem.*, **1964**, *239*, 2370-2378.

## Chapter 5

# Artificial metalloenzymes for in situ regeneration of the reduced nicotinamide cofactor

This chapter is based on

V. Kohler, Y. M. Wilson, M. Durrenberger, D. Ghislieri, <u>E. Churakova</u>, T. Quinto, L. Knorr, D. Haussinger, F. Hollmann, N. J. Turner, T. R. Ward

Nat. Chem., 2013, 5, 93-99

## Chapter 5

## Artificial metalloenzymes for in situ regeneration of the reduced nicotinamide cofactor

#### Introduction

The interest in the application of biocatalysis in industrial processes has been growing continuously <sup>[1-7]</sup>. Oxidoreductases have a great potential for organic synthesis due to their high chemo-, regio- and stereoselectivity combined with high activity <sup>[8-9]</sup>. However, the practical application of oxidoreductases is still limited due to cofactor challenge: in order to promote the reaction, oxidoreductases require redox equivalents that classically are supplied by natural nicotinamide cofactors such as nicotinamide adenine dinucleotide (NAD) or nicotinamide adenine dinucleotide phosphate (NADP) (Figure 1).

Figure 1. Structures and basic redox chemistry of oxidized and reduced nicotinamide cofactors.

Stoichiometric use of NAD(P) is not feasible due to its high cost (Table 1). Therefore, for preparative applications NAD(P) cofactors are usually applied in the catalytic amount and continuously regenerated in the reaction media.

Table 1. Cost of cofactors from Alfa-Aesar (Prices from the catalogue of May 2013)

Cofactor	€/ g
$NAD^{^{+}}$	21
NAD(P) <sup>+</sup>	37
NADH	315
NAD(P)H	850

Up to date cofactor regeneration is mainly achieved by: (a) using whole cells; (b) addition of a sacrificial co-substrate (substrate-coupled reaction system) or (c) addition of a second enzyme and a co-substrate (enzyme-coupled reaction system) <sup>[8, 10]</sup>. Formate dehydrogenase (FDH), glucose dehydrogenase (GDH), alcohol dehydrogenases (ADHs), phosphite dehydrogenase (PDH), glutamate dehydrogenases (GDHs) are the enzymatic regeneration systems most commonly employed for the synthetic application <sup>[10-13]</sup>.

In addition to the above mentioned enzymatic approaches, chemical and electrochemical NAD(P)H recycling systems have been investigated intensively [14-20]. The organometallic pentamethylcyclopentadienyl rhodium bipyridine [Cp\*Rh(bipy)(H<sub>2</sub>O)]<sup>2+</sup> complex has emerged as the most successful catalyst for the regiospecific reduction of NAD(P)<sup>+</sup>. Its catalytically active hydrido form [Cp\*Rh(bipy)H]<sup>+</sup> produces exclusively enzymatically active 1,4-NAD(P)H due to coordination of NAD<sup>+</sup> to the metal center via the amide-carbonyl-O-atom of NAD<sup>+</sup> forming a kinetically favorable sixmembered ring transition state [21-22] (Scheme 1)

The hydrido form  $[Cp*Rh(bipy)H]^+$  can be obtained by various chemical, electrochemical and photochemical methods <sup>[23-29]</sup>. Sodium formate (NaHCO<sub>2</sub>) is widely used as hydride source: it is cheap and leads to formation of  $CO_2$  as by-product shifting the equilibrium of the regeneration reaction (Scheme 1).

Unlike most of the enzymatic regeneration systems  $[Cp*Rh(bipy)(H_2O)]^{2+}$  does not distinguish between NAD<sup>+</sup> and NADP<sup>+</sup> and is active and stable under a broad range of reaction conditions (pH, T, etc.) [29-30]. However, mutual inactivation between  $[Cp*Rh(bipy)(H_2O)]^{2+}$  and enzymes is commonly encountered [17, 20, 31]. Most likely nucleophilic protein residues (e.g. histidine, cysteine) coordinate to the vacant rhodium coordination site. Such an interaction precludes NADH regeneration as  $[Cp*Rh(bipy)(H_2O)]^{2+}$  binding site is tightly coordinated to the protein residue preventing the reduction into  $[Cp*Rh(bipy)H]^+$  complex (i.e. coordination of formate is impeded). Simultaneously, enzyme activity is impaired if the binding occurs with catalytically relevant amino acids, blocks the active site or interferes with the tertiary and quaternary enzyme structure.

Scheme 1. Catalytic cycle for regioselective reduction of NAD(P)<sup>+</sup> using sodium formate as a hydride source proposed by <sup>[22]</sup>.

A range of potential solutions to the mutual inactivation of  $[Cp*Rh(bipy)(H_2O)]^{2+}$  and enzymes have been reported. Application of a nucleophilic buffer or addition of a non-reactive proteins (bovine albumin) to saturate the coordination site of  $[Cp*Rh(bipy)(H_2O)]^{2+}$  showed to be efficient to preserve the enzyme activity  $^{[32-33]}$ . However, regeneration activity of  $[Cp*Rh(bipy)(H_2O)]^{2+}$  under formate-driven conditions has been impaired. It was shown that physical separation of the enzyme(s) and  $[Cp*Rh(bipy)(H_2O)]^{2+}$  greatly stabilize both  $^{[17, 34]}$ . For example, derivatizing peripheral SH- or  $NH_2$ -groups of enzyme with epoxide containing polymer prevented undesired interaction of Rh-catalyst and enzyme. However, the performance of both, biocatalyst and metallocatalyst, was restricted in terms of turnover frequency and total turnover number (TTN) due to diffusion limitations.

Following the concept of physical separation of  $[Cp*Rh(bipy)(H_2O)]^{2+}$  and enzymes, we hypothesized that the encapsulation of Rh-complex into a protein scaffold would shield the complex preventing the interaction between metallocomplex and enzyme. The well-known, strong non-covalent interaction between biotin and streptavidin (Ka> $10^{13}$  M $^{-1}$ ) is widely applied for creating of so-called artificial metalloenzymes  $^{[35-38]}$ . Hence, metallocomplexes [Cp\*M(biot-p-L)Cl] bearing a biotinylated ligand could be efficiently incorporated into streptavidin scaffold, preventing the mutual inactivation of the metallocomplex and an enzyme (Figure 2). We envisioned that incorporation of a biotinylated complex [Cp\*M(Biot-p-L)Cl] (M = Rh, Ir) within a host protein streptavidin (Sav) could afford an

artificial transfer hydrogenase (ATHase) that can be applied for NAD(P)H regeneration using sodium formate as a hydride source.

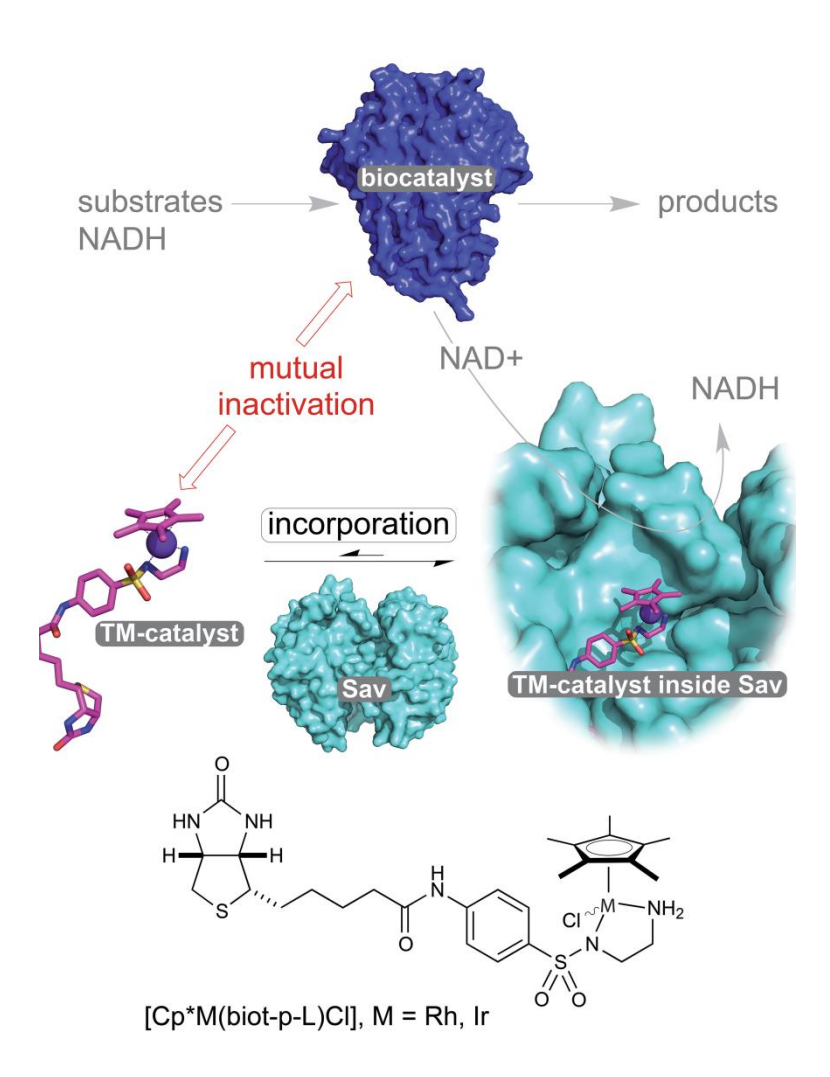


Figure 2. Reaction cascades resulting from combining an ATHase with a biocatalyst. Relying on the strength of the biotin - streptavidin interaction, incorporation of the biotin-bearing complex [Cp\*Ir(biot-p-L)Cl] within streptavidin (Sav) affords an ATHase that can be applied for NADH regeneration. TM-catalyst: a transition metal catalyst.

To prove the concept, we combined ATHase catalyzed NAD(P)H regeneration system with 2-hydroxylbiphenyl monooxygenase (HbpA, EC1.14.13.44, an NADH- and FAD-dependent enzyme) (Scheme 2). HbpA monooxygenase catalyzes ortho-specific hydroxylation of  $\alpha$ -substituted phenols to the corresponding catechols [39-40]. As exemplary case we chose a selective hydroxylation of 2-hydroxybiphenyl to 2,3-dihydrohybiphenyl.

Scheme 2. Hydroxylation of 2-hydroxybiphenyl coupled to an ATHase catalyzed NADH regeneration process.

#### **Results and discussion**

#### NADH regeneration activity of [Cp\*M(Biot-p-L)Cl] and [Cp\*M(Biot-p-L)Cl]·Sav

In a first set of experiments we evaluated the potential of [Cp\*M(biot-p-L)Cl] (M=Rh, Ir) and metallocomplex embedded into streptavidin [Cp\*M(biot-p-L)Cl]·Sav towards NAD<sup>+</sup> reduction using formate as a hydride source. The formation of NADH was monitored spectrophotometrically at NADH characteristic absorption wavelength 340 nm. Representative UV spectra of the [Cp\*Ir(Biot-p-L)Cl] and [Cp\*Ir(Biot-p-L)Cl]·Sav - mediated reduction of NAD<sup>+</sup> are shown in Figure 3. Following the time-course of NADH formation we identified the turnover frequencies (TF) for the metallocomplexes (Figure 4). TF was defined as the quantity (mole) of NADH formed per minute divided by the quantity (mole) of the catalyst. According to the acquired data, the Ir-complex exhibited higher catalytic activity than the corresponding Rh-complex towards in situ NADH regeneration. We determined TF of 4.6 min<sup>-1</sup> for [Cp\*Ir(biot-p-L)Cl that is 65 fold higher than [Cp\*Rh(biot-p-L)Cl] and 17 fold higher than activity of the prototypical complex [Cp\*Rh(bipy)(H<sub>2</sub>O)]<sup>2+</sup> (Table 2).

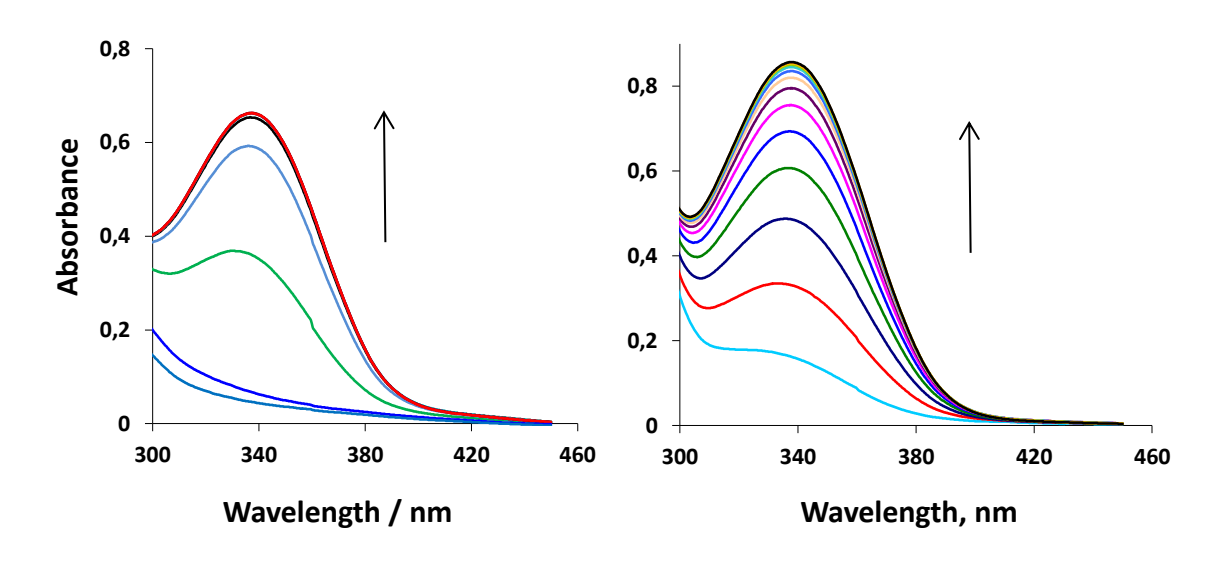


Figure 3. UV-spectra recorded during the [Cp\*Ir(Biot-p-L)Cl] (left) and [Cp\*Ir(Biot-p-L)Cl]·Sav (right)-mediated reduction of NAD<sup>†</sup>. Spectra were recorded at 10 sec and 60 sec intervals in case of [Cp\*Ir(Biot-p-L)Cl] (left) and [Cp\*Ir(Biot-p-L)Cl]·Sav (right), respectively. General conditions: [Cp\*Ir-biot-p-L)Cl] or [Cp\*Ir-biot-p-L)Cl]·Sav = 10  $\mu$ M, [NaHCO<sub>2</sub>] = 200 mM, [NAD<sup>†</sup>] = 100  $\mu$ M, [KP<sub>i</sub> buffer] = 50 mM,  $\mu$ H = 7.5, T = 30 °C, V = 1 mL.

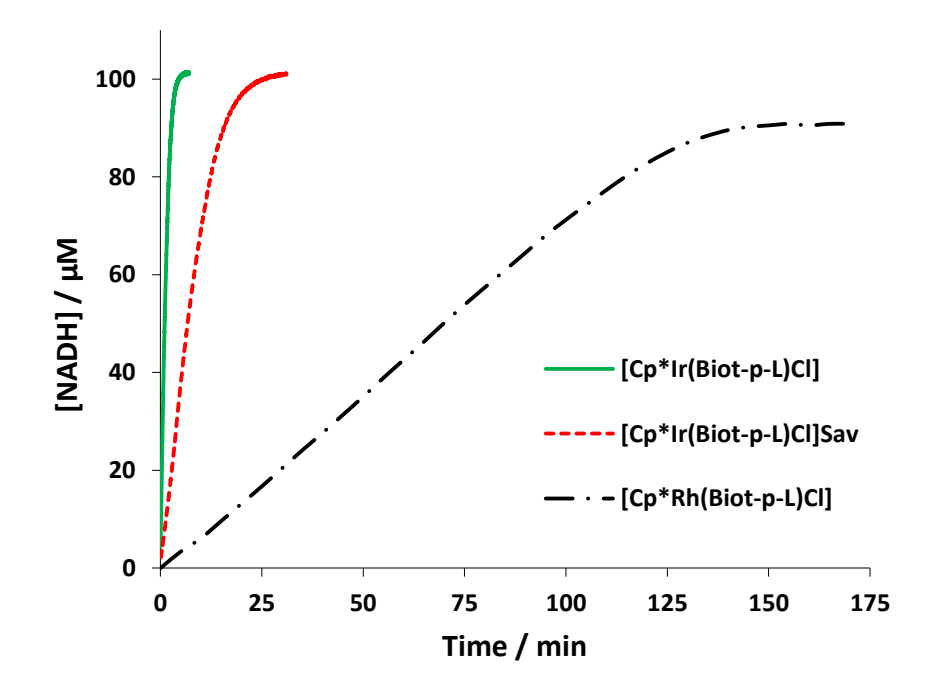


Figure 4. Time course of the metal-catalyzed reductions of NAD<sup> $^+$ </sup>. [Cp\*Ir(Biot-p-L)Cl]: solid line (green), [Cp\*Ir(Biot-p-L)Cl]·Sav: dashed line (red); [Cp\*Rh(Biot-p-L)Cl]: dash-dot line (black), recorded to prove formation of NADH catalyzed by novel [Cp\*Ir(biot-p-L)Cl] complexes at the characteristic NADH absorption wavelength 340 nm. General conditions: [Cp\*M-biot-p-L)Cl] or [Cp\*M-biot-p-L)Cl]·Sav (M= Rh, Ir) = 10  $\mu$ M, [NaHCO<sub>2</sub>] = 200 mM, [NAD $^+$ ] = 100  $\mu$ M, [KP<sub>1</sub> buffer] = 50 mM, pH = 7.5, T = 30  $^{\circ}$ C, V = 1 mL.

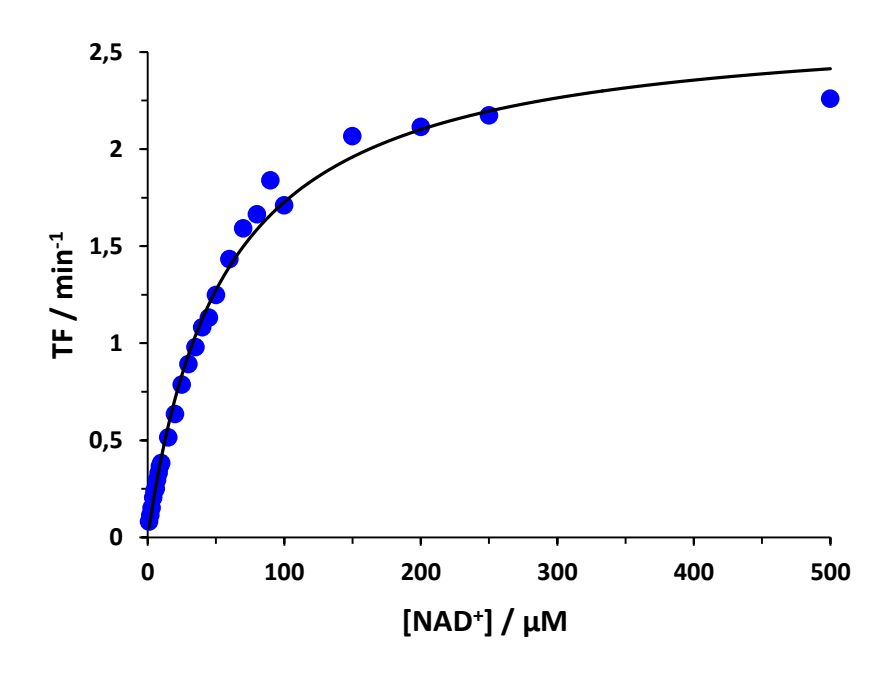
The ability of [Cp\*Ir(biot-p-L)Cl] embedded into the streptavidin environment to catalyze NADH regeneration was investigated under identical experimental conditions as for the isolated complexes. The Ir-complex incorporated into the streptavidin [Cp\*Ir(biot-p-L)Cl]·Sav showed only 15% of the activity with respect to the isolated complex. A loss in activity might be due to the diffusion

limitations: a NAD<sup>+</sup> has a complex structure entailing ribose, pyrophosphate and adenosine groups, hence its access towards Ir might be hindered by the protein environment. Nevertheless,  $[Cp*Ir(biot-p-L)CI]\cdot Sav$  performed higher activity in terms of TF than the prototypical rhodium complex  $[Cp*Rh(bipy)(H_2O)]^{2+}$  (Table 2).

Table 2. Comparison of initial rates for NAD $^+$  reduction for graph in Figure 3 (right). General conditions: [Cp\*M-biot-p-L)Cl] or [Cp\*M-biot-p-L)Cl]·Sav (M = Rh, Ir) = 10  $\mu$ M, [NaHCO $_2$ ] = 200 mM, [NAD $^+$ ] = 100  $\mu$ M, [KP $_i$  buffer] = 50 mM, pH = 7.5, T = 30 °C, V = 1 mL.

Compound	TF [min <sup>-1</sup> ]	relative activity [%]
[Cp*Rh(bipy)(H <sub>2</sub> O)] <sup>2+</sup>	0.27	386
[Cp*Rh(Biot-p-L)Cl]	0.07	100
[Cp*Ir(Biot-p-L)Cl]	4.6	6571
[Cp*Ir(Biot-p-L)Cl]·Sav	0.7	1000

To elucidate further the striking difference in the catalytic activity of Ir-complex and Ir-complex embedded into streptavidin, we studied the influence of NAD<sup>+</sup> concentration on the initial NADH regeneration rate catalyzed by [Cp\*Ir(biot-p-L)Cl] and [Cp\*Ir(biot-p-L)Cl]·Sav at fixed formate concentration (Figure 5). A Michaelis - Menten type of dependence was observed for both catalysts, as previously reported in literature also for the  $[Cp*Rh(bipy)(H_2O)]^{2+[30]}$ . The  $K_m$  and  $V_{max}$  for  $NAD^+$ were determined for both [Cp\*Ir(biot-p-L)Cl] and [Cp\*Ir(biot-p-L)Cl]·Sav from non - linear regression analysis of the data according to Michaelis - Menten equation (Figure 5). Incorporation of the metallocomplex into the streptavidin moderately affected the kinetic parameters (Table 3). The difference in  $K_m$  values for NAD<sup>+</sup> in case of [Cp\*Ir(biot-p-L)Cl] and [Cp\*Ir(biot-p-L)Cl]·Sav are probably due to the aforementioned diffusion limitation. The difference in  $k_{cat}$  is most likely related to the change of electronic properties of the Ir-complex due to the incorporation into streptavidin. A similar observation was reported by Haquette and co-authors conjugating [Cp\*Rh(2,2'-dipyridylamine)Cl]<sup>+</sup> complex to the papain:  $K_m$  (NAD<sup>+</sup>) of 27.1  $\mu$ M and  $k_{cat}$  of 43.5 h<sup>-1</sup> were defined for the isolated complex, whereas linking the complex to the papain gave a  $K_m$  (NAD<sup>+</sup>) of 59  $\mu$ M and  $k_{cat}$  of 30.5 h<sup>-1</sup> [16].



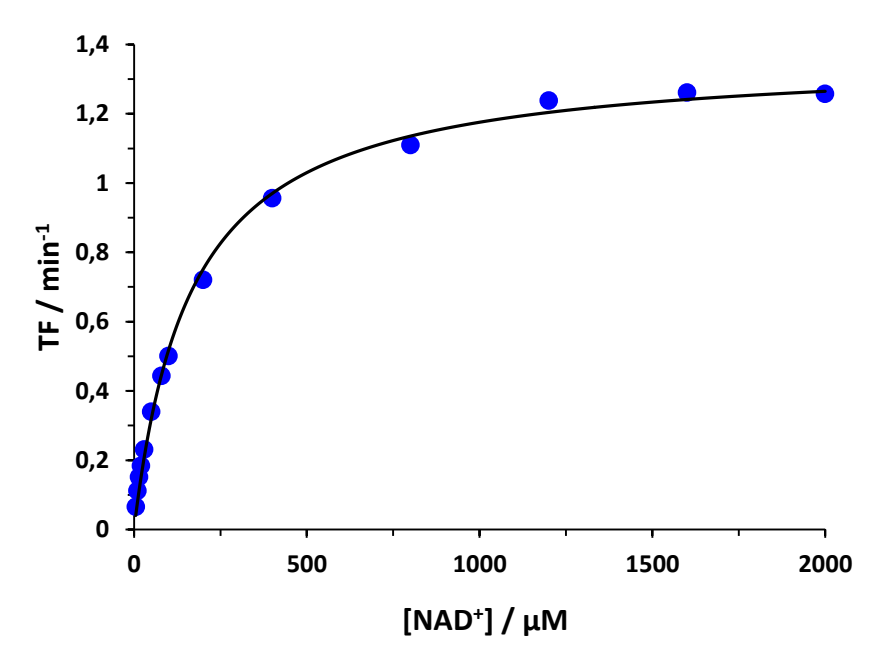


Figure 5. Estimation of Michaelis - Menten constants for the reduction of NAD $^{+}$ . Top: [Cp\*Ir(biot-p-L)Cl]; Bottom: [Cp\*Ir(biot-p-L)Cl]·Sav (ATHase). General conditions: c([Cp\*Ir(biot-p-L)Cl]) = 10  $\mu$ M or c(ATHase) = 5  $\mu$ M, [NaHCO $_{2}$ ] = 200 mM, KP $_{1}$ 50 mM, pH =7.5, T = 30  $^{\circ}$ C. The apparent Michaelis - Menten parameters  $k_{cat}$  and  $K_{m}$  were obtained applying sigmoidal fit corresponding to the Michaelis - Menten equation using OriginPro 8.5.1 $^{\circ}$ .

Table 3. Kinetic parameters of ATHase and [Cp\*Ir(biot-p-L)Cl] for reduction of NAD<sup>+</sup>.

Catalyst	$K_m$ [ $\mu$ M]	k <sub>cat</sub> [min <sup>-1</sup> ]
[Cp*Ir(biot-p-L)Cl]	55.2 ± 3.1	2.68 ± 0.06
[Cp*Ir(biot-p-L)Cl]·Sav	164.5 ± 5.7	1.369 ± 0.013

#### The effect of Sav on the mutual deactivation of the Ir-catalyst and HbpA

The stabilities of enzyme and Ir-catalyst play a crucial role with respect to preparative application. Efforts to combine HbpA with NAD<sup>+</sup> reduction catalyst have proven challenging: both HbpA and [Cp\*Ir(Biot-p-L)L] were rapidly deactivated when brought into contact (Table 4). Since HbpA and [Cp\*Ir(Biot-p-L)L] are rather stable under reaction conditions, we assume a mutual inactivation between metallocomplex and biocatalyst. The deactivation was largely alleviated if the Ir-catalyst was preincubated with Sav. Hence, we concluded that indeed, Sav shielded the Ir-complex efficiently from interaction with HbpA and thereby protected both catalysts from mutual deactivation.

Table 4. Residual activity of HbpA and Ir-catalyst after co-incubation. General conditions: [HbpA] = 0.2 mg/mL = 0.128 U/mL, c ([Cp\*Ir-biot-p-L)Cl]·Sav) =  $10 \mu\text{M}$  or c ([Cp\*Ir-biot-p-L)Cl]) =  $10 \mu\text{M}$ ; T =  $30^{\circ}\text{C}$ , [KP<sub>1</sub>] = 50 mM, pH = 7.5.

	residual HbpA a	ectivity [%]	residual Ir-a	ectivity [%]	
		incubation time			
	1h	2h	1h	2h	
[Cp*Ir(biot-p-L)L]	<1	0	29	0	
[Cp*Ir(biot-p-L)L]·Sav	62	49	68	57	
KP <sub>i</sub> buffer	97.8	94.4	100	100	

#### The effect of Sav on the chemoenzymatic hydroxylation of 2-hydroxybiphenyl

To test the validity of the molecular compartmentalization concept outlined in Figure 2, we investigated the regeneration of NADH in the presence of HbpA monooxygenase using the ATHase. The time courses of the reactions in the presence and absence of Sav demonstrate essential difference in final conversion (Figure 6). If Sav was omitted from the reaction mixture, accumulation of the product ceased soon after start of the reaction yielding less than 5% conversion of the starting material. In the presence of Sav, however, the mutual inactivation of [Cp\*Ir(Biot-p-L)Cl] and HbpA was efficiently prevented and robust hydroxylation activity was achieved (Figure 6). Full conversion of 2-hydroxybiphenyl to 2,3-dihydroxybiphenyl was accomplished in 2 h. We conclude that Sav shields the Ir-complex from the enzyme, allowing the NADH regeneration with formate as hydride source.

The catalytic performance [Cp\*Ir(Biot-p-L)Cl]·Sav in terms of TF (0.32 min<sup>-1</sup>) was in range with TF defined spectrophotometrically (Table 2). However, the HbpA performance was rather limited as just 1.5% of its specific activity has been achieved. We assume the significant loss of HbpA activity is most likely due to the slow NADH regeneration catalyzed by ATHase, that represent a rate limiting step of the overall reaction.

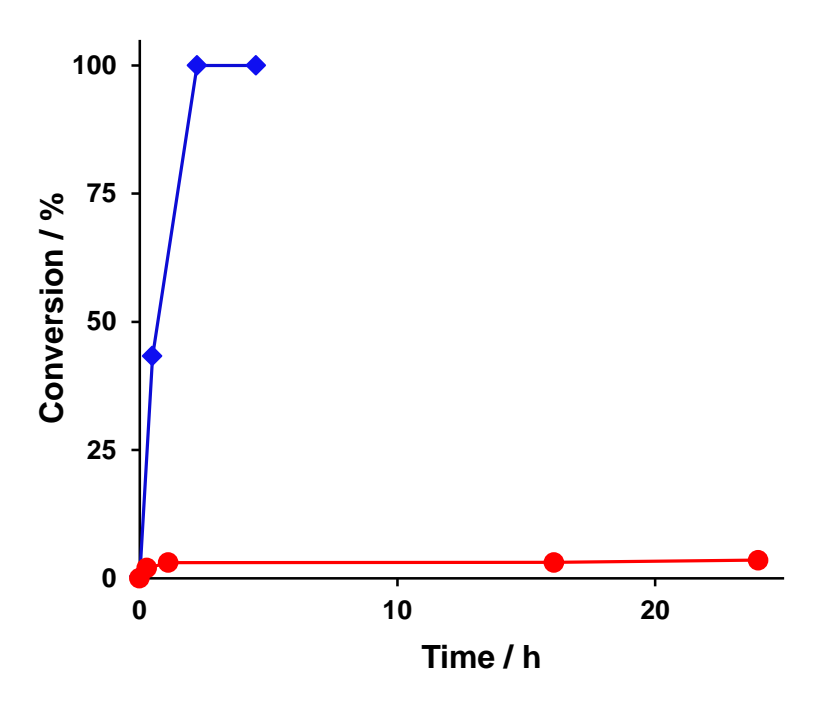


Figure 6. Comparison of the chemoenzymatic hydroxylation of 2-phenylphenole in the presence ( $\spadesuit$ , blue) and absence ( $\spadesuit$ , red) of Sav. General conditions: [NaHCO<sub>2</sub>] = 168 mM, [2-phenylphenole] = 0.5 mM; [HbpA] = 0.5 mg/mL = 0.44 U/mL, [NAD<sup>†</sup>] = 0.5 mM, [FAD] = 10  $\mu$ M; ( $\spadesuit$ , blue): c([Cp\*Ir-biot-p-L)CI]·Sav) = 20  $\mu$ M, ( $\spadesuit$ , red): c([Cp\*Ir-biot-p-L)CI]) = 20  $\mu$ M; T = 30 °C, [KP<sub>i</sub>] = 50 mM, pH =7.5.

Due to the low solubility of the substrate (2-phenylphenol) in aqueous reaction media also the performance of the catalysts in terms of TTN (mol product/mol catalyst) was somewhat limited. Therefore, we advanced to a so-called two liquid phase system (2 LPS) wherein a hydrophobic organic solvent (e.g. 1-decanol) serves as substrate reservoir and product sink (Scheme 3). Applying 2 LPS concept also prevents inhibition of HbpA by 2,3-dihydroxybiphenyl by in situ removal of the product [41], [Chapter 7].

The biphasic system displayed again mutual inactivation of HbpA and metallocomplex in the absence of Sav, whereas a TTN of > 100 (calculated for [Cp\*Ir(Biot-p-L)Cl]) was achieved when Sav was present (Figure 7). Moreover TTN of 10 were achieved for NAD<sup>+</sup>. Here both ATHase and HbpA showed rather low initial activity (TF<sub>ATHase</sub> = 0.084 min<sup>-1</sup>; HbpA activity = 0.003 U/mg corresponding to less than 1% of specific activity). We assume that significant drop in initial activity can be attributed to diffusion of 2-phenylphenol from the organic to aqueous phase limiting the overall reaction rate. Nevertheless, the decrease of initial rate in two phase system is compensated by higher TTN.

Scheme 3. Schematic representation of two liquid phase system (2 LPS) for hydroxylation of 2-phenylphenol catalyzed by HbpA in the presence of the proposed NADH regeneration system.

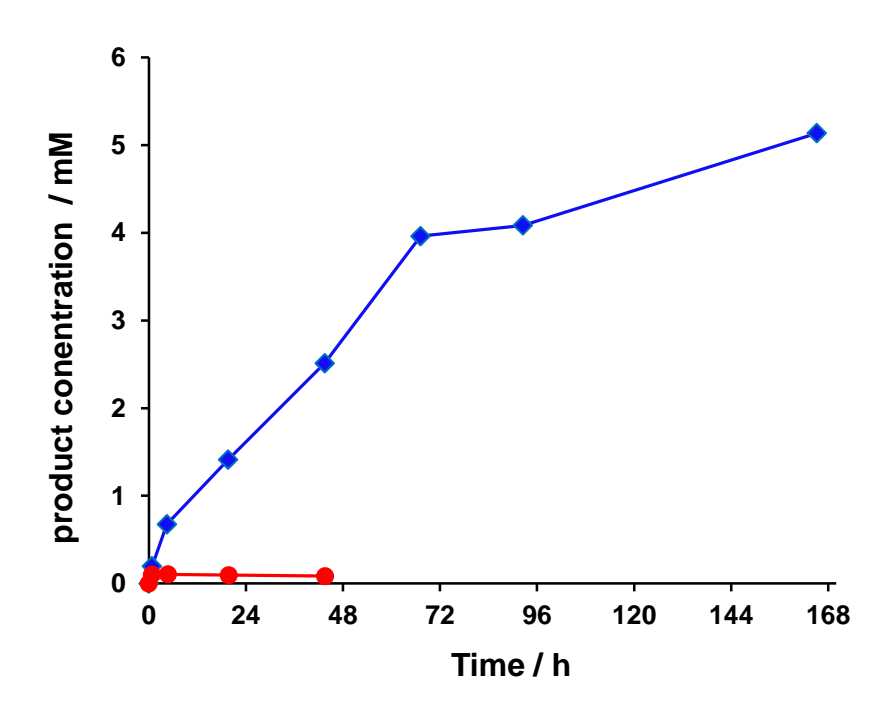


Figure 7. Time course of chemoenzymatic hydroxylation of 2-phenylphenol in 2 LPS in the presence ( $\spadesuit$ , blue) and absence ( $\spadesuit$ , red) of Sav. General conditions: aqueous phase: [KP<sub>i</sub>] = 42 mM, pH =7.5; [NaHCO<sub>2</sub>] = 168 mM; [HbpA] = 1.6 mg/mL = 0.88 U/mL, [NAD<sup>†</sup>] = 0.5 mM, [FAD] = 20  $\mu$ M; ( $\spadesuit$ , blue): c([Cp\*Ir-biot-p-L)Cl]·Sav) = 50  $\mu$ M; ( $\spadesuit$ , red): c([Cp\*Ir-biot-p-L)Cl]) = 50  $\mu$ M; organic phase: [2-phenylphenol] = 100 mM in 1-decanol, V = 1 mL; T = 30°C.

#### **Conclusions and outlook**

Here we showed that [Cp\*M(biot-p-L)Cl] (M = Rh, Ir) are active and efficient catalysts for the regeneration of NADH with formate as a hydride donor. Comparison of the catalytic activity towards NAD<sup>+</sup> reduction showed that the Ir-complex exhibits higher activity than Rh-complex in terms of TF.

The introduction of the biotin-bearing complex [Cp\*Ir(biot-p-L)CI] into streptavidin resulted in an artificial transfer hydrogenase (ATHase). This ATHase resemble the catalytic activity of initial metallocomplex and can be applied for NAD $^+$  reduction.

Combining the ATHase with a NADH-dependent enzyme namely HbpA showed full conversion of 2-phenylphenol, accumulating the desired product only. On the contrary combining the novel [Cp\*Ir(biot-p-L)Cl] complex with HbpA in the absence of streptavidin showed that accumulation of the product ceased soon after start of the reaction, affording less than 5% conversion of the starting material. Hence, we conclude that Sav efficiently shields the Ir-complex from interaction with HbpA and thereby protects both catalysts from mutual deactivation.

Furthermore, the possibility of running the system in pure aqueous phase or as a biphasic system highlights the applicability of the ATHase regeneration system under a variety of reaction conditions. Moreover TTN for both NAD<sup>+</sup> and Ir-catalyst could be significantly improved in biphasic system.

Further studies should aim the full characterization of the proposed regeneration system coupled to biocatalytic transformation. Thus optimized ratio of ATHase /biocatalyst may result in higher reaction rates and TTN. Also the dependence of NADH regeneration rate on formate concentration needs to be elucidated. Therefore, catalytic activity of the Ir-complex might be enhanced under formate-optimized conditions. Besides, advancing the biphasic system to a microemulsion system may lead to better performance of the system overcoming putative diffusion limitations.

Preliminary results suggest an applicability of ATHase catalyzed NADH regeneration also to an enoate reductase-catalyzed C=C double-bond reduction. Further the application of novel ATHase will be elucidated for variety of redox enzymes relying on NAD(P)H, FADH<sub>2</sub> and heme cofactors to demonstrate the general applicability of the regeneration system.

#### **Experimental**

#### **Stock solutions:**

All chemicals were obtained from Sigma-Aldrich in analytical grade. Potassium phosphate buffer (KPi) was prepared by dissolving  $K_2HPO_4$  (114.8 mg) and  $KH_2PO_4$  (590.2 mg) in distilled water (100mL, final conc. 50 mM, pH 6.0). Then sodium formate was dissolved in phosphate buffer (final 200mM). The pH was adjusted with NaOH to final pH 7.5. Streptavidin (Sav) mutant S112A and [Cp\*M(biot-p-L)Cl] (M = Rh, Ir) complexes were kindly supplied by Prof. Dr. Thomas Ward, The University of Basel. Streptavidin (Sav) mutants were produced, purified and characterized as previously described in [42]. Stock solutions of lyophilized streptavidin Sav-S112A corresponding to 1 mM free binding sites (assuming 3 free binding sites per tetramer) were prepared by dissolving Sav-S112A (21.9 mg) in H<sub>2</sub>O (1 mL) directly before the experiment. The mixture was stirred until all protein was dissolved. For a

detailed synthesis procedure of [Cp\*Ir(biot-p-L)Cl] see reference <sup>[43]</sup>. The stock solutions of the metal complexes were prepared in DMF to the final concentration of 1 mM. NAD and NADH stock solutions were prepared in  $H_2O$  to the final concentration of 10 mM and stored at -20°C. FAD stock solutions were prepared in water to the final concentration of 1 mM.

#### **HbpA** preparation

The enzyme 2-hydroxybiphenyl-3-monooxygenase (HbpA, E.C.1.14.13.44) was kindly supplied by Prof. Dr. Andreas Schmid (TU Dortmund, Dortmund, Germany). The enzyme had been produced using *Escherichia coli* recombinantly expressing HbpA (*E. coli* JM101 pHBP461 containing hbpA) following a published procedure <sup>[39, 41]</sup>. For enrichment, the cell crude extracts (cell disruption was achieved by two passages through a French Press) were submitted to anion exchange chromatography (Streamline DEAE anion exchanger - Pharmacia). HbpA was eluted with 20 mM Tris HCl pH 7.5 using a linear gradient of NaCl from 0 to 1 M NaCl. HbpA was recovered in pooled fractions at 150 to 200 mM NaCl. The final enzyme preparation (pooled fractions) contained partially purified HbpA. Specific activities of purified fractions were determined at 30°C, 0.5 mM 2-hydroxybiphenyl and 0.3 mM NADH. HbpA was stored as a lyophilised powder at -20 °C. HbpA stock solution (typically 12.5 mg/mL) was prepared directly before the experiments in KP<sub>i</sub> buffer (50 mM, pH 7.5). HbpA specific activity towards NADH oxidation defined spectrophotometrically was ~0.88 ± 0.14 U/mg (batch used for monophasic reaction) and ~0.55 ± 0.02 U/mg (batch used for biphasic reaction).

## NADH regeneration activity of [Cp\*Ir(Biot-p-L)Cl], [Cp\*Ir(Biot-p-L)Cl]·Sav and [Cp\*Rh(Biot-p-L)Cl]

The activity measurements of the biotinylated metal-complexes (in the absence or presence of Sav) for NADH regeneration was carried out in disposable UV cuvettes (polystyrene) at 30 °C (Shimadzu UV-2401 PC spectrophotometer; Julabo F12 Refrigerated/Heating Circulator). The reaction buffer (980  $\mu$ L (or 970  $\mu$ L for the reaction with Sav), 50 mM KPi, 200 mM NaHCO<sub>2</sub>, pH 7.5) was supplemented with [Cp\*Ir(Biot-*p*-L)Cl] or [Cp\*Rh(Biot-*p*-L)Cl], respectively (10  $\mu$ L of a 1 mM solution in DMF). If indicated, Sav-S112A stock solution (10  $\mu$ L, 1 mM in free binding sites in H<sub>2</sub>O; 3 free binding sites per tetramer assumed) was added and the mixture was incubated at ambient temperature for 15 minutes to allow the binding of the metal complex to Sav. The reactions were started by addition of NAD<sup>+</sup> (10  $\mu$ L of a 10 mM solution in H<sub>2</sub>O). The reaction progress was followed spectrophotometrically by recording UV spectra or simply by following the absorption change at 340 nm. For quantification of NADH formed, the molar absorption coefficient of 6220 M<sup>-1</sup> cm<sup>-1</sup> was used.

#### The effect of Sav-S112A on the robustness of the chemoenzymatic hydroxylation reactions

In a first set of experiments the mutual inactivation of [Cp\*Ir(Biot-p-L)Cl] and HbpA as well as the protecting effect of [Cp\*Ir-biot-p-L)Cl]·Sav(S112A) was examined. For this, following assays were performed: To phosphate buffer (1560 μL, 50 mM, pH 7.5) was added [Cp\*Ir(Biot-p-L)Cl] (20 μL of a 1 mM solution in DMF) and either Sav-S112A (20 μL, 1 mM free binding sites in H<sub>2</sub>O; 3 free binding sites per tetramer assumed) or H<sub>2</sub>O (20 μL), respectively. Subsequently the mixtures were supplemented with HbpA stock solution (400 μL, 1 mg/mL in 50 mM KPi buffer, pH 7.5). These mixtures were incubated in a shaking incubator at 30 °C. At 1 and 2 hours aliquots were taken to measure the residual activity spectrophotometrically. Residual HbpA activity: An aliquot of the incubated mixture (200 μL) was added to a mixture of phosphate buffer (752 μL, 50 mM, pH 7.5), NADH stock (30 µL of a 10 mM solution in H<sub>2</sub>O) and FAD (10 µL of a 1 mM solution in H2O) in a disposable UV-cuvette (polystyrene). The resulting solution was placed in a UV spectrometer at 30 °C and background activity was recorded for 1.5 min. Residual substrate-related activity was followed after adding 2-hydroxybiphenyl (8 μL of a 25 mM methanolic solution) by the decrease in absorption at 340nm (NADH). For residual [IrCp\*(Biot-p-L)L] activity an aliquot of the incubated mixture (100 μL) was added to formate containing buffer (890 μL, 50 mM in KPi, 200 mM in NaHCO<sub>2</sub>, pH 7.5) and the reactions were started by addition of NAD (10  $\mu$ L of a 10 mM solution H<sub>2</sub>O).

#### The effect of Sav-S112A on the chemoenzymatic hydroxylation of 2-hydroxybiphenyl

A first set of experiments was performed in aqueous medium only: Formate containing buffer solution (1.68 ml of 50 mM KPi, 200 mM NaHCO<sub>2</sub>, pH adjusted to 7.5 with NaOH) was placed in a 2 mL PP-tube, Sav-S112A stock solution (40  $\mu$ L, 1 mM free binding sites in H<sub>2</sub>O; 3 free binding sites per tetramer assumed) was added, followed by [Cp\*Ir(Biot-*p*-L)Cl] (40  $\mu$ L, 1 mM in DMF). This mixture was incubated for 15 minutes at room temperature. Afterwards, the mixture was supplemented with FAD solution (20  $\mu$ L of a 1 mM solution in H<sub>2</sub>O) and HbpA stock solution (80  $\mu$ L, 12.5 mg/ml, 11 U/ml in KPi buffer). After addition of the substrate 2-hydroxybiphenyl (40  $\mu$ L of a 25 mM stock solution in methanol) the reaction was started by addition of NAD<sup>+</sup> (100  $\mu$ L of a 10 mM stock solution in H<sub>2</sub>O). The reaction mixtures were placed in a thermoshaker (TWISTER comfort) and incubated at 30 °C and 400 rpm. Samples of 50  $\mu$ L were withdrawn at the indicated time points, diluted with ACN/water (0.95 mL of a 50:50 (v/v) mixture containing 0.1 % TFA) and analyzed by RP-HPLC. (Shimadzu LC-20 system with a Shimadzu SPD-20A Photo Diode Array detector using a Waters Xterra column (RP18, 3.5  $\mu$ M, 4.6 × 150 mm). The temperature was controlled to 40°C by a Shimadzu CTO-20AC column oven. The eluent was acetonitrile/water (50/50) isocratic and contained 0.1% TFA; flow rate: 1.1 mL/min, detection wavelength 254 nm). The quantification was based on calibration curves using

authentic standards. Typical chromatograms are shown in Figure 8. The reaction without Sav-S112A was performed under identical conditions but leaving out the Sav-S112A addition step.

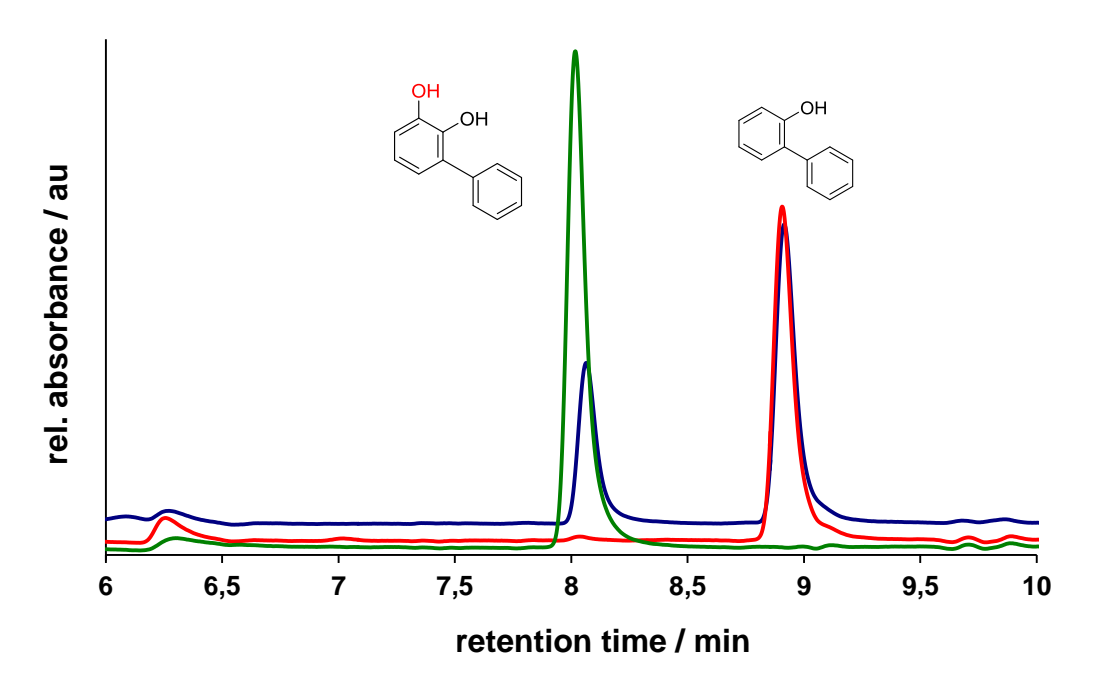


Figure 8. Chromatograms of a typical chemoenzymatic hydroxylation reaction. Red: Sample taken immediately after initiation of the reaction, blue: sample taken after 40 min reaction time, green: sample taken after 24 h reaction time.

A typical procedure for two-phase system was the following: to a buffered solution of NaHCO $_2$  (712  $\mu$ L, 200 mM in NaHCO $_2$ , 50 mM in KPi, pH adjusted with NaOH to 7.5) was added [Cp\*Ir-biot-p-L)Cl] (50  $\mu$ L of a 1 mM solution in DMF) and either Sav-S112A (50  $\mu$ L, 1 mM free binding sites in H $_2$ O; 3 free binding sites per tetramer assumed) or H $_2$ O (50  $\mu$ L), respectively. The mixture then was supplemented with FAD solution (10  $\mu$ L of a 1 mM solution in H $_2$ O) as well as HbpA stock solution (128  $\mu$ L, 12.5 mg/mL, 6.9 U/mL in KPi buffer, pH of buffer 7.5). Immediately afterwards 2-hydroxybiphenyl in 1-decanol (1 mL of a 100 mM solution) was added. The reaction mixtures were placed in a thermoshaker and incubated at 30°C and 800 rpm. After a short mixing period (approx. 1 minute) a sample (0.1 mL) was withdrawn and centrifuged to induce phase separation. 10  $\mu$ L of the organic phase were withdrawn (the remaining sample was added back to the reaction mixture), diluted with ACN/water (0.99 mL of a 50:50 (v/v) mixture containing 0.1 % TFA) and analyzed by RP-HPLC as described above. The reaction was subsequently initiated by addition of NAD\* stock solution (50  $\mu$ L of a 10 mM solution in H $_2$ O). Samples were taken at the indicated time points and treated as described above. For analysis, only the substrate and product concentrations in the organic phase were considered.

#### Determination of apparent kinetic constants of ATHase catalyzed NAD reduction

Note: the reaction conditions for the kinetic measurement (50 mM KPi-buffer, 200 mM NaHCO<sub>2</sub>) are not identical to the conditions used in the monophasic reaction set-up (42 mM KPi-buffer, 168 mM NaHCO<sub>2</sub>). The following buffers and stock solutions were used: buffer (50 mM KPi pH 7.5), NaHCO<sub>2</sub> (400 mM in KPi-buffer, pH adjusted with NaOH to 7.5), NAD $^+$  (0.025 mM, 0.05 mM, 0.075 mM, 0.1 mM, 0.15 mM, 0.25 mM, 0.4 mM, 0.5 mM, 1 mM, 4 mM, 6 mM, 8 mM, 10 mM in KPi buffer); [Cp\*Ir(Biot-p-L)Cl] - 1.00 mM (M $_{\rm W}$  803 g/mol, weight 2.32mg in 2.889 ml of DMF); ATHase: 10.23 mg of Sav S112A were dissolved in Buffer 1 (4.209 mL) and Ir-stock solution (467  $\mu$ L) was added. This leads to a final concentration of approximately 100  $\mu$ M (in respect to Ir) and a ratio of Ir/free binding sites of 1/1 (3 binding sites per tetramer assumed).

All stock solutions were incubated at 30 °C prior use. The samples were prepared in the cuvette (polystyrene) by adding first KPi buffer (250  $\mu$ L), followed by the ATHase (50  $\mu$ L, final conc. 5  $\mu$ M), and then NAD<sup>+</sup> (200  $\mu$ L from the corresponding stock). The reactions were started by the addition of NaHCO<sub>2</sub> (500  $\mu$ L, final 200 mM).

Each measurement was performed in triplicate in a Shimadzu UV-1800 UV spectrophotometer (at 30 °C) and analyzed with UV Probe, Version 2.34. Absorption was detected at 340 nm and an absorption coefficient of 6220  $M^{-1}cm^{-1}$  for NADH was used for calculation of the kinetic parameters. Rates were determined by considering the linear part of increase in absorbance over time. The apparent Michaelis-Menten parameters  $k_{cat}$  and  $K_m$  were obtained applying sigmoidal fit using OriginPro 8.5.1® corresponding to the Michaelis-Menten equation.

#### References

- [1] S. Aldridge, Industry backs biocatalysis for greener manufacturing, *Nat. Biotechnol.*, **2013**, *31*, 95-96.
- [2] A. Liese, K. Seelbach, A. Buchholz, J. Haberland, in Industrial Biotransformations (Eds.: A. Liese, K. Seelbach, C. Wandrey), *Wiley-VCH Verlag GmbH & Co. KGaA*, **2006**, p. 153.
- [3] M. Breuer, K. Ditrich, T. Habicher, B. Hauer, M. Keßeler, R. Stürmer, T. Zelinski, Industrial Methods for the Production of Optically Active Intermediates, *Angew. Chem. Int. Ed.*, **2004**, 43, 788-824.
- [4] A. Schmid, J. S. Dordick, B. Hauer, A. Kiener, M. Wubbolts, B. Witholt, Industrial biocatalysis today and tomorrow, *Nature*, **2001**, *409*, 258-268.
- [5] A. Schmid, F. Hollmann, J. B. Park, B. Buhler, The use of enzymes in the chemical industry in Europe, *Curr. Opin. Biotechnol.*, **2002**, *13*, 359-366.
- [6] K. M. Koeller, C. H. Wong, Enzymes for chemical synthesis, *Nature*, **2001**, *409*, 232-240.
- [7] A. J. J. Straathof, S. Panke, A. Schmid, The production of fine chemicals by biotransformations, *Curr. Opin. Biotechnol.*, **2002**, *13*, 548-556.

- [8] D. Monti, G. Ottolina, G. Carrea, S. Riva, Redox Reactions Catalyzed by Isolated Enzymes, *Chem. Rev.*, **2011**, *111*, 4111-4140.
- [9] F. Hollmann, I. Arends, K. Buehler, A. Schallmey, B. Buhler, Enzyme-mediated oxidations for the chemist, *Green Chem.*, **2011**, *13*, 226-265.
- [10] R. Wichmann, D. Vasic-Racki, in Technology Transfer in Biotechnology, *Vol. 92* (Ed.: U. Kragl), *Springer Berlin Heidelberg*, **2005**, pp. 225-260.
- [11] H. Chenault, G. Whitesides, Regeneration of nicotinamide cofactors for use in organic synthesis, *Appl. Biochem. Biotechnol.*, **1987**, *14*, 147-197.
- [12] W. Kroutil, H. Mang, K. Edegger, K. Faber, Biocatalytic Oxidation of Primary and Secondary Alcohols, *Adv. Synth. Catal.*, **2004**, *346*, 125-142.
- [13] W. A. van der Donk, H. M. Zhao, Recent developments in pyridine nucleotide regeneration, *Curr. Opin. Biotechnol.*, **2003**, *14*, 421-426.
- [14] S. Betanzos-Lara, Z. Liu, A. Habtemariam, A. M. Pizarro, B. Qamar, P. J. Sadler, Organometallic Ruthenium and Iridium Transfer-Hydrogenation Catalysts Using Coenzyme NADH as a Cofactor, *Angew. Chem. Int. Ed.*, **2012**, *51*, 3897-3900.
- [15] J. Canivet, G. Suess-Fink, P. Stepnicka, Water-soluble phenanthroline complexes of rhodium, iridium and ruthenium for the regeneration of NADH in the enzymatic reduction of ketones, *Eur. J. Inorg. Chem.*, **2007**, 4736-4742.
- [16] P. Haquette, B. Talbi, L. Barilleau, N. Madern, C. Fosse, M. Salmain, Chemically engineered papain as artificial formate dehydrogenase for NAD(P)H regeneration, *Org. Biomol. Chem.*, **2011**, *9*, 5720-5727.
- [17] F. Hildebrand, S. Luetz, Stable Electroenzymatic Processes by Catalyst Separation, *Chem. Eur. J.*, **2009**, *15*, 4998-5001.
- [18] F. Hollmann, K. Hofstetter, A. Schmid, Non-enzymatic regeneration of nicotinamide and flavin cofactors for monooxygenase catalysis, *Trends Biotechnol.*, **2006**, *24*, 163-171.
- [19] Y. Maenaka, T. Suenobu, S. Fukuzumi, Efficient Catalytic Interconversion between NADH and NAD(+) Accompanied by Generation and Consumption of Hydrogen with a Water-Soluble Iridium Complex at Ambient Pressure and Temperature, J. Am. Chem. Soc., 2012, 134, 367-374.
- [20] M. Poizat, I. Arends, F. Hollmann, On the nature of mutual inactivation between Cp\*Rh(bpy)(H2O) (2+) and enzymes analysis and potential remedies, *J. Mol. Catal. B-Enzym.*, **2010**, *63*, 149-156.
- [21] H. C. Lo, O. Buriez, J. B. Kerr, R. H. Fish, Bioorganometallic chemistry part 11. Regioselective reduction of NAD(+) models with Cp\*Rh(bpy)H (+): Structure-activity relationships and mechanistic aspects in the formation of the 1,4-NADH derivatives, *Angew. Chem. Int. Ed.*, 1999, 38, 1429-1432.
- [22] H. C. Lo, C. Leiva, O. Buriez, J. B. Kerr, M. M. Olmstead, R. H. Fish, Bioorganometallic Chemistry. 13. Regioselective Reduction of NAD+ Models, 1-Benzylnicotinamde Triflate and β-Nicotinamide Ribose-5'-methyl Phosphate, with in Situ Generated [Cp\*Rh(Bpy)H]+: Structure–Activity Relationships, Kinetics, and Mechanistic Aspects in the Formation of the 1,4-NADH Derivatives†, *Inorg. Chem.*, **2001**, *40*, 6705-6716.
- [23] M. M. Grau, M. Poizat, I. Arends, F. Hollmann, Phosphite-driven, Cp\*Rh(bpy)(H2O) (2+)-catalyzed reduction of nicotinamide and flavin cofactors: characterization and application to promote chemoenzymatic reduction reactions, *Appl. Organomet. Chem.*, **2010**, *24*, 380-385.

- [24] Z. Jiang, C. Lü, H. Wu, Photoregeneration of NADH Using Carbon-Containing TiO2, *Ind. Eng. Chem. Res.*, **2005**, *44*, 4165-4170.
- [25] U. Kölle, M. Grützel, Organometallic Rhodium(III) Complexes as Catalysts for the Photoreduction of Protons to Hydrogen on Colloidal TiO2, *Angew. Chem. Int. Ed. Engl.*, **1987**, *26*, 567-570.
- [26] S. H. Lee, D. H. Nam, J. H. Kim, J.-O. Baeg, C. B. Park, Eosin Y-Sensitized Artificial Photosynthesis by Highly Efficient Visible-Light-Driven Regeneration of Nicotinamide Cofactor, *ChemBioChem*, **2009**, *10*, 1621-1624.
- [27] C. B. Park, S. H. Lee, E. Subramanian, B. B. Kale, S. M. Lee, J.-O. Baeg, Solar energy in production of l-glutamate through visible light active photocatalyst-redox enzyme coupled bioreactor, *Chem. Commun.*, **2008**, *0*, 5423-5425.
- [28] R. Ruppert, S. Herrmann, E. Steckhan, Efficient indirect electrochemical in-situ regeneration of NADH: Electrochemically driven enzymatic reduction of pyruvate catalyzed by D-LDH, *Tetrahedron Lett.*, **1987**, *28*, 6583-6586.
- [29] R. Ruppert, S. Herrmann, E. Steckhan, Very efficient reduction of NAD(P)+ with formate catalysed by cationic rhodium complexes, *Journal of the Chemical Society, Chemical Communications*, **1988**, 1150-1151.
- [30] F. Hollmann, B. Witholt, A. Schmid, Cp\*Rh(bpy)(H2O) (2+): a versatile tool for efficient and non-enzymatic regeneration of nicotinamide and flavin coenzymes, *J. Mol. Catal. B-Enzym.*, **2002**, *19*, 167-176.
- [31] J. D. Ryan, R. H. Fish, D. S. Clark, Engineering Cytochrome P450 Enzymes for Improved Activity towards Biomimetic 1,4-NADH Cofactors, *ChemBioChem*, **2008**, *9*, 2579-2582.
- [32] V. Höllrigl, K. Otto, A. Schmid, Electroenzymatic Asymmetric Reduction of rac-3-Methylcyclohexanone to (1S,3S)-3-Methylcyclohexanol in Organic/Aqueous Media Catalyzed by a Thermophilic Alcohol Dehydrogenase, *Adv. Synth. Catal.*, **2007**, *349*, 1337-1340.
- [33] F. Hildebrand, S. Luetz, Electroenzymatic synthesis of chiral alcohols in an aqueous organic two-phase system, *Tetrahedron-Asymmetry*, **2007**, *18*, 1187-1193.
- [34] J. Lutz, F. Hollmann, T. V. Ho, A. Schnyder, R. H. Fish, A. Schmid, Bioorganometallic chemistry: biocatalytic oxidation reactions with biomimetic NAD(+)/NADH co-factors and Cp\*Rh(bpy)H (+) for selective organic synthesis, *J. Organomet. Chem.*, **2004**, *689*, 4783-4790.
- [35] T. R. Ward, Artificial Metalloenzymes Based on the Biotin-Avidin Technology: Enantioselective Catalysis and Beyond, *Acc. Chem. Res.*, **2011**, *44*, 47-57.
- [36] F. Rosati, G. Roelfes, Artificial Metalloenzymes, *ChemCatChem*, **2010**, *2*, 916-927.
- [37] M. R. Ringenberg, T. R. Ward, Merging the best of two worlds: artificial metalloenzymes for enantioselective catalysis, *Chem. Commun.*, **2011**, *47*, 8470-8476.
- [38] Y. Lu, N. Yeung, N. Sieracki, N. M. Marshall, Design of functional metalloproteins, *Nature*, **2009**, *460*, 855-862.
- [39] W. A. Suske, M. Held, A. Schmid, T. Fleischmann, M. G. Wubbolts, H. P. E. Kohler, Purification and characterization of 2-hydroxybiphenyl 3-monooxygenase, a novel NADH-dependent, FAD-containing aromatic hydroxylase from Pseudomonas azelaica HBP1, *J. Biol. Chem.*, **1997**, 272, 24257-24265.
- [40] W. A. Suske, W. J. H. van Berkel, H. P. E. Kohler, Catalytic mechanism of 2-hydroxybiphenyl 3-monooxygenase, a flavoprotein from Pseudomonas azelaica HBP1, *J. Biol. Chem.*, **1999**, *274*, 33355-33365.

- [41] A. Schmid, I. Vereyken, M. Held, B. Witholt, Preparative regio- and chemoselective functionalization of hydrocarbons catalyzed by cell free preparations of 2-hydroxybiphenyl 3-monoxygenase, *J. Mol. Catal. B-Enzym.*, **2001**, *11*, 455-462.
- [42] V. Köhler, J. Mao, T. Heinisch, A. Pordea, A. Sardo, Y. M. Wilson, L. Knörr, M. Creus, J.-C. Prost, T. Schirmer, T. R. Ward, OsO4·Streptavidin: A Tunable Hybrid Catalyst for the Enantioselective cis-Dihydroxylation of Olefins, *Angew. Chem. Int. Ed.*, **2011**, *50*, 10863-10866.
- [43] C. Letondor, A. Pordea, N. Humbert, A. Ivanova, S. Mazurek, M. Novic, T. R. Ward, Artificial transfer hydrogenases based on the biotin-(strept)avidin technology: Fine tuning the selectivity by saturation mutagenesis of the host protein, *J. Am. Chem. Soc.*, **2006**, *128*, 8320-8328.

# Chapter 6

# Hydrophobic formic acid esters for cofactor regeneration in aqueous/organic two-liquid phase systems

This chapter is based on

E. Churakova, B. Tomaszewski, K. Buehler, A. Schmid, I. Arends, F. Hollmann

Top. Catal., 2014, 57, 385-391

# Chapter 6

# Hydrophobic formic acid esters for cofactor regeneration in aqueous/organic two-liquid phase systems

#### Introduction

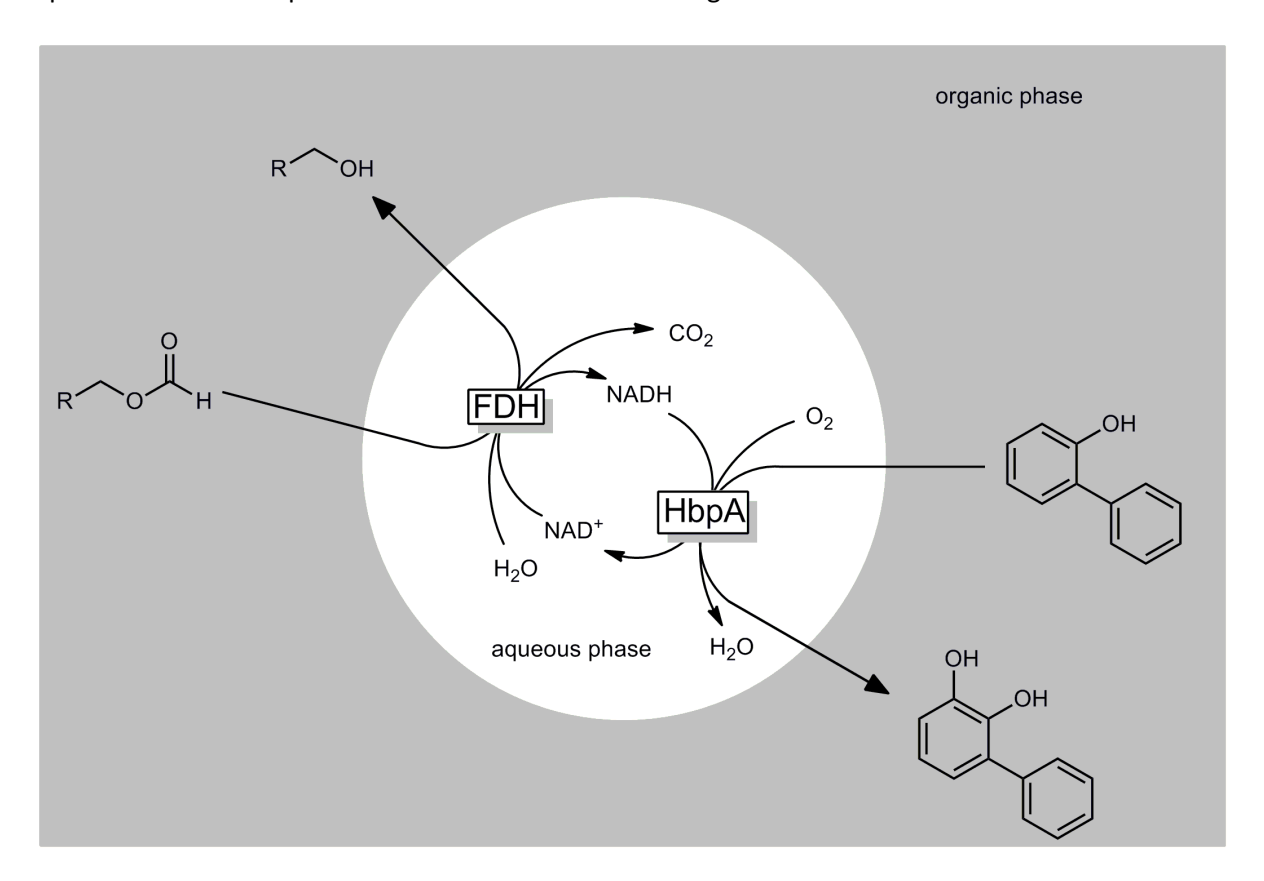
Formate dehydrogenase (FDH, E.C. 1.2.1.2) is certainly one of the most widely applied cofactor regeneration systems  $^{[1-4]}$  used to promote NADH-dependent reductions and oxidations  $^{[5-11]}$ . The formate - driven NAD $^+$  reduction yields volatile CO $_2$  as by-product, thus efficiently shifting the reaction equilibrium towards NADH formation.

One drawback of the FDH regeneration system is its dependence on highly polar formic acid or formates as sacrificial electron donors to drive the regeneration reaction. As a result, classical FDH-based reaction systems are limited to mainly aqueous media. Considering that the majority of the (industrially) relevant substrate/product couples are rather hydrophobic, purely aqueous reaction systems suffer from poor substrate loadings and inherently poor space-time-yields. One possible solution to this dilemma is the use of aqueous/organic two-liquid phase systems (2 LPS) wherein the bulk of reagents is dissolved in the water-immiscible organic phase and partitions into the, biocatalyst-containing, aqueous phase for transformation according to their partition coefficient <sup>[9-13], [Chapter 2]</sup>. In order to obtain high volumetric productivities, large volumetric ratios of organic to aqueous phase are desirable. In this case, formate has to be supplied at high concentration in the aqueous layer to attain stoichiometric amounts of the sacrificial reductant. The resulting high ionic strength in the aqueous phase can pose a significant challenge to activity and stability of the dissolved biocatalysts.

Inspired by a recent contribution by Bertau and coworkers who reported FDH-activity on formate esters <sup>[14]</sup>, we hypothesized that hydrophobic formic acid esters may serve as sacrificial electron donors to promote NADH-dependent reactions in 2 LPS. Hence, hydrophobized formates can be supplied in the apolar organic phase in stoichiometric amounts without impairing the biocatalyst(s) due to high ionic strengths in the aqueous layer. Ideally, the formic acid esters themselves form the organic phase thereby avoiding the need of additional solvent. Provided the alcohol part of the formic acid ester is a hydrophobic alcohol its accumulation in the organic phase in the course of the reaction should not alter the (hydrophobic) properties of the organic phase too much.

To test the hypothesis of FDH-catalyzed NADH regeneration using formate esters in 2 LPS we chose 2-hydroxybiphenyl-3-monooxygenase (HbpA, E.C. 1.14.13.44, an NADH- and FAD-dependent

enzyme) as a model enzyme <sup>[10-11, 15-19]</sup>. As organic phase we chose octyl formate since both the ester and 1-octanol are sufficiently hydrophobic to serve as second, water-immiscible phase. Overall, a biphasic reaction setup as shown in Scheme 1 was envisaged.



Scheme 1. The 'hydrophobized formates concept' to promote a NADH - dependent oxyfunctionalization reaction. Formic acid esters, such as octyl formate, form the organic phase also serving as substrate reservoir and product sink. Formate dehydrogenase (FDH) mediates the oxidative hydrolysis of the formic acid esters into  $CO_2$  and alcohol while regenerating NADH [14]. The latter is consumed in the course of the HbpA (2-hydroxybiphenyl-3-monooxygenase) - catalyzed hydroxylation of 2-hydroxybiphenyl.

#### **Results**

In a first set of experiments we examined the influence of increasing formate concentrations on the activity of both HbpA and FDH (Figure 1).

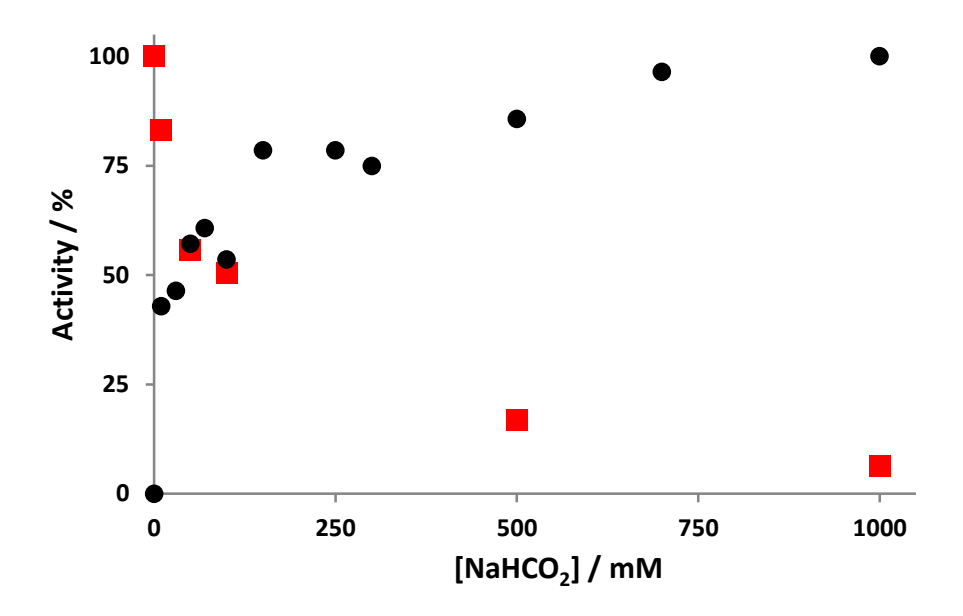


Figure 1. Influence of [NaHCO<sub>2</sub>] on the activity of HbpA ( $\blacksquare$ ) and FDH ( $\bullet$ ). General conditions: KPi buffer 50mM, pH = 7.5, V = 1 mL, T = 30°C, ( $\blacksquare$ ): [HbpA] = 0.066 U mL<sup>-1</sup> = 0.04 mg mL<sup>-1</sup>, [2-hydroxybiphenyl] = 0.2 mM, [NADH] = 0.3 mM, [FAD] = 2  $\mu$ M; ( $\bullet$ ) [FDH] = 0.018 U mL<sup>-1</sup> = 0.017 mg mL<sup>-1</sup>, [NAD<sup>+</sup>] = 1 mM.

Interestingly, both enzymes showed an opposite behaviour with increasing sodium formate concentrations. Whereas FDH was apparently not inhibited by the presence of up to 1 M sodium formate, HbpA activity decreased significantly. Already in the presence of 100 mM of sodium formate HbpA activity was reduced by 50%. This is in line with previous observations made with HbpA <sup>[18]</sup>. Suske et al. have observed a significant influence of monovalent anions (such as azide and chloride) on the stability of the intermediate hydroperoxoflavin <sup>[19]</sup>, which may also account for the apparent inhibition observed with formate. Also, a negative influence of the increasing ionic strength on the structural integrity of the biocatalyst may be hypothesized. Further studies will be necessary to fully understand the nature of the apparent inhibition of HbpA by NaHCO<sub>2</sub>. Overall, we concluded that HbpA catalyzed hydroxylation reaction (being inhibited by already comparably low sodium formate concentrations) is a suitable model system to evaluate the 'hydrophobized formates concept'.

Next, we went on to test the feasibility of the 'hydrophobic formates concept'. Under arbitrarily chosen reaction conditions (see Figure 2, caption) we were pleased to observe stable hydroxylation activity over at least 3 weeks wherein the desired product 2,3-dihydroxybiphenyl continuously accumulated in the organic phase (Figure 2). It is worth mentioning here that in the absence of either HbpA, FDH or NAD<sup>+</sup>, no conversion was observed.

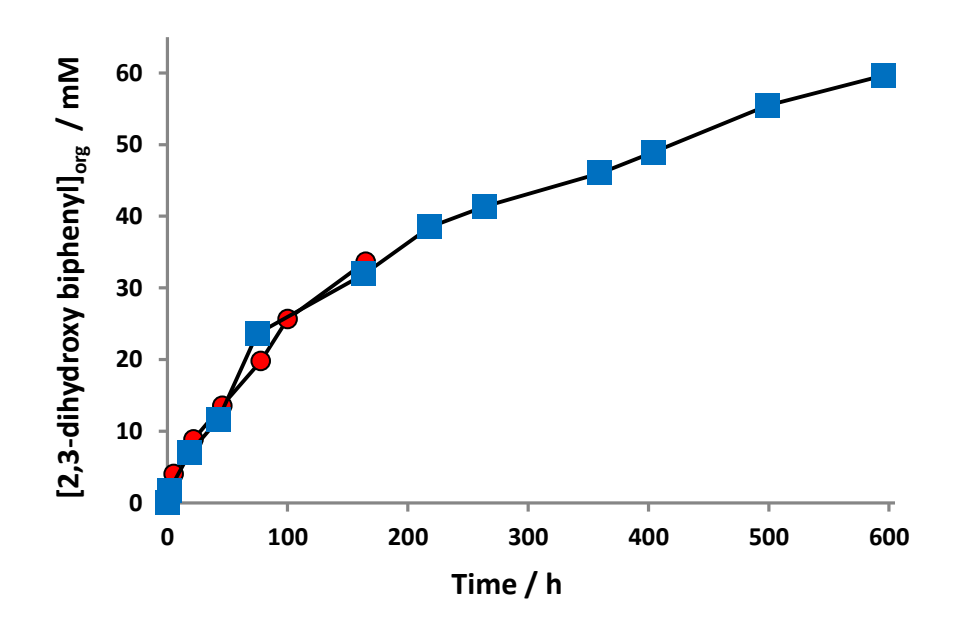


Figure 2. Time-course of 2,3-dihydroxybiphenyl formation in a 2 LPS using octyl formate as a second organic phase. General conditions: octyl formate: KPi = 9:1 (v/v);  $V_{total} = 10 \text{ ml}$ ,  $T = 30^{\circ}\text{C}$ ; aqueous concentrations:  $[HbpA] = 5.4 \text{ U mL}^{-1} = 3.6 \text{ mg mL}^{-1}$ ,  $[FDH] = 5.4 \text{ U mL}^{-1} = 5.1 \text{ mg mL}^{-1}$ ,  $[NAD^{+}] = 2 \text{ mM}$  ( $\blacksquare$ ); organic concentrations: [2-hydroxybiphenyl] = 500 mM.

On average (over the whole period), the productivity reached was 0.1 mMh<sup>-1</sup><sub>org</sub>. Nevertheless, the reaction yielded the desired 2,3-dihydroxybiphenyl in 12% yield with very promising turnover numbers (TN = final amount of product divided by amount of catalyst used) for NAD<sup>+</sup> and HbpA of 2680 and 9540, respectively. Also the extraordinary high robustness of the reaction (steadily accumulating the product over at least 3 weeks) is worth pointing out.

The high robustness of the overall reaction was astonishing as control experiments in the absence of substrate and NAD<sup>+</sup> under otherwise identical conditions to the reaction shown in Figure 2 indicated half-life times of 16h and 24h for HbpA and FDH, respectively (Figure 3). We attribute this to slow, spontaneous hydrolysis of octyl formate and subsequent accumulation of formic acid in the aqueous medium, leading to inactivation of the biocatalysts.

In fact, we attempted to accelerate the overall reaction rate via lipase-mediated<sup>1</sup> octyl formate hydrolysis, thus generating formic acid in situ for NADH regeneration. However, only trace amounts of product were observed accompanied with a pH drop to less than 2, therefore leading to instantaneous acid-induced enzyme inactivation.

Overall, provided the consumption of formic acid proceeds faster than its formation via hydrolysis, a pH-stable system can be achieved. Therefore, water-induced octyl formate hydrolysis may contribute to the overall FDH activity but acid induced enzyme inactivation under reaction conditions is unlikely.

-

<sup>&</sup>lt;sup>1</sup> See an experimental section

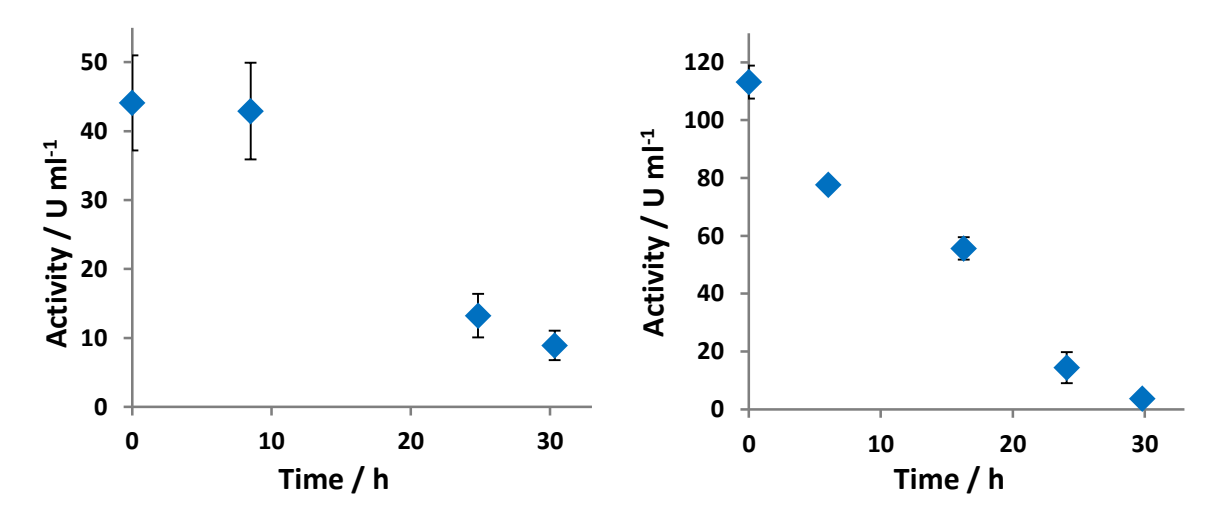


Figure 3. Stability of FDH (left) and HbpA (right) under the conditions of a 2 LPS applied in this study. General conditions: octyl formate: KPi = 9:1 (v/v), [KPi] = 50 mM, PM = 7.5, PM = 10 mJ, PM = 1.5, PM = 1.5

It should be mentioned here that the productivity of the reaction system (shown in Figure 2) significantly fell back behind the values expected from the enzyme activities applied. An initial product formation rate of a bit more than 1 mMh<sup>-1</sup> (in the organic phase, corresponding to approx. 9 mMh<sup>-1</sup> in the aqueous layer) was determined. This corresponds to a formal specific HbpA activity of 0.15 U mL<sup>-1</sup>, which is significantly lower than (approx. 3%) the theoretical HbpA activity of 5.4 U mL<sup>-1</sup> determined in independent spectrophotometric experiments. Similar calculation also applies for the formal activity of FDH.

On the one hand, significant decline in activity of overall two enzymes system might be explained by slow NADH regeneration catalyzed by FDH using octyl formate. Thus Bertau and co-authors defined that *Vmax* values for FDH - mediated formate ester cleavage are lower than for "natural" substrate sodium formate by a factor 2-3 <sup>[14]</sup>. Hence, using octyl formate for NADH regeneration may result in lower activity of FDH, subsequently retarding the activity of the overall system. On the other hand, diffusion of the (co)-substrates (octyl formate and 2-hydroxybiphenyl) from organic to aqueous phase could be overall rate limiting thereby accounting for the low formal specific enzyme activities.

To clarify this, we systematically varied the concentrations of all reagents and catalysts to identify the overall rate-limiting component. Interestingly, varying the concentration of either HbpA, FDH or NAD<sup>+</sup> did not significantly influence the overall rate of the system; within experimental error, all rates were identical. Exemplarily the influence of varying [NAD<sup>+</sup>] is shown in Figure 2 (circles 2 mM and boxes 0.2 mM). Similar results were also obtained when changing the biocatalysts concentration.

As the catalysts concentrations had no apparent effect on the overall reaction rate, we suspected that diffusion limitation over the interphase might be overall rate - limiting. In fact, changing the

concentration of both octyl formate and 2-hydroxybiphenyl had a clear impact on the reaction rate (Figure 4 and Figure 5).

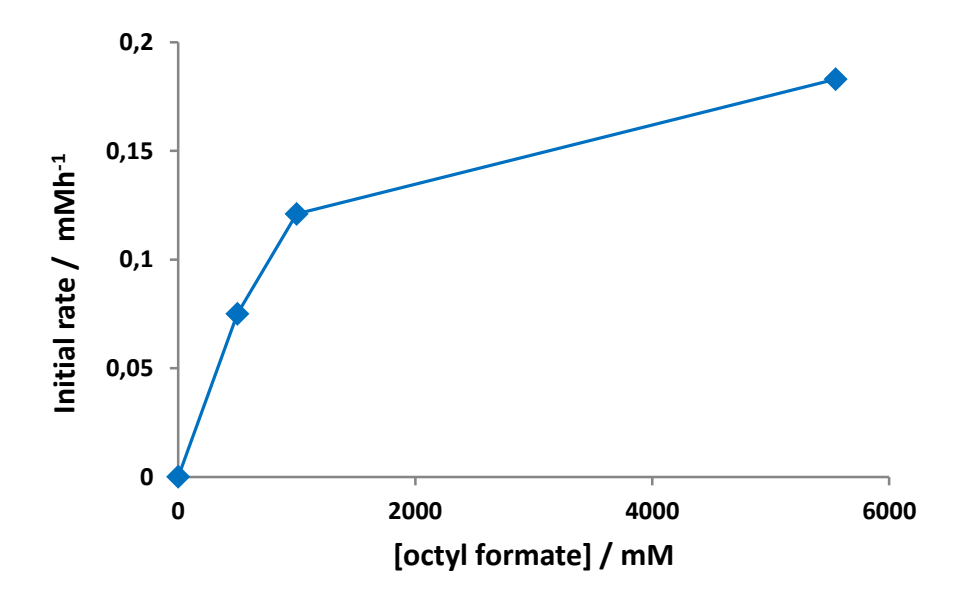


Figure 4. Influence of octyl formate concentration on the rate of 2,3-dihydroxybiphenyl formation (determined in the organic phase). General conditions: organic phase: KPi = 9:1 (v/v), V total = 1 ml; aqueous phase: [HbpA] = 5.4 U mL<sup>-1</sup>, [FDH] = 5.4 U mL<sup>-1</sup>, [NAD<sup>+</sup>] = 2 mM; organic phase: different ratios of 1-decanol to octyl formate were used resulting in the molar octyl formate concentrations shown; [2-hydroxybiphenyl] = 10 mM.

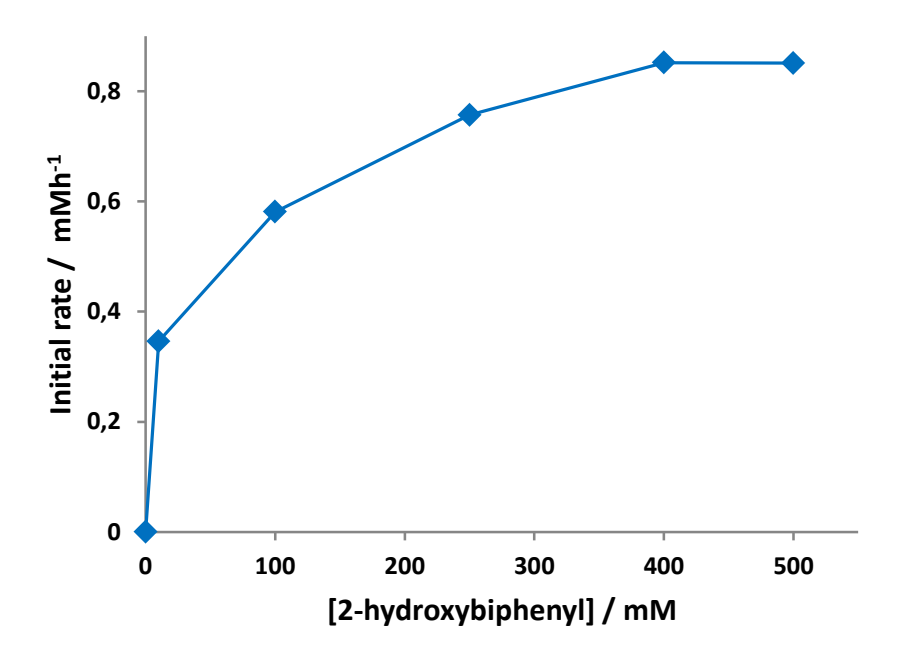


Figure 5. Influence of 2-hydroxybiphenyl concentration on the rate of 2,3-dihydroxybiphenyl formation (determined in the organic phase). General conditions: octyl formate: KPi = 9:1 (v/v); V total = 1 ml. Aqueous phase:  $[HbpA] = 5.4 \text{ U mL}^{-1}$ ,  $[FDH] = 5.4 \text{ U mL}^{-1}$ ,  $[NAD^{+}] = 2 \text{ mM}$ ; organic phase: 2-hydroxybiphenyl dissolved in octyl formate at shown concentrations.

In both series saturation-type behaviour of the reaction rate on the concentration of 2-hydroxybiphenyl and octyl formate in the organic layers was observed. We interpret these results in terms of phase-transfer limiting the overall rate of the reaction system. It should be mentioned

that overall system might be also restricted by oxygen diffusion due to its low solubility in aqueous media (approximately 0.25 mM).

The intrinsic influence of the octyl formate and 2 - hydroxybiphenyl concentrations on the initial reaction rate imply the diffusion of the substrates from organic to aqueous phase indeed significantly confines the system. Hence, the interfacial area of aqueous and organic layers should also have a significant influence on the overall rate [Chapter 2]. Indeed, changing the reaction setup from gently shaken (Figure 2) to vigorously mixed (performing the reaction in baffled Erlenmeyer flasks) almost doubled the reaction rate albeit at the expense of a significantly reduced stability of the production system: under the mechanically very demanding conditions the enzymes denatured rapidly leading to an almost complete loss of activity after 1h.

#### **Discussion**

For many biocatalytic reactions water is not the ideal solvent as hydrophobic reactants are only poorly solubilized. The resulting low reactant concentrations, combined with sometimes tedious reaction work-up, render biocatalytic procedures unpractical. Therefore it is not astonishing that a growing number of publications aim at 'water-free' or minimal water-content biocatalysis [10-11, 13, 20-26]. For production systems necessitating diffusible nicotinamide cofactors (for example monooxygenases where a NADH-regenerating system is inevitable), the so-called two-liquid phase system (2 LPS) approach may be a good compromise as here a hydrophobic organic solvent serves as substrate reservoir and product sink enabling overall high substrate loadings. In addition, 2 LPSs can also render biocatalytic reactions more efficient by controlling the aqueous concentrations of substrates and products. Thereby, inhibitory effects of excess reagents can be minimized as well as undesired side reactions, such as the non-productive uncoupling of NADH oxidation from substrate hydroxylation resulting in  $H_2O_2$  formation, as observed e.g. with HbpA [18-19].

Although FDH cofactor regeneration is widely applied, high substrate loadings are difficult to achieve using formate salts as stoichiometric reductants as the resulting high ionic strengths in the aqueous layer may significantly impair the biocatalysts' activity and stability. In the current contribution we have demonstrated the principal feasibility of using hydrophobized formic acids (by means of hydrophobic formic acid esters) in the 2 LPS approach. Thereby, hydrophobic formic acid esters not only serve as substrate reservoir and product sink but also as source of reducing equivalents.

The major limitation of the current reaction setup is the sluggish phase transfer kinetics of both 2-hydroxybiphenyl and octyl formate. Possibly, also low oxygen availability contributes to the overall slow reaction rate. Increasing the phase transfer rate, especially via emulsification should be in the focus of further investigations.

Despite the early stage of development of this system and many challenges still to be faced en route for practical applications, we believe that hydrophobized formates represent an interesting future development in FDH-based redox biocatalysis.

#### **Conclusions and outlook**

In this contribution we have demonstrated the principle applicability of the 'hydrophobized formates concept' to promote NADH-dependent redox reactions. Hydrophobic esters of formic acid can serve as organic phase in biocatalytic 2 LPS reactions and as source of reducing equivalents at the same time; thereby paving the way towards low-water content redox biotransformations.

The current setup is limited by poor mass transfer rates over the interphase, which should be addressed in future investigations. For example, creating emulsions stabilized with surfactant might be a solution to the diffusion limitations. Here, the major challenge to be addressed is to reduce the mechanical stress induced by the emulsification process avoiding the biocatalysts inactivation. Additionally, engineering measures to maintain sufficient oxygen concentration have to be taken. Furthermore, the novel concept of using formic acid esters for NADH regeneration might be extended for various ADHs and P450 monooxygenases as well. Depending on the nature of the enzymes chosen, the biocatalyst stability issues might be addressed by immobilization or using stabilizing additives, e.g. different polyols [27-29].

#### **Experimental**

#### **Materials**

Enzymes: HbpA (119.4 mg/mL) and FDH (52 mg/mL) glycerol stocks of lyophilized enzymes were provided by prof. A. Schmid, TU Dortmund University, Germany. Enzymes were produced and purified following to previously published procedure [10-11, 30-31].

Chemicals: All chemicals were purchased from Sigma-Aldrich, Fluka or Acros in the highest purity available and used as received. The following buffers and stock solutions were used: buffer (50 mM KP<sub>i</sub> pH 7.5), NADH (25 mM in buffer), NAD<sup>+</sup> (10 mM in buffer), HbpA (3.98 mg mL<sup>-1</sup> in buffer), FDH (1.74 mg mL<sup>-1</sup> in buffer), NaHCO<sub>2</sub> (2 M in buffer, pH adjusted to 7.5), 2-hydroxybiphenyl (25 mM in methanol), FAD (0.2 mM in buffer).

#### UV spectrophotophotometric activity measurements

The activity of both HbpA and FDH was determined using a spectrophotometric assay following the depletion (HbpA) or formation (FDH) of the characteristic UV-absorption band of NADH at 340 nm ( $\epsilon$  = 6220 M<sup>-1</sup>cm<sup>-1</sup>). The experiments were performed using 1.5 mL disposable UV cuvettes (polystyrene)

at 30 °C on a Shimadzu UV-2401 PC spectrophotometer with Julabo F12 Refrigerated/Heating Circulator. All experiments were performed at 30 °C.

**HbpA** assay: HbpA was diluted in buffer to a final concentration of 0.04 mg mL<sup>-1</sup> and supplemented with FAD (0.002 mM final). The assay was started by addition of NADH (0.3 mM final) to determine the non-substrate related NADH oxidation rate (background activity). After one minute, 2-hydroxybiphenyl (0.2 mM final) was added to determine the total NADH oxidation rate. The specific 2-hydroxybiphenyl hydroxylation activity of the HbpA preparation (1.66 U mg<sup>-1</sup>) was obtained by subtracting the background activity from the total activity.

**FDH-assay:** FDH was diluted in buffer to a final concentration of 0.017 mg mL<sup>-1</sup> and supplemented with NAD<sup>+</sup> (1 mM final) and NaHCO<sub>2</sub> (100 mM final). The specific NAD<sup>+</sup>-reduction activity of the FDH-preparation used was 1.06 U mg<sup>-1</sup>. A spectroscopic determination of the FDH activity towards octyl formate proved to be difficult due to its poor solubility in aqueous media (diffusion limitation and/or formation of optically intransparent emulsions) and the slow hydrolysis of octyl formate leading to the formation of aqueous formic acids.

#### **Stability measurements**

The stabilities of HbpA and FDH under reaction conditions were determined by incubating 5.4 U mL<sup>-1</sup> of each enzyme at 30 °C for 30 hours in a 2 mL reaction tube containing a biphasic mixture (phase ratio 9:1 organic to aqueous) consisting of 100  $\mu$ L of KPi buffer (50 mM, pH = 7.5) and 900  $\mu$ L of octyl formate, in the presence of TWEEN 20 (0.2 mg mL<sup>-1</sup>). TWEEN 20 was chosen as surfactant to facilitate the formation of stable emulsions with minimal shear force [Chapter 2]. At intervals, 10  $\mu$ L samples of the aqueous phase were withdrawn and analysed using the photometric assay described above.

#### Coupling of FDH catalyzed NADH regeneration to the HbpA reaction

Unless mentioned otherwise, the coupled reaction of FDH and HbpA was performed in 2 mL tubes at 30  $^{\circ}$ C and mixed at 1200 rpm. The reaction mixtures consisted of a biphasic mixture of KP<sub>i</sub> buffer and octyl formate with the ratio 1:9 (v/v). The organic phase contained 2-hydroxybiphenyl in a concentration range of 10-500 mM and the aqueous phase contained HbpA (5.4 U mL<sup>-1</sup>), FDH 5.4 U mL<sup>-1</sup>), NAD<sup>+</sup> (2 mM) and FAD (20  $\mu$ M). The reaction mixture was supplemented with TWEEN 20 (0.2 mg mL<sup>-1</sup>). We have refrained from adding catalase to the experiments since the cell crude extracts (originating from aerobic E. coli cultivations) presumably contained endogenous catalase activity. Aliquots of 10  $\mu$ L of the organic phase were withdrawn at intervals, diluted with 990  $\mu$ L of acetonitrile containing 0.1% of TFA (v/v) and analysed by RP-HPLC.

The time course of 2,3-dihydroxybiphenyl formation was done under the aforementioned conditions at 10 mL scale (50 mL tubes) with an initial ratio between the organic and aqueous phase of 9:1 (v/v). The final phase ratio was approximately 8.84:1 (v/v) after 16 samples of 10  $\mu$ L.

The effect of lipase addition was investigated under following conditions: the coupled reaction of FDH and HbpA was performed as described in standard procedure in 50 mL tubes using NAD $^+$  (0.2 mM) and 2-HBP (500 mM). To the reaction assay ( $V_{total} = 10$  mL), 0.1 g of immobilized Lipase B (CalB) from Candida Antarctica (Novozyme 435) was added.

All experiments had been performed in duplicates (unfortunately not always sampling at identical times). Therefore, no error bars are given in the figures. Nevertheless, the deviation between the single experiments was maximally 14%.

#### **HPLC** analysis

The progress of the reactions was measured by RP-HPLC on a Shimadzu LC-20 system equipped with a Shimadzu SPD-20A Photo Diode Array detector using a Waters Xterra column (RP18, 3.5  $\mu$ M, 4.6  $\times$  150 mm). The temperature was controlled at 40°C by a Shimadzu CTO-20AC column oven. As eluent an acetonitrile/water (containing 0.1% TFA) (40/60) mixture was used isocratically. The flow rate was set to 1.1 mL min<sup>-1</sup> and the detection wavelength to 210 nm. Retention times were 2.94 min for 2,3-dihydroxibiphenyl, 3.67 min for 2-hydroxybiphenyl and 6.47 min for octyl formate. 1-Octanol was not quantified due to its low response in the detection method (UV). Data were processed using the LC solution software. The final concentrations were calculated based on standard curves obtained using 2-hydroxybiphenyl and 2,3-dihydroxybiphenyl standards in the concentration range of 10-500 mM.

#### References

- [1] A. Weckbecker, H. Groger, W. Hummel, Regeneration of nicotinamide coenzymes: principles and applications for the synthesis of chiral compounds, *Adv. Biochem. Eng. Biotechnol.*, **2010**, *120*, 195-242.
- [2] W. A. van der Donk, H. M. Zhao, Recent developments in pyridine nucleotide regeneration, *Curr. Opin. Biotechnol.*, **2003**, *14*, 421-426.
- [3] F. Hollmann, I. Arends, K. Buehler, A. Schallmey, B. Buhler, Enzyme-mediated oxidations for the chemist, *Green Chem.*, **2011**, *13*, 226-265.
- [4] C. Rodriguez, I. Lavandera, V. Gotor, Recent Advances in Cofactor Regeneration Systems Applied to Biocatalyzed Oxidative Processes, *Curr. Org. Chem.*, **2012**, *16*, 2525-2541.
- [5] Z. Shaked, G. M. Whitesides, Enzyme-catalyzed organic synthesis: NADH regeneration by using formate dehydrogenase, *J. Am. Chem. Soc.*, **1980**, *102*, 7104-7105.
- [6] Y. Chen, S. L. Goldberg, R. L. Hanson, W. L. Parker, I. Gill, T. P. Tully, M. A. Montana, A. Goswami, R. N. Patel, Enzymatic Preparation of an (S)-Amino Acid from a Racemic Amino Acid, *Org. Process Res. Dev.*, **2010**, *15*, 241-248.

- [7] K. Kühnel, S. C. Maurer, Y. Galeyeva, W. Frey, S. Laschat, V. B. Urlacher, Hydroxylation of Dodecanoic Acid and (2R,4R,6R,8R)-Tetramethyldecanol on a Preparative Scale using an NADH-Dependent CYP102A1 Mutant, *Adv. Synth. Catal.*, **2007**, *349*, 1451-1461.
- [8] S. C. Maurer, H. Schulze, R. D. Schmid, V. Urlacher, Immobilisation of P450BM-3 and an NADP(+) cofactor recycling system: Towards a technical application of heme-containing monooxygenases in fine chemical synthesis, *Adv. Synth. Catal.*, **2003**, *345*, 802-810.
- [9] K. Hofstetter, J. Lutz, I. Lang, B. Witholt, A. Schmid, Coupling of Biocatalytic Asymmetric Epoxidation with NADH Regeneration in Organic–Aqueous Emulsions, *Angew. Chem. Int. Ed.*, **2004**, *43*, 2163-2166.
- [10] J. Lutz, V. V. Mozhaev, Y. L. Khmelnitsky, B. Witholt, A. Schmid, Preparative application of 2-hydroxybiphenyl 3-monooxygenase with enzymatic cofactor regeneration in organic-aqueous reaction media, *J. Mol. Catal. B-Enzym.*, **2002**, *19*, 177-187.
- [11] A. Schmid, I. Vereyken, M. Held, B. Witholt, Preparative regio- and chemoselective functionalization of hydrocarbons catalyzed by cell free preparations of 2-hydroxybiphenyl 3-monooxygenase, *J. Mol. Catal. B-Enzym.*, **2001**, *11*, 455-462.
- [12] M. Eckstein, M. Villela Filho, A. Liese, U. Kragl, Use of an ionic liquid in a two-phase system to improve an alcohol dehydrogenase catalysed reduction, *Chem Commun (Camb)*, **2004**, 1084-1085.
- [13] S. C. Maurer, K. Kühnel, L. A. Kaysser, S. Eiben, R. D. Schmid, V. B. Urlacher, Catalytic Hydroxylation in Biphasic Systems using CYP102A1 Mutants, *Adv. Synth. Catal.*, **2005**, *347*, 1090-1098.
- [14] P. Frohlich, K. Albert, M. Bertau, Formate dehydrogenase a biocatalyst with novel applications in organic chemistry, *Org. Biomol. Chem.*, **2011**, *9*, 7941-7950.
- [15] F. Hollmann, A. Schmid, E. Steckhan, The first synthetic application of a monooxygenase employing indirect electrochemical NADH regeneration, *Angew. Chem. Int. Ed.*, **2001**, *40*, 169-171.
- [16] M. Held, A. Schmid, H. P. Kohler, W. Suske, B. Witholt, M. G. Wubbolts, An integrated process for the production of toxic catechols from toxic phenols based on a designer biocatalyst, *Biotechnol. Bioeng.*, **1999**, *62*, 641-648.
- [17] M. Held, W. Suske, A. Schmid, K.-H. Engesser, H.-P. E. Kohler, B. Witholt, M. G. Wubbolts, Preparative scale production of 3-substituted catechols using a novel monooxygenase from Pseudomonas azelaica HBP 1, J. Mol. Catal. B: Enzym., 1998, 5, 87-93.
- [18] W. A. Suske, M. Held, A. Schmid, T. Fleischmann, M. G. Wubbolts, H. P. E. Kohler, Purification and characterization of 2-hydroxybiphenyl 3-monooxygenase, a novel NADH-dependent, FAD-containing aromatic hydroxylase from Pseudomonas azelaica HBP1, *J. Biol. Chem.*, **1997**, *272*, 24257-24265.
- [19] W. A. Suske, W. J. H. van Berkel, H. P. E. Kohler, Catalytic mechanism of 2-hydroxybiphenyl 3-monooxygenase, a flavoprotein from Pseudomonas azelaica HBP1, *J. Biol. Chem.*, **1999**, *274*, 33355-33365.
- [20] J. B. Park, D. S. Clark, New reaction system for hydrocarbon oxidation by chloroperoxidase, *Biotechnol. Bioeng.*, **2006**, *94*, 189-192.
- [21] G. de Gonzalo, I. Lavandera, K. Faber, W. Kroutil, Enzymatic Reduction of Ketones in "Microaqueous" Media Catalyzed by ADH-A from Rhodococcus ruber, *Org. Lett.*, **2007**, *9*, 2163-2166.

- [22] B. Orlich, H. Berger, M. Lade, R. Schomacker, Stability and activity of alcohol dehydrogenases in W/O-microemulsions: enantioselective reduction including cofactor regeneration, *Biotechnol. Bioeng.*, **2000**, *70*, 638-646.
- [23] L. H. Dai, A. M. Klibanov, Peroxidase-catalyzed asymmetric sulfoxidation in organic solvents versus in water, *Biotechnol. Bioeng.*, **2000**, *70*, 353-357.
- [24] J. Grunwald, B. Wirz, M. P. Scollar, A. M. Klibanov, Asymmetric oxidoreductions catalyzed by alcohol dehydrogenase in organic solvents, *J. Am. Chem. Soc.*, **1986**, *108*, 6732-6734.
- [25] A. M. Klibanov, Asymmetric enzymatic oxidoreductions in organic solvents, *Curr. Opin. Biotechnol.*, **2003**, *14*, 427-431.
- [26] A. M. Klibanov, Improving enzymes by using them in organic solvents, *Nature*, **2001**, *409*, 241-246.
- [27] K. Nagayama, A. C. Spiess, J. Buchs, Enhanced catalytic performance of immobilized Parvibaculum lavamentivorans alcohol dehydrogenase in a gas phase bioreactor using glycerol as an additive, *Chem. Eng. J.*, **2012**, *207*, 342-348.
- [28] A. Ö. Triantafyllou, E. Wehtje, P. Adlercreutz, B. Mattiasson, How do additives affect enzyme activity and stability in nonaqueous media?, *Biotechnol. Bioeng.*, **1997**, *54*, 67-76.
- [29] S. A. Costa, T. Tzanov, A. F. Carneiro, A. Paar, G. M. Gubitz, A. Cavaco-Paulo, Studies of stabilization of native catalase using additives, *Enzyme Microb. Technol.*, **2002**, *30*, 387-391.
- [30] A. Schmid, H.-P. E. Kohler, K.-H. Engesser, E. coli JM109 pHBP461, a recombinant biocatalyst for the regioselective monohydroxylation of ortho-substituted phenols to their corresponding 3-substituted catechols, *J. Mol. Catal. B: Enzym.*, **1998**, *5*, 311-316.
- [31] H. Slusarczyk, S. Felber, M. R. Kula, M. Pohl, Stabilization of NAD-dependent formate dehydrogenase from Candida boidinii by site-directed mutagenesis of cysteine residues, *Eur. J. Biochem.*, **2000**, *267*, 1280-1289.

# Chapter 7

# **Conclusions and outlook**

# Chapter 7

#### **Conclusions and outlook**

Biocatalysts attract considerable attention for synthetic organic oxyfunctionalization chemistry due to their high chemo-, regio-, and stereoselectivity, which can be difficult to achieve by chemical means. Enzymatic oxyfunctionalizations are mainly performed by peroxygenases and oxygenases. The aim of this thesis was to setup robust and scalable biocatalytic oxyfunctionalizations using heme - dependent peroxygenases. Unlike oxygenases, peroxygenases are single component proteins, independent of an expensive NAD(P)H cofactor utilizing simple and cheap  $H_2O_2$  as an oxidant. However, the application of peroxygenases is hampered by their low operational stability, which impairs the overall productivity. Hence, the major topic of this thesis was to improve the operational stability and the overall productivity of peroxygenase - catalyzed oxyfunctionalization.

#### Stabilization by the controlled in situ H<sub>2</sub>O<sub>2</sub> generation from O<sub>2</sub>

The operational stability of peroxygenases is mainly hampered by  $H_2O_2$ , which oxidatively inactivates the peptide and the prosthetic group. To alleviate this inactivation, we have developed two alternative catalytic approaches for the controlled in situ  $H_2O_2$  generation from  $O_2$ . The photocatalytic method for in situ generation of  $H_2O_2$  has been applied to CPO catalyzed sulfoxidation and AaeAPO catalyzed hydroxylation/epoxidation reactions. The operational stability, and consequently the overall productivity (in terms of TTN), of both CPO and AaeAPO has been significantly improved in comparison with stoichiometric use of  $H_2O_2$  as illustrated for thioanisole and ethylbenzene oxidations (Table 1, entries 1 - 3).

Table 1. a) Sulfoxidation of thioanisole catalyzed by CPO; b) ethylbenzene hydroxylation catalyzed by AaeAPO using different  $H_2O_2$  generation/dosage methods

	H <sub>2</sub> O <sub>2</sub> generation method/addition mode	TTN (CPO) <sup>a</sup>	TTN (AaeAPO) <sup>b</sup>	Ref.
1	Stoichiometric H <sub>2</sub> O <sub>2</sub>	4 900	6000	[1]; Chapter 3
2	Flavin/ EDTA/ hv/ O <sub>2</sub> (monophasic)	22 400	18 080	[1]; Chapter 3
3	Glucose oxidase/glucose/O <sub>2</sub>	250 000	-	[2]
4	Continuous addition	108 000	43 000	[3-4]
5	Sensor – controlled	148 000	-	[5]
6	Flavin/ EDTA/ hv/ O <sub>2</sub> (biphasic)	126 000	200 000	Chapter 2; Chapter 3

In monophasic set - up, TTN for photocatalytic approach remained lower than for previously reported methods (Table 1, entries 3 - 5). However, photocatalytic approach showed a drastic increase in TTN in the biphasic system already under non-optimized conditions (Table 1, entry 6). Further optimization of the reaction system may lead to even higher productivities.

One of the major advantages of the in situ  $H_2O_2$  generation is the constant reaction volume, whereas continuous or sensor controlled addition of  $H_2O_2$  require diluted concentrations of  $H_2O_2$  leading to constant increase of the reaction volume, high water consumption and laborious product isolation.

One of the drawbacks for in situ generation of  $H_2O_2$ , is the need for an excess of a sacrificial electron donor for oxygen reduction, and the concomitant byproduct formation. Therefore, the initially applied reductant EDTA, leading to the formation of significant amounts of problematic byproducts such as formaldehyde and ethylene diamine, has been substituted by innocuous ascorbic acid [Chapter 3]. In addition, ascorbic acid is known as a radical scavenger, which further facilitates enzymatic stability and suppresses radical – induced side reactions.

As was shown in Chapters 2-3 oxygen diffusion from ambient atmosphere represents one of the major limitations of the photoenzymatic system. Partially this problem can be solved by increasing the oxygen pressure, however it somehow influences the safety of the whole process. External oxygen supply may lead to the formation of air (oxygen) bubbles and cause the hydrodynamic stress at the liquid - gas interphase, which can impair the enzyme activity and stability. To overcome this drawback, bubble - free oxygenation might be applied by e.g. using an oxygen - permeable composite membrane [6-7].

The second approach for in situ generation of  $H_2O_2$  catalysis employs 1-benzyldihydronicotinamide (mNADH) as sacrificial reductant of flavin [Chapter 4]. mNADH is a strong reducing reagent <sup>[8]</sup>, therefore light excitation of flavin is not required for the reduction of flavin. This approach has been applied for P450 peroxygenase - catalyzed hydroxylation of myristic acid. The operational stability of P450 peroxygenases could be enhanced by applying in situ generation of  $H_2O_2$ . However, the final productivities remained low (TTN of 200) because of the low substrate loadings. Further experiments using higher substrate loading, e.g. in 2 LPS may improve the final productivities. Additionally, an efficient and stable regeneration system of catalytic amount mNADH needs to be developed <sup>[9-10]</sup>

#### Two - liquid phase system

To increase the overall productivity of studied biotransformations, the two - liquid phase system (2 LPS) approach has been applied throughout this thesis permitting high substrate loadings and reducing reactants toxicity for enzymes. For example, in case of the CPO - catalyzed enantiospecific

sulfoxidation of thioanisole, application of the 2 LPS concept greatly enhanced the overall productivity as compared to the aqueous reaction system (Table 1). CPO activity and selectivity remained stable using thioanisole as a second liquid phase. Interestingly, the enantioselectivity and stability of *Aae*APO markedly depended on the solvent used as a second phase [Chapters 2-3]. Preliminary results showed that encapsulation of *Aae*APO into a sol - gel matrix enhanced enzyme stereospecificity. Therefore, different immobilization techniques would be interesting to test in order to prevent enzymes inactivation and permit its recycling.

In addition, the direct use of *Aae*APO in organic solvents would be interesting to investigate. In biphasic system enzymes retain their conformational flexibility. Thus, hydrophilic protein motives tend to expose to aqueous phase, wherein hydrophobic protein motives incline towards organic media. Such a hydrophilic - hydrophobic interaction may lead to the change of the enzyme conformation, which is favorable for catalysis, and its denaturation over longer periods. However, it has been demonstrated that enzymes are very rigid in the absence of water, which plays the role of molecular lubricant. Therefore, various enzymes retain their native structure even in anhydrous organic solvents [11]. Although, the catalytic activity of enzymes in neat solvents is generally lower than in water [12-13], this approach 1) makes high concentrations of substrate possible, simplifying downstream processes and 2) obviate the water consumption, which is essential in a view of oncoming problem of fresh water sources.

#### Future prospects for application of peroxygenases

The recently discovered *Aae*APO peroxygenase possesses a remarkable activity towards oxyfunctionalizations of (non) - activated C-H bonds over broad range of substrates [Chapter 3]. Furthermore, already under non - optimized conditions high productivities have been obtained for hydroxylation of ethylbenzene derivatives catalyzed by *Aae*APO [Chapter 3]. On the contrary, CPO is a good catalyst only for sulfoxidations, whereas its performance in hydroxylation of C-H bonds and epoxidation reactions drops by several orders of magnitude [5, 14-15].

As for catalysis with P450 peroxygenases, further experiments using higher substrate loading, e.g. in 2 LPS may shed light on possibilities for preparative applications. However, the substrate scope of these enzymes needs to be further extended, by means of protein engineering or by using decoy molecules with a carboxy group, which allows to generate active species and catalyze non-natural reactions [16-17].

Generally, in order to establish profitable industrial processes based on peroxygenases, large - scale enzymes production is necessary to reduce the cost of the catalyst. However, so far only CPO is

produced as a fine chemical. Despite of promiscuity and high productivities achieved by *Aae*APO, its production has not been established yet. This hampers the commercial application of *Aae*APO.

Nevertheless, comparing the publication track between lipases (which are easy to handle and widely applied in industry <sup>[18]</sup>), and peroxygenases, we can conclude that the research area on these enzymes is rather young. The information available on this enzymes hardly reach 30 publications per year in comparison with thousands articles published on lipases. Therefore, we can assume that commercial application of promising peroxygenases, such as *Aae*APO, is only a question of time. In this respect, collaborative research is needed including the development of efficient and stable peroxygenase production systems, and combined enzyme, reaction and process engineering. Finally, the discovery of novel peroxygenases may enrich the scope of desirable oxyfunctionalizations for organic synthesis.

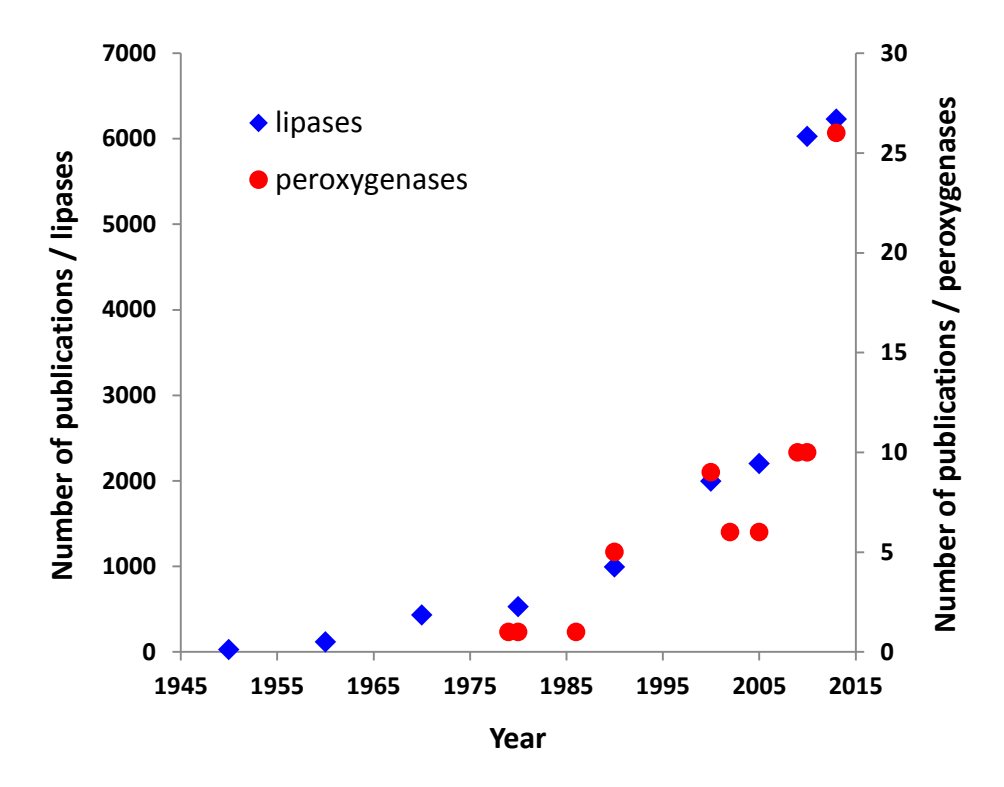


Figure 1. Publication track on lipases and peroxygenases according to Web Of Science [19]

This thesis showed that industrial viability of peroxygenases can be improved by a) using in situ generation of  $H_2O_2$  and b) applying two liquid phase system for substrate supply/product removal, which leads to enhanced productivity.

#### NADH cofactor regeneration

In addition to peroxygenases, various oxyfunctionalizations can be performed by oxygenases. However, the application of isolated oxygenases, relies on efficient cofactor regeneration techniques. Therefore, the second objective of this thesis was the development of alternative NADH regeneration systems for oxygenase - based catalysis.

First, we proposed a chemical method for NAD(P)H regeneration using a transition metal catalyst [Chapter 5]. To overcome the issue of the commonly encountered mutual inactivation between the metallocomplex and the enzyme, we proposed using artificial transfer hydrogenases (ATHs) wherein the biotin - coordinated transition metal complex is sterically shielded by complexation with streptavidin. The applicability of the concept was illustrated by combining the ATHase with HbpA, demonstrating that the general catalytic properties of ATHase and enzyme are preserved. However, the efficiency of the proposed regeneration system remains noncompetitive with e.g. the well established FDH-catalyzed NADH regeneration. Nevertheless, this concept opens the door towards attractive one - pot concurrent chemo - enzymatic cascades.

Second contribution relied on the FDH catalyzed NADH regeneration using formic acid esters as 'hydrophobized' formic acid equivalents, which simultaneously served as an organic phase in 2 LPS reaction and as source of reducing equivalents [Chapter 6]. This concept elegantly addresses 3 issues, such as NADH regeneration, substrate supply, and enzyme inhibition. Although robust productivity of HbpA catalyzed aromatic hydroxylation has been achieved, the productivity of the system has been severely limited by the diffusion limitations, which have to be addressed in future research, by e.g. creating emulsions stabilized with surfactant. Furthermore, the activity of FDH towards formic acid esters might be further enhanced by protein engineering techniques.

#### References

- [1] D. I. Perez, M. M. Grau, I. W. C. E. Arends, F. Hollmann, Visible light-driven and chloroperoxidase-catalyzed oxygenation reactions, *Chem Commun*, **2009**, 6848-6850.
- [2] F. van de Velde, N. D. Lourenço, M. Bakker, F. van Rantwijk, R. A. Sheldon, Improved operational stability of peroxidases by coimmobilization with glucose oxidase, *Biotechnol. Bioeng.*, **2000**, *69*, 286-291.
- [3] M. P. J. van Deurzen, I. J. Remkes, F. van Rantwijk, R. A. Sheldon, Chloroperoxidase catalyzed oxidations in t-butyl alcohol/water mixtures, *J. Mol. Catal. A: Chem.*, **1997**, *117*, 329-337.
- [4] M. Kluge, R. Ullrich, K. Scheibner, M. Hofrichter, Stereoselective benzylic hydroxylation of alkylbenzenes and epoxidation of styrene derivatives catalyzed by the peroxygenase of Agrocybe aegerita, *Green Chem.*, **2012**, *14*, 440-446.
- [5] F. Van Rantwijk, R. A. Sheldon, Selective oxygen transfer catalysed by heme peroxidases: Synthetic and mechanistic aspects, *Curr. Opin. Biotechnol.*, **2000**, *11*, 554-564.
- [6] W. Van Hecke, R. Ludwig, J. Dewulf, M. Auly, T. Messiaen, D. Haltrich, H. Van Langenhove, Bubble-free oxygenation of a bi-enzymatic system: effect on biocatalyst stability, *Biotechnol. Bioeng.*, **2009**, *102*, 122-131.
- [7] M. Schneider, F. Reymond, I. W. Marison, U. Vonstockar, Bubble-free oxygenation by means of hydrophobic porous membranes, *Enzyme Microb. Technol.*, **1995**, *17*, 839-847.

- [8] K. E. Taylor, J. B. Jones, Nicotinamide coenzyme regeneration by dihydropyridine and pyridinium compounds, *J. Am. Chem. Soc.*, **1976**, *98*, 5689-5694.
- [9] J. D. Ryan, R. H. Fish, D. S. Clark, Engineering Cytochrome P450 Enzymes for Improved Activity towards Biomimetic 1,4-NADH Cofactors, *ChemBioChem*, **2008**, *9*, 2579-2582.
- [10] J. Lutz, F. Hollmann, T. V. Ho, A. Schnyder, R. H. Fish, A. Schmid, Bioorganometallic chemistry: biocatalytic oxidation reactions with biomimetic NAD(+)/NADH co-factors and Cp\*Rh(bpy)H (+) for selective organic synthesis, *J. Organomet. Chem.*, **2004**, *689*, 4783-4790.
- [11] A. M. Klibanov, Improving enzymes by using them in organic solvents, *Nature*, **2001**, *409*, 241-246.
- [12] A. M. Klibanov, Why are enzymes less active in organic solvents than in water?, *Trends Biotechnol.*, **1997**, *15*, 97-101.
- [13] F. van de Velde, M. Bakker, F. van Rantwijk, R. A. Sheldon, Chloroperoxidase-catalyzed enantioselective oxidations in hydrophobic organic media, *Biotechnol. Bioeng.*, **2001**, *72*, 523-529.
- [14] M. Hofrichter, R. Ullrich, Heme-thiolate haloperoxidases: versatile biocatalysts with biotechnological and environmental significance, *Appl. Microbiol. Biotechnol.*, **2006**, *71*, 276-288.
- [15] M. Hofrichter, R. Ullrich, M. J. Pecyna, C. Liers, T. Lundell, New and classic families of secreted fungal heme peroxidases, *Appl. Microbiol. Biotechnol.*, **2010**, *87*, 871–897.
- [16] O. Shoji, T. Fujishiro, H. Nakajima, M. Kim, S. Nagano, Y. Shiro, Y. Watanabe, Hydrogen Peroxide Dependent Monooxygenations by Tricking the Substrate Recognition of Cytochrome P450BSβ, *Angew. Chem.*, **2007**, *119*, 3730-3733.
- [17] T. Fujishiro, O. Shoji, N. Kawakami, T. Watanabe, H. Sugimoto, Y. Shiro, Y. Watanabe, Chiral-substrate-assisted stereoselective epoxidation catalyzed by H2O2-dependent cytochrome P450 SPα, *Chem. Asian J.*, **2012**, *7*, 2286-2293.
- [18] A. Schmid, J. S. Dordick, B. Hauer, A. Kiener, M. Wubbolts, B. Witholt, Industrial biocatalysis today and tomorrow, *Nature*, **2001**, *409*, 258-268.
- [19] <a href="http://apps.webofknowledge.com">http://apps.webofknowledge.com</a>

## Summary

Biocatalytic oxyfunctionalizations, especially of non-activated hydrocarbons, attract considerable attention for synthetic organic chemistry thanks to their high chemo-, regio-, and stereoselectivity, which difficult to achieve by chemical means. Many enzymatic oxyfunctionalizations have been described. However, there are many hurdles towards large scale applications, such as low activity and stability of enzymes, substrate toxicity, overoxidation, oxygen mass transfer, etc. Therefore, the aim of this thesis is to setup robust and scalable biocatalytic oxyfunctionalizations.

**Chapter 1** gives a general introduction on enzymatic C-H oxyfunctionalizations highlighting the great potential of heme - iron peroxygenases. Peroxygenases do not rely on expensive NAD(P)H cofactors and catalyze a variety of useful synthetic transformations utilizing  $H_2O_2$  as an oxidant. However, the practical applicability of heme - peroxygenases is limited by their low stability towards  $H_2O_2$ . To avoid the inactivation of the enzymes, we have developed two alternative catalytic approaches for the controlled in situ  $H_2O_2$  generation from  $O_2$ . General applicability of the proposed methods has been demonstrated for various peroxygenase - based biotransformations in **Chapters 2, 3, 4**.

Thus, in *Chapter 2* a photocatalytic approach for in situ H<sub>2</sub>O<sub>2</sub> generation has been applied for the CPO (chloroperoxidase from *Caldariomyces fumago*) catalyzed thioanisole sulfoxidation. The enzyme stability has been drastically improved; however, the productivity of the system was severely limited by low solubility and evaporation of the substrate. Therefore, the photocatalytic approach was demonstrated at preparative - scale using a surfactant - stabilized two – liquid phase system (2 LPS). Both, initial rate and robustness of the system could be enhanced significantly leading to an increase of the final product concentration by more than one order of magnitude in comparison with monophasic set - up.

In *Chapter 3* the proposed photocatalytic in situ generation of  $H_2O_2$  proved to be a suitable approach for *Aae*APO (*Agrocybe aegerita* aromatic peroxygenase) catalyzed epoxidation and hydroxylation reactions. High productivities and excellent enantiomeric excesses (>97%) were obtained with a broad range of substrates. Furthermore, preliminary results indicate that hundreds of thousands of turnovers can be achieved after reaction engineering, demonstrating the high potential of *Aae*APO for oxyfunctionalization catalysis.

In *Chapter 4* an alternative in situ  $H_2O_2$  generation method has been developed using a synthetic nicotinamide cofactor mimic and flavin. This method has been applied for the specific  $\alpha$ - or  $\beta$ -hydroxylation of fatty acid catalyzed by the cytochrome P450 peroxygenases. The cytochrome P450 peroxygenases P450bs $\beta$  from *Bacillus subtilis* and P450cl $\alpha$  from *Clostridium acetobutylicum* belong to

a unique group of P450s which consume  $H_2O_2$  and therefore do not require additional electron transfer proteins and NAD(P)H cofactor. Using the new method for in situ  $H_2O_2$  generation the final productivity of P450 peroxygenases could be enhanced due to higher enzyme stability under operation conditions.

In addition to peroxygenases, various oxyfunctionalizations can be performed by oxygenases. However, the application of isolated oxygenases, relies on efficient cofactor regeneration techniques. Formate dehydrogenase (FDH) is widely applied for NAD(P)H regeneration. However, classical FDH - based reaction systems are limited to mainly aqueous media, wherein the majority of substrates are poorly soluble. In order to circumvent this limitation we propose in *Chapter 6* using formic acid esters as 'hydrophobized' formic acid equivalents, which simultaneously can serve as an organic phase in 2LPS reaction and as source of reducing equivalents. The concept was demonstrated using 2-hydroxybiphenyl-3-monooxygenase (HbpA)-catalyzed specific *ortho*-hydroxylation of phenols as model reaction.

In addition, chemical methods for NAD(P)H regeneration have been employed as an alternative to enzymatic methods. The organometallic compound  $[Cp*Rh(bpy)(H_2O)]^{2+}$  has emerged as a catalyst of choice. However, the mutual inactivation between  $[Cp*Rh(bpy)(H_2O)]^{2+}$  and enzymes is usually encountered. To overcome this issue, in *Chapter 5*, we propose using artificial transfer hydrogenases (ATHs) wherein the biotin-coordinated transition metal complex is sterically shielded by complexation with streptavidin. Thereby, the mutual inactivation of the regeneration catalysts and the production enzyme(s) can be efficiently circumvented. The applicability of the concept was illustrated by combining the ATHase with HbpA, demonstrating that the general catalytic properties of ATHase and enzyme are preserved.

In conclusion, this thesis addresses some major challenges of oxyfunctionalization catalysis including enzyme stability, cofactor dependency and substrate supply. The proposed methods to overcome these issues have been implemented to various enzymatic oxyfunctionalizations. Furthermore, their practical applicability has been demonstrated at preparative - scale using a two liquid phase approach. Promising results in terms of productivity and selectivity have been obtained, thereby paving the way to preparative biocatalytic oxyfunctionalization. Nevertheless, further studies, e.g. combining enzyme immobilization techniques with reaction and process engineering, are needed to substantiate the full potential of biocatalytic oxyfunctionalizations.

## Samenvatting

Biokatalytische oxyfunctionaliseringen, vooral die van niet-geactiveerde koolwaterstoffen, zijn van grote interesse binnen de synthetische organische chemie vanwege hun hoge chemo-, regio en stereoselectiviteit die normaalgesproken lastig te verkrijgen zijn met chemische routes. Veel enzymatische oxyfunctionaliseringen zijn inmiddels gerapporteerd, maar de toepassing op grote schaal ondervindt problemen, zoals lage activiteit en lage stabiliteit van enzymen, giftigheid van substraten, overoxidatie, massatransportlimitaties van zuurstof etc. Dit vormt de aanleiding voor dit proefschrift namelijk onderzoek naar robuuste en opschaalbare biokatalytische oxyfunctionaliseringen.

**Hoofdstuk 1** geeft een algemene introductie tot de enzymatische C-H oxyfunctionaliseringen waarin de grote potentie van heme-iron peroxygenases wordt onderstreept. Deze peroxygenases zijn niet afhankelijk van NAD(P)H cofactoren en katalyseren een variëteit aan waardevolle synthetische transformaties waarin  $H_2O_2$  als oxidant wordt gebruikt. Echter, de praktische toepassing van de heme-peroxygenases wordt beperkt door hun lage stabiliteit ten aanzien van  $H_2O_2$ . Algemene toepassing van de voorgestelde methodes voor verschillende peroxygenase-gebaseerde biotransformaties wordt onderzocht in de **Hoofdstukken 2, 3, 4**.

In *Hoofdstuk 2* wordt een fotokatalytische benadering voor de in-situ productie van H<sub>2</sub>O<sub>2</sub> toegepast voor de CPO (chloroperoxide van *Caldariomyces fumago*) gekatalyseerde sulfoxidatie van thioanisole. Hoewel de stabiliteit van het enzym aanmerkelijk was verbeterd, bleek de productiviteit van het systeem sterk beperkt door lage oplosbaarheid en verdamping van het substraat. Dit is waarom de fotokatalytische benadering wordt uitgevoerd op preparatieve schaal met behulp van een oppervlakte-actieve stof die een vloeibaar twee-fase systeem stabiliseert (2 LPS). Zowel de aanvankelijke reactiesnelheid als de robuustheid van het systeem bleken sterk verbeterd, wat tot een orde-van-grootte toename van de concentratie van het product leidde in vergelijking met een één-fase systeem.

In *Hoofdstuk 3* wordt aangetoond dat de voorgestelde fotokatalytische in-situ generatie van H<sub>2</sub>O<sub>2</sub> een goede benadering is voor *Aae*APO (*Agrocybe aegerita* aromatisch peroxygenase) gekatalyseerde epoxidatie en hydroxylatie reacties. Hoge productiviteitswaarden en uitstekende enantiomerische selectiviteiten (>97%) zijn verkregen met een groot scala aan substraten. Verder geven de voorlopige resultaten aan dat technologische aanpassingen kunnen leiden tot honderdduizenden katalytische omlopen, wat de grote potentie van *Aae*APO voor oxyfunctionaliseringskatalyse demonstreert.

In **Hoofdstuk 4** wordt de ontwikkeling van een alternatieve methode voor  $H_2O_2$  productie omschreven, gebruikmakend van een gesynthetiseerd analoog van nicotine cofactor en flavine. Deze methode wordt toegepast voor de specifieke  $\alpha$ - of  $\beta$ -hydroxylatie van vetzuren, gekatalyseerd door

cytochrome P450 peroxygenases. De cytochrome P450 peroxygenases P450bs $\beta$  van *Bacillus subtilis* en P450cl $\alpha$  van *Clostridium acetobuylicum* behoren tot een unieke groep P450s die H<sub>2</sub>O<sub>2</sub> als substraat gebruiken en daardoor geen verdere electronenoverdracht en NAD(P)H cofactor nodig hebben. Het was, gebruikmakend van de nieuwe methode voor in-situ H<sub>2</sub>O<sub>2</sub> generatie, mogelijk de uiteindelijke productiviteit van de P450 peroxygenases te verbeteren door de stabiliteit van de enzymen te verhogen onder operationele omstandigheden.

Naast peroxygenases is het ook mogelijk om verschillende oxyfunctionaliseringen uit te voeren met oxygenases. Echter, de toepassing van geïsoleerde oxygenases hangt af van de mogelijkheden tot het regenereren van de cofactor. Formaat dehydrogenase (FDH) is breed toegepast voor NAD(P)H regeneratie, maar de klassieke FDH-gebaseerde reactiesystemen beperken zich tot waterige fases, wat de oplosbaarheid van het merendeel van de substraten niet ten goede komt. Om deze limitatie te omzeilen stellen we in *Hoofdstuk 6* voor esters van mierenzuur te gebruiken als 'gehydrofobeerde' mierenzuurequivalenten, die tegelijkertijd als organische fase in dit twee-fase systeem, en als bron van reducerende equivalenten kunnen fungeren. Dit concept is aangetoond met 2-hydroxybiphenyl-3-monooxygenase (HbpA)-gekatalyseerde specifieke *ortho*-hydroxylatie van fenolen als modelreactie.

Als alternatief voor enzymatische methodes zijn chemische methoden voor NAD(P)H regeneratie gebruikt. De organometallische [Cp\*Rh(bpy)(H<sub>2</sub>O)]<sup>2+</sup> verbinding werd hiervoor bestudeerd. Echter, het komt vaak voor dat er onderlinge inactivatie tussen [Cp\*Rh(bpy)(H<sub>2</sub>O)]<sup>2+</sup> en de enzymen optreedt. Om dit probleem op te lossen, stellen we in *Hoofdstuk 5* voor 'artificial transfer hydrogenases' (ATHs) te gebruiken waarin de biotin-gecoördineerde transitiemetaalcomplexen sterisch worden gehinderd door complexatie met streptavidin. Hierdoor wordt de onderlinge inactivatie van de regeneratiekatalysatoren en de producerende enzymen op een efficiënte wijze omzeild. De toepasbaarheid van dit concept wordt geïillustreerd door ATHase met HbpA te combineren, waarin wordt aangetoond dat de algemene katalytische eigenschappen van ATHase en het enzym worden behouden.

Concluderend: dit proefschrift pakt enkele grote uitdagingen binnen het veld van de oxyfunctionaliseringskatalyse aan, zoals enzyme-stabiliteit, cofactor-afhankelijkheid en substraatafgifte. De methodes die zijn voorgesteld om deze problemen op te lossen zijn geïmplementeerd in verscheidende enzymatische oxyfunctionaliseringen. Daarnaast is de praktische toepassing aangetoond op preparatieve schaal, gebruikmakend van een twee-fase benadering. Veelbelovende resultaten met betrekking tot productiviteit en selectiviteit zijn behaald. Desalniettemin is verder onderzoek noodzakelijk om de volle potentie van biokatalytische oxyfunctionalisering te realiseren. Gedacht kan worden aan bv. het combineren van enzym-immobilisatie met reactie- en procestechnologie.

# Acknowledgements

First of all, I would like to express my deep gratitude and respect to my supervisor Frank Hollmann and my promoter Isabel Arends. Frank, thank you very much for support and inspiration, for being positive and also strict, when it was necessary, for nice "beer" talks. Thanks for being an inspiring teacher, an enthusiastic supervisor, and even more so, a good friend. I think, it was my luckiest coincidence to meet you in the middle of nowhere at that Russian conference. You are the person who convinced me to start PhD, honestly saying that it might be a very exciting, but also a painful experience. Thank you for making me ready for ups and downs. Nevertheless, I enjoyed it and never had doubts about finishing my thesis under your guidance and persistent enthusiasm.

Isabel, thank you for being always positive and friendly, for support and help, especially in the last stages of writing the thesis. Thanks for treating all the foreigners in the group the way we feel like home!

Heel hartelijk bedankt to Maartin Gorselin, who day by day helped me intensively with all the equipment, analytics, any small and big problems. Without Maarten, my research would take ten years instead of four. Thank you very much for always being in positive mood and willing to help, for your never-ending optimism, for being supportive and for devoting the time, which you even did not have. The lesson from you: "I do not have time, but later I will have even less. Let's solve this problem now!"

Hans – Peter de Hoog is the person who has contributed significantly to my thesis. He helped to start research at the very beginning, and it is the most important to have a good and positive start. Thank you for introducing me to the lab, guiding the very first experiments, explaining many basics in enzymatic catalysis, which made the follow-up research comprehensible and easier going.

Serena remained my labmate, my officemate and, a good friend during the whole PhD. People were coming and going away, but you were always there helping me with advices, discussions, and even with important lab work. We traveled together for all the project meetings, we were nervous together before presentations, we had a lot of joyful time on the conferences and parties, we discovered The Netherlands together and adapted together to the culture. PhD made us great friends. Thank you very much for all your support!

Son is my older brother in science. We always had a lot of fruitful discussions about science and life; we had some arguments as well. Nevertheless, we always had joyful time at work, conferences, lunch breaks, dinners, and travelling. You gave various helpful advices, constructive criticism and you

were always ready to share your experience. You helped enormously in correcting my thesis and discussing my propositions. Thank you very much for being a scientific mentor, for philosophical discussions, for soulful talks, for loving Cheburashka, for being a good and really supportive friend!

I would like to acknowledge all the co-authors of my articles. Special thanks to Bartlomej Tomasewskij and Tomasso Quinto for a pleasant and productive collaboration, and a lot of fun during experimental work (even in the stressful deadline time!). You made a great contribution to my thesis! Work made us friends, and I had a great time having talks and dinners with you!

I would like to acknowledge Katja Buehler for her kind supervision during my stay in Dortmund. I would like to thank Ron Wever, Michael van der Horst, Louis Hartog for the kind supervision during my stay at the Amsterdam University. Thanks to Vlada Urlacher and Marco Girhard for all the valuable advices and assistance. It was a pleasure to collaborate with all of you. I have learnt a lot and gained the great experience!

Federica and Elmer, my great students, thank you for the joy of teaching and the joy of learning that you have given to me. It was a great experience and important contribution to my thesis! Elmer, it is hard to believe, but we even made it to a publication!

I would like to express my appreciation to Alessio, who helped me to design the cover of my thesis. I am thankful to Maarten Goesten for translating my Summary to Samenvatting and for all the linguistic advices.

I would like to thank cordially my colleagues - Selin, Paul, Daniela Sordi, Adeline, Jeroen, Sanjib, Jörg, Verena, Caroline, Florian, Tobias, Aida, Kristina, Linda, Ulf, Peter-Leon, Simon, Fred van Rantwijk, Fred Hagen, Mieke who were always ready to help, share experience and give advices. Many thanks to all members and guests of the BOC group - Kathrin, Cintia, Guzman, Bishuang, Yan Ni, Mauro, Jonathan, Wayne, Yi Cheng, Federico, Pedro, Monica, Remco, Jannis, Sinan for the great time in the lab, relaxing social events, hilarious and funny discussions during coffee breaks, lunches and conferences. Thanks to all my officemates, we always had a lot of fun! Special thanks to Selin, Verena and Caroline, who helped me a lot with corrections of the thesis! Special thanks to Jörg, Florian, Sibel, and Kristina for help with NMR analysis.

I would like to express my deep gratitude to our secretary – Mieke. It is not easy to have a Russian passport, and you helped me so much in resolving all the challenges to keep me legal, to travel and to deal with all PhD bureaucracy! Thank you very much!

Special thanks to my friend Alina, who was always sharing exciting scientific ideas with me, always made me think wider, and who gave me worthy advices during writing the thesis. Thanks a lot for

inspiring me to write some propositions with follow-up fruitful discussions. Thank you just for being a very supportive and a good friend!

Many thanks to my friends Daniela Ullien, Misha, Roma, Rodrigo, Diana, who were there from the very first days of my PhD and helped me a lot to adapt to The Netherlands, who always remained positive and supportive, and contributed greatly with fruitful discussions to my propositions. Special thanks to Daniela for the valuable help during writing the thesis.

Thanks a lot to my dance partners Damani, Nina, Dro, Denis. You might be not aware, but you truly supported me by dancing together, freeing my mind, giving me energy, and inspiring for new ideas. Thanks to Portuguese community for relaxing dinners and for sharing the knowledge on port wine drinking. Many thanks to Marie Curie Initial Training Network for the financial support and all the members of the BIOTRAINS for the fruitful projects meeting followed by pleasant networking.

Thanks to my greatest friends Zhenya, Nikita, Sasha, Irina, Ksusha who are always close even when we are far away and who always give me support! Many thanks to my amazing sister Masha, who is always positive, always gives me a smile, and always makes me see things better. I know that I always can count on you and this makes me happy. Thanks to my parents for the best support, trust and love. Thanks to my beloved Samur for motivation, for support, for love and for the crazy journey through life and across the world – from Siberia to Brazil.

# List of publications

- [1] C. E. Paul, E. Churakova, E. Maurits, M. Girhard, V. B. Urlacher, F. Hollmann, In situ formation of H<sub>2</sub>O<sub>2</sub> for P450 peroxygenases, submitted to *Bioorg. Med. Chem.*
- [2] E. Churakova, B. Tomaszewski, K. Buehler, A. Schmid, I. Arends, F. Hollmann, Hydrophobic Formic Acid Esters for Cofactor Regeneration in Aqueous/Organic Two-Liquid Phase Systems, *Top. Catal*, **2014**, *57*, 385-391.
- [3] V. Koehler, Y. M. Wilson, M. Duerrenberger, D. Ghislieri, E. Churakova, T. Quinto, L. Knoerr, D. Haeussinger, F. Hollmann, N. J. Turner, T. R. Ward, Synthetic cascades are enabled by combining biocatalysts with artificial metalloenzymes, *Nat. Chemistry*, 2013, 5, 93-99.
- [4] E. Churakova, I. W. C. E. Arends, F. Hollmann, Increasing the Productivity of Peroxidase-Catalyzed Oxyfunctionalization: A Case Study on the Potential of Two-Liquid-Phase Systems, *ChemCatChem*, **2013**, *5*, 565-568.
- [5] E. Churakova, M. Kluge, R. Ullrich, I. Arends, M. Hofrichter, F. Hollmann, Specific Photobiocatalytic Oxyfunctionalization Reactions, *Angew. Chem. Int. Ed.*, 2011, 50, 10716-10719.